DYNAMICS OF LONG-TERM ESSENTIAL HYPERTENSION AND PHARMACOTHERAPY OPTIONS

by

Zeynep Hasgul

B.S., Industrial Engineering, Istanbul Technical University, 2019

Submitted to the Institute for Graduate Studies in
Science and Engineering in partial fulfillment of
the requirements for the degree of
Master of Science

Graduate Program in Industrial Engineering
Boğaziçi University

2022

ACKNOWLEDGEMENTS

First and foremost, express my deepest gratitude to my thesis supervisor Assoc. Prof. Gönenç Yücel for his invaluable guidance, support and patients at all stages of this study.

Also, I would like to thank to Assoc. Prof. Dr. Aybek Korugan and Assist. Prof. Dr. Mert Edalı for taking part in my thesis committee and providing valuable comments.

I am grateful to Hasan Ali Barman, M.D. and Serhan Ozyıldırım, M.D. from Istanbul University Cerrahpaşa Institute of Cardiology for supporting this study with their cardiology knowledge.

I am also thankful to the members of SESDYN Research Group for their support and motivation. I finally wish to thank all of my friends and colleagues for being by my side during my study.

Most importantly, I would like to express my deepest gratitude to my parents for supporting and encouraging me throughout all my decisions in life.

ABSTRACT

DYNAMICS OF LONG-TERM ESSENTIAL HYPERTENSION AND PHARMACOTHERAPY OPTIONS

Hypertension is a preventable and treatable disease however; blood pressure control remains insufficient in many countries. An incomplete understanding of the highly complex mechanism of blood pressure regulation is one of the reasons for poor hypertension management. Physiological differentiation in individuals causes optimal antihypertensive treatment strategies to vary for patients. Consequently, instead of one fits all treatments, personalized treatments can offer improved results on therapeutic goals. Due to the sheer number of feedback loops and interconnected mechanisms, we developed and validated a system dynamics model for understanding and interpreting relationships within hypertension treatment. We aim to demonstrate the use of simulation modeling to study inter-patient physiological variations and their effects on hypertension treatment outcomes. The model includes the central nervous system and renal control mechanisms, vascular elasticity, and kidney function, capturing long-term dynamics of blood pressure. Three pathogenesis mechanisms of primary hypertension (the over-active nervous system, the over-active renin-angiotensin-aldosterone system, and low sodium excretion) are examined to represent different patient profiles. Later, treatment outcomes are analyzed on the identified patient profiles by comparing the decline in kidney and vascular functions under various treatment options. This study presented the potential benefit of using dynamic simulation models to compare treatment options for patients with physiological differences. Even though obtaining granular empirical data is challenging, they can be used for calibrating simulation models such as these to get closer to individualized treatments in clinical settings. As a future study, cost-effectiveness and value of information aspects can be incorporated to assess the benefit of personalized treatments.

ÖZET

PRİMER HİPERTANSİYONUN UZUN DÖNEM DİNAMİKLERİ VE FARMAKOTERAPİ SEÇENEKLERİNİN DEĞERLENDİRİLMESİ

Hipertansiyon önlenebilir, tedavi edilebilir bir hastalık olmasına rağmen kontrolü birçok ülkede yetersiz kalmaktadır. Karmaşık mekanizmasının tam anlaşılmaması, başarısız hipertansiyon tedavisinin nedenlerinden biridir. Bireysel fizyolojik farklılaşma, ideal antihipertansif tedavi stratejileri değişmektedir. Sonuç olarak, tüm hastaları kapsayan tek bir tedavi yerine, kişiselleştirilmiş tedaviler, tedavi hedeflerinde daha iyi sonuçlar sağlayabilir. Çok sayıda geri bildirim döngüsü ve birbirine bağlı mekanizmalar bulunduran hipertansiyon tedavisindeki ilişkileri anlamak ve yorumlamak için bir sistem dinamiği modeli geliştirdik ve test ettik. Hastalar arası fizyolojik çeşitliliklerin hipertansiyon tedavi sonucu üzerindeki etkilerini incelemede simülasyon modelleme kullanımını göstermeyi amaçladık. Model, kan basıncının uzun vadeli dinamiklerini yakalayan merkezi sinir sistemi ve böbrek kontrol mekanizmalarını, damar elastikiyetini ve böbrek fonksiyonunu kapsamaktadır. Primer hipertansiyonun üç patogenez mekanizması (aktif sinir sistemi, aktif renin-anjiyotensin-aldosteron sistemi ve düşük sodyum atılımı) farklı hasta profillerini temsil etmek üzere incelendi. Sonra, çeşitli tedavi seçenekleri altında böbrek ve damar fonksiyonlarındaki düşüş karşılaştırılarak belirlenen hasta profillerinde tedavi sonuçları analiz edildi. Bu çalışma, fizyolojik farklılıkları olan hastalar tedavi seçeneklerini karşılaştırmada dinamik simülasyon modelleri kullanmanın potansiyel faydasını sundu. Granüler ampirik veriler elde etmek zor olsa da, klinik kullanımda bireyselleştirilmiş tedavilere yaklaşmak için bu gibi simülasyon modellerini kalibre etmek için kullanılabilirler. Bu çalışmanın devamı olarak, kişiselleştirilmiş tedavileri değerlendirmek için maliyet etkinliği ve bilgi değeri analiz edilebilir.

TABLE OF CONTENTS

LIST OF FIGURES

LIST OF TABLES

LIST OF ACRONYMS/ABBREVIATIONS

ACE-I	Angiotensin Converting Enzyme Inhibitor
ADH	Antidiuretic Hormone
Adj	Adjustment
ALD	Aldosterone
AT1	Angiotensin 1
AT2	Angiotensin 2
ARB	Angiotensin Receptor Blocker
BP	Blood Pressure
CCB	Calcium Channel Blocker
CNS	Central Nervous System
CO	Cardiac Output
ECF	Extracellular Fluid
EDV	End Diastolic Volume
Eff	Effect
ESV	End Systolic Volume
GFR	Glomerular Filtration Rate
HR	Hearth Rate
MAP	Mean Arterial Pressure
Na	Sodium
PNS	Parasympathetic Nervous System
RAAS	Renin–Angiotensin–Aldosterone System
RSNS	Renal Sympathetic Nervous System
SNS	Sympathetic Nervous System
SV	Stroke Volume
TBW	Total Body Water
TPR	Total Peripheral Resistance

1. INTRODUCTION

According to WHO, heart disease has remained the leading cause of death globally for the last 20 years. An estimated 17.9 million people died from cardiovascular diseases in 2019, accounting for 32% of global deaths [1]. Hypertension, also known as high or elevated blood pressure, is a medical condition that increases the risk of developing heart, brain, and kidney diseases. Therefore, it is considered the leading preventable risk factor for cardiovascular disease, premature death, and disability worldwide [2].

Hypertension is an important determinant of quality of life and premature death and is also highly prevalent. Estimates suggest that 1 in 3 adults has hypertension [3]. Moreover, the prevalence of the disease is rising globally due to the aging population and increases in unhealthy diets and sedentary lifestyles [4]. The number of people that suffer from hypertension has more than doubled globally during the last four decades, from 594 million in 1975 to 1.13 billion in 2015 [3].

The change in hypertension prevalence is not uniform in all regions. The prevalence of the disease in developed countries has improved over time yet worsened in low- and middle-income areas. Therefore, the burden of the disease has shifted from high-income to low-income countries [5]. Possible disparities in healthcare access make the problem all the more complicated, and the economic impact of hypertension cannot be overlooked. Direct healthcare expenses such as medications, tests, clinic visits, hospitalizations, and indirect costs of lost productivity due to premature mortality and disability add up to the financial burden of the disease [6]. It is estimated that the global financial toll of hypertension is 10% of overall global healthcare expenditure [7].

Hypertension is an ongoing problem in the modern world that significantly impacts well-being. Due to its high prevalence, contribution to premature death, and financial burden, it is an important global health challenge. Therefore in 2013, WHO Member States agreed on a global action plan to reduce the burden of avoidable noncommunicable diseases [1]. Two among nine global targets defined in the program directly focus on preventing and controlling cardiovascular diseases. One of them is to reduce the prevalence of hypertension by 25% by 2025. The second target is to be able to provide drug therapy and counseling to at least 50% of eligible people to avoid cardiovascular events. Nonetheless, these goals seem far to be achieved based on more recent reports, as the COVID-19 pandemic has disrupted hypertension management services in half of the countries around the world [8].

2. PROBLEM DEFINITION AND RESEARCH OBJECTIVES

According to the medical guidelines, hypertension is diagnosed when a person's systolic blood pressure is greater than 140 mm Hg; diastolic blood pressure is greater than 90 mm Hg on repeated examinations [9]. After hypertension is diagnosed, it is a treatable disease. There is a wide range of drugs used to treat high blood pressure, such as diuretics, angiotensin-converting enzyme inhibitors (ACE-I), angiotensin II-AT 1 receptor blockers (ARB), beta-blockers, calcium channel blockers (CCB). Furthermore, lifestyle improvements can prevent or delay the onset of the disease and enhance antihypertensive drug treatment [9].

Despite available treatment options, it is estimated that less than half of the patients get a diagnosis and treatment [3]. However, achieving blood pressure control is challenging even after being diagnosed and receiving treatment. A globally conducted meta-analysis indicates that only 40% of diagnosed and treated hypertension patients can reach therapeutic goals [10]. Even in the best-performing countries, target blood pressure was achieved by less than 70% of the patients [11]. Successful treatment rates in low-income and middle-income countries go as low as 9.6% [12]. As a result, it is estimated that fewer than 1 in 5 people have their problem under control [3].

Reasons behind this suboptimal control rate can be listed as the patient's non-adherence to lifestyle modifications and medical treatments, therapeutic inertia, and insufficient use of multiple drug combination strategies. Non-adherence, where a patient intentionally refuses to receive treatment or does not follow the prescribed treatment, is one of the main reasons for the poor control rate [9]. However, physician-related barriers, particularly therapeutic inertia, were also identified as significant challenges to achieving blood pressure control [13].

Therapeutic inertia occurs when a healthcare provider fails to initiate or intensify drug therapy in a patient with suboptimal blood pressure. The factors for clinical inertia include overestimation of possible care, insufficient training to achieve target pressure, and clinicians' avoidance of strengthening treatment [13]. Furthermore, it was shown that avoiding intensification and multiple drug combination strategies can harm patients' adherence to the treatment and patient-physician trust [14]. Therefore, adjusting therapy to a patient's needs is critical for a good treatment outcome.

Recommended treatment algorithm in high-impact medical guidelines [15, 16] is presented in Figure 2.1. Lifestyle modifications such as following a healthy diet, weight control, increased physical activity, and smoking cessation are the initial interventions for hypertension management. Yet, lifestyle modifications were found to be challenging to maintain, and often drug therapy is required [17].

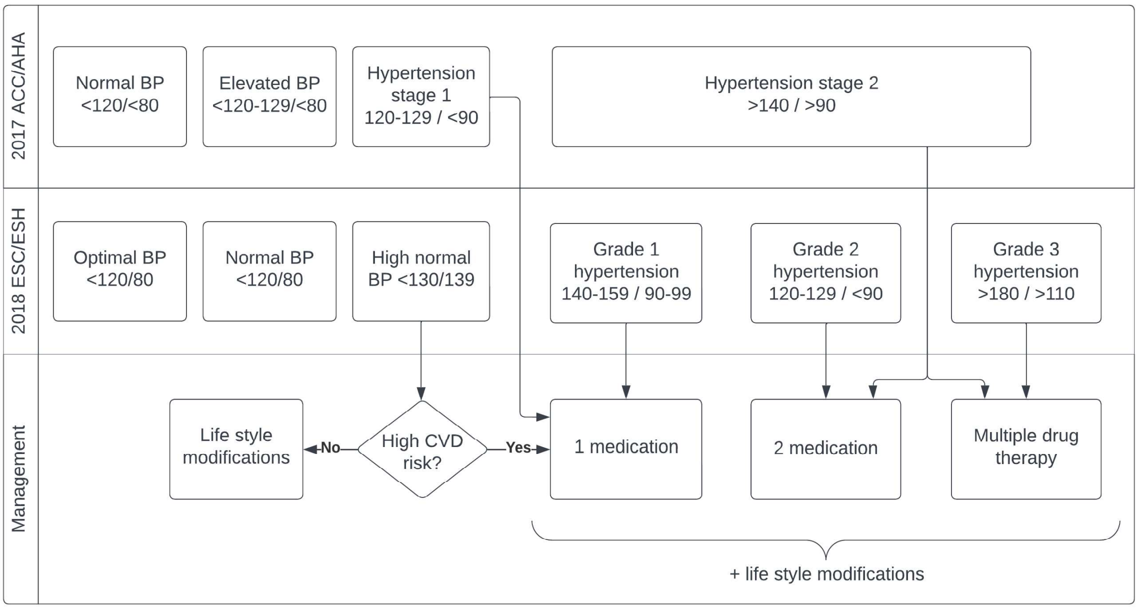

Figure 2.1. Hypertension treatment algorithm in medical guidelines (adopted from [15, 16]).

For a long time, prescribing monotherapy, a treatment that involves a single drug, has been considered the first treatment option for antihypertensive medications. However, monotherapy is often insufficient to achieve adequate blood pressure control in most patients. As a next step, previous guidelines suggested switching from one monotherapy to another, which was often ineffective and time-consuming [9].

One-fourth to one-third of patients cannot achieve therapeutic goals even with dual combination therapies, requiring more antihypertensive agents [18]. Recent studies on low-dose triple combination therapy have shown benefits among severe hypertension patients that could not be treated by dual therapy [19]. But the guidelines recommend multiple drug combination strategies only in persistent hypertension scenarios with a gradual increase [15, 16].

On the other hand, recent studies have demonstrated the benefits of low-dose drug combinations for first-line treatment over monotherapy. In a multi-year study, initiating treatment with a triple pill containing low doses of 3 antihypertensive drugs (ARB, CCB, diuretic) led to more patients achieving adequate blood pressure than usual care [19]. Starting and following a combination of antihypertensive therapy is associated with a more significant reduction of blood pressure, an earlier achievement of control, and higher therapeutic success rates [18, 20].

It can be concluded that there are alternative treatment strategies and various factors to treat hypertension successfully. Additionally, studies show that patients are more responsive to some classes of antihypertensive agents than others [21]. There is no one-fits-all treatment, and the debate over the best treatment approaches remains. These differential responses are observed due to inter-patient differences in hypertension pathophysiology [22]. Therefore, an incomplete understanding of the mechanisms involved in blood pressure control plays a role in suboptimal hypertension management [18].

Blood pressure control remains insufficient worldwide as the mechanisms regulating blood pressure are incredibly complex. Various interconnected subsystems are involved, including neural, hormonal, renal, cardiac, and vascular factors, operating on different time scales. More than sixty years ago, the mosaic theory for hypertension was proposed to express this complexity [23]. The partial failure of one or more control mechanisms can lead to suboptimal blood pressure as represented in Figure 2.2 [24, 25]. Moreover, in 90-95% of the patients, the direct cause of the disease is not identifiable [26], called primary hypertension. In this study, secondary hypertension, where the cause of the disease can be attributed to another medical condition such as renal artery stenosis, hyperthyroidism, or pregnancy, is left out of scope.

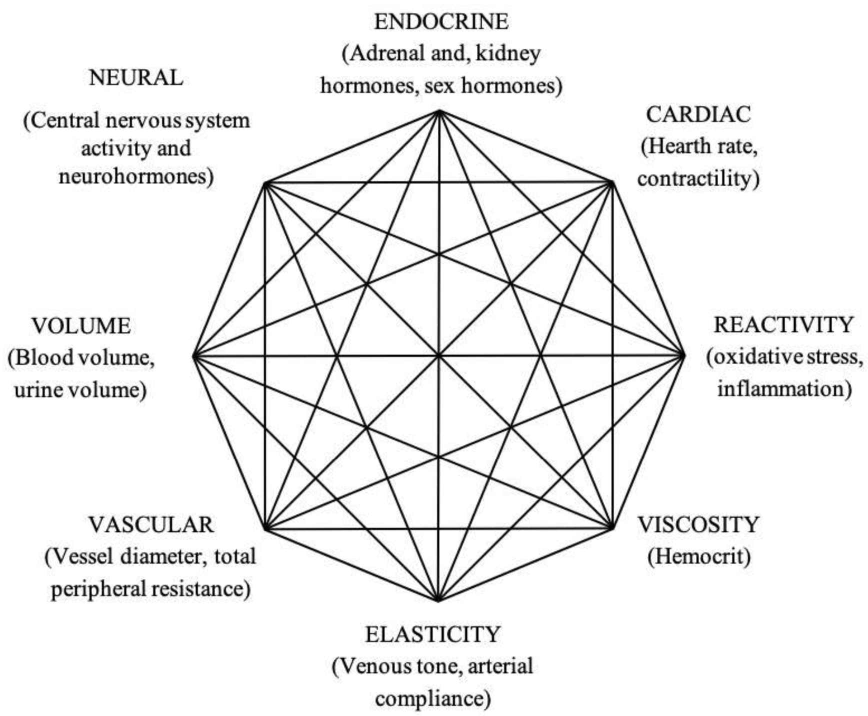

Figure 2.2. Systems responsible from blood pressure control (reproduced from [24,25]).

Hypertension has been a persistent public health problem despite healthcare interventions and research going back decades. Hypertension is manageable with simple lifestyle adaptations and medical treatments; however, achieving therapeutic goals remains challenging even in patients that receive diagnosis and treatment. The dynamic hypothesis of this study suggests that the optimal antihypertensive treatment strategies can vary for individuals due to inter-patient physiological variations. Consequently, instead of one fits all treatments, personalized treatments can offer improved results on therapeutic goals.

Modeling is an effective tool to evaluate different hypotheses, identify knowledge gaps, and propose new theories. Models are essential in understanding complex systems' quantitative relationships and feedback mechanisms. Modeling and computer simulations offer valuable contributions for studying physiological systems, such as demonstrating the system as a whole, providing a tool to be used in clinical settings and experimental design, enabling software-based teaching aid, and many more. Models enable making health predictions and testing treatment policies where empirical research on living beings is limited [25].

A hypertension physiological model can bring us closer to understanding regulatory mechanisms and help us improve treatment processes for patients. Also, it can be used to assess the value of individualized treatment. Furthermore, the patient subgroups most likely to suffer from a one-fits-all treatment practice can be identified. Hence, objective of this study is to build a physiological system dynamics model to evaluate long-term hypertension management with pharmacotherapy alternatives and their combinations. Furthermore, this study aims to demonstrate the potential use of simulation models and highlight the advantages of using such models.

3. LITERATURE REVIEW

The literature review focuses on the studies that develop models of cardiovascular mechanisms. Studies on these topics have addressed the problem in different methodologies and scopes. These studies are analyzed to identify important factors of the system, improve understanding of the relationships, and identify research gaps.

The literature review section consists of two sections. Firstly, mathematical models of blood pressure control mechanisms and the pathophysiology of hypertension are investigated. Later, system dynamics models on cardiovascular health are emphasized.

3.1. Mathematical Models

The cardiovascular system can be represented as a closed electrical circuit system, and the blood circulation follows fluid dynamics principles [27]. Models can be classified based on dimensions considered for the vessels. Zero-dimensional or lumped parameter models represent cardiovascular dynamics as a whole. Higher dimensional models consider factors such as capacitance, axial symmetry, and local flow in the vessels [28]. As this study aims to build a model on cardiovascular dynamics as a whole, lumped parameter models were focused on for the literature review.

Mathematical modeling in cardiology has a rich history, with the first known model dating back to the nineteenth century [29]. A significant milestone in the mathematical modeling of the cardiovascular system was the physiological model developed by Guyton *et al.* [30]. This comprehensive circulatory dynamics and regulation model includes eighteen subsystems: kidneys, lungs, metabolism, and autonomics. The model built by Guyton *et al.* has been the basis for numerous studies and is still used with modifications and expansions.

In further studies, the authors used the model to study arterial pressure [31] and its effects on hypertension [32, 33]. Also, the model was developed further by other authors [34–37].

Later, discoveries in physiology showed that in the Guyton model the role of the central nervous system was lacking [38, 39]. Also, one of the main assumptions of the Guyton model is that arterial pressure solely determines the kidney's ability to remove sodium. However, later this idea was challenged by pointing out that other physiological mechanisms also had involvement [40].

Based the paradigm shift from kidney focus, Averina *et al.* [41,42] and Karaaslan *et al.* [43, 44] developed mathematical models that emphasized the importance of the central nervous system on blood pressure regulation. Furthermore, in recent years, mathematical models started to focus on factors affecting arterial function loss, such as inflammation, as hypotheses for hypertension pathophysiology [45–47].

As this study aims to evaluate drug therapies for blood pressure regulation, mathematical models that include pharmacodynamics are analyzed [48, 49]. Furthermore, the scope of this study is hypertension dynamics over years of models. Therefore, models that included related elements, such as arterial stiffening [50] and compliance loss [51, 52], were also reviewed.

Also, some mathematical models in the literature focus on more specific conditions such as pulmonary hypertension [53, 54], intracranial hypertension [55, 56], and portal hypertension [57, 58]. Due to hormonal differences, blood pressure regulation mechanisms vary among male and female patients. Even though most hypertension models in the literature are gender-neutral, some mathematical models take sexual dimorphism into account [59]. However, these factors were left out of the scope of this study.

3.2. System Dynamics Models

System dynamics applications in healthcare can be classified under three main groups [60]. The first category includes models on administrative concerns of healthcare management. The second model group is developed to challenge regional community public health concerns. In the last group of studies, the models are focused on a specific disease. While modeling a particular disease, the problem can be handled as a population concern or at an individual physiological level. Based on this classification, system dynamics models on cardiovascular health are examined in Table 3.1.

Table 3.1. System dynamics models on cardiovascular health.

Reference	**Topic**	**Model focus**
[61]	Myocardial infarction	Population
[67]	Heart failure	Population
[71]	Risk factors for cardiovascular health	Population
[62–65, 72]	Cardiovascular interventions and health outcomes	Population
[73]	Weight related cardiovascular problems	Population
[75]	Hypertension and other chronic diseases	Population
[69]	Stroke	Population
[66]	Myocardial infarction	Population
[74]	Environment and cardiovascular problems	Population
[76]	Hypertension and chronic kidney disease	Population
[77]	Hypertension and cardiovascular outcomes	Population
[78]	Hypertension	Physiological
[79]	Hypertension and kidney damage	Physiological
[80]	Sleep apnea and blood pressure	Physiological
[70]	Blood cholesterol	Physiological
[68]	Heart failure	Physiological
[81]	Disorders of the body water mechanism	Physiological

System dynamics modeling is often used to address public health problems and interventions, including cardiovascular diseases. The first applications of system dynamics on cardiovascular health date back to the 1980s [61]. Later, many other models were developed to define risk factors, propose policies, and compare interventions based on casualties and costs [62–65].

Some of the studies focus on a specific cardiovascular disorder such as; myocardial infarction [61, 66], heart failure [67, 68], stroke [69], and blood cholesterol [70]. In contrast, other studies in the literature analyze all cardiovascular diseases and risk factors collectively [62–65, 71, 72]. Alternatively, cardiovascular diseases can be investigated by focusing on specific risk factors such as unhealthy diet, overweight [73], and environmental stress [74].

Hypertension is one of the common public health concerns; therefore, it has been a popular element to be included in system dynamics models. Hypertension is integrated into studies investigating chronic and cardiovascular diseases [75] as a group. Some studies examine the relationship of hypertension [62–65] with other conditions and risk factors such as diabetes and smoking [76, 77].

The first system dynamics model that considers hypertension from a physiological perspective dates back to the 1980s [78]. Incioglu [79] modeled long-term hypertension and its effect on kidney function. Even though it is the most comprehensive physiological model that captures long-term blood pressure dynamics, it does not include the central nervous system control mechanism.

Ozgun [80] built a physiological model to investigate sleep apnea's impact on hypertension over months. The model consists of the effects of both nervous and renal system activities. Other physiological models of cardiovascular health include heart failure dynamics [68] and body water mechanism disorders [81].

3.3. Findings from the Literature Review

Because of the significance of hypertension, it has been a popular area of study in mathematical modeling. However, proposed mathematical models on hypertension often model the pathophysiology of hypertension rather than modeling the treatment and management of the disease. Very few models include medical interventions [49], yet they do not investigate the long-term dynamics of treatment. In Table 3.2, related research in the literature are identified and compared with this study.

Table 3.2. Comparison of the study with the literature.

Study	**Time**	**Renal system**	**Nervous system**	**Vascular function**	**Treatment**
This study	years	✓	✓	✓	✓
[30]	days	✓			
[44]	days	✓	✓		
[42]	days	✓	✓		
[50]	years	✓	✓	✓	
[49]	weeks	✓	✓		✓
[68]	weeks	✓	✓		✓
[79]	years	✓			✓
[81]	days	✓			
[80]	weeks	✓	✓		✓

Due to the sheer number of feedback loops and interconnected mechanisms involved in blood pressure regulation, the system dynamics modeling approach can be beneficial. Most hypertension studies using system dynamics models tackle the problem at the population level as a public health problem. Limited system dynamics models consider cardiovascular diseases in the literature on an individual patient level [68, 70, 79, 80].

Even though some of these cardiovascular models include common mechanisms with blood pressure regulation [68, 80], they focus on the short-term dynamics considering a time frame of days. System dynamics study in the literature focusing on hypertension over the years only captures the renal regulation mechanisms and does not consider treatment alternatives [79].

It can be concluded that there is a gap in the literature for a system dynamics model that comprehensively includes physiological mechanisms of blood pressure regulation and treatment alternatives in the long run. However, previous models in the literature will guide this study in formulation, parametrization, and validation aspects.

4. OVERVIEW OF THE MODEL

The model consists of four sectors; cardiovascular, central nervous system, renal, and treatment sector. In this section, the model development process is explained, then the model overview is presented, and finally, the mathematical formulations of the model and equations are described in detail. Furthermore, the physiological and medical background for model assumptions and simplifications are elucidated.

Complete list of equations is provided in the Appendix A and the visualization that includes all sectors and variables is given in the Appendix B.

4.1. Model Development

The purpose of this model is to capture physiological mechanisms that lead to essential hypertension and long-term blood pressure dynamics in response to pharmacological treatments. While building the model's structure, physiology books were initially used [82–84]. Later it was revised by two subject matter experts, one specializing in cardiology and the other in physiology. Based on the experts' feedback, the model structure was modified and presented to them in follow-up interviews. This iterative process was followed until the experts confirmed that the model could capture long-term essential hypertension feedback mechanisms observed in clinical practice.

In the model development process, guidelines set for system dynamics were followed [85, 86]. Unit consistency was considered during the model-building process in all equations. Equations, parameter values, and graphical functions are defined according to the information obtained from the literature and established mathematical models [32,33,43,44]. A complete list of equations is given in Appendix A. The Vensim DSS 9.3.3 software was used for modeling and simulation. The time unit of the model is one day, and the time step is selected as 0.0625.

4.2. Overview of the Model

Blood vessels carry blood from the heart to the body with each heartbeat. With the contraction of the hearth, pumped blood applies a force into the vessels. Blood pressure is the force applied by circulating blood against the walls of the arteries. Mean arterial pressure, the average systolic and diastolic pressure over time represents this force. Systolic blood pressure occurs when the heart contracts or beats, whereas diastolic blood pressure occurs when the heart rests between beats.

Many mechanisms impact mean arterial pressure; however, two immediate factors are total peripheral resistance and cardiac output. Total peripheral resistance is the amount of force exerted on circulating blood by the vessels. Cardiac output, the amount of blood pumped by the heart each minute, creates a pressure gradient between arteries and veins that drives the flow through the vascular system.

Various factors are involved in regulating total peripheral resistance and cardiac output. The central nervous and renal systems are the main systems responsible for keeping blood pressure at desired levels. Therefore, the model includes two main balancing feedback structures, B1-a, B1-b, B2-a and B2-b, as given in Figure 4.1.

The variables in boxes represent stock variables in the model. These variables have inertia and to change their values a there is a longer delay. Balancing feedback loops B1-a and B1-b include mechanisms of the central nervous system. Baroreceptors detect blood pressure changes and deliver these signals to the central nervous system. If the pressure is elevated, the parasympathetic system is activated, and the sympathetic system is inhibited.

Loop B1-a represents the effect of the nervous system on cardiac output. The sympathetic nervous system can increase heart rate, causing an elevation in cardiac output. It can also increase contractility, stretching the heart muscle and increasing cardiac output with more vigorous contractions. Loop B1-b represents the effect of the nervous system on total peripheral resistance. Activating the sympathetic nervous system can increase peripheral resistance by constricting the vascular walls.

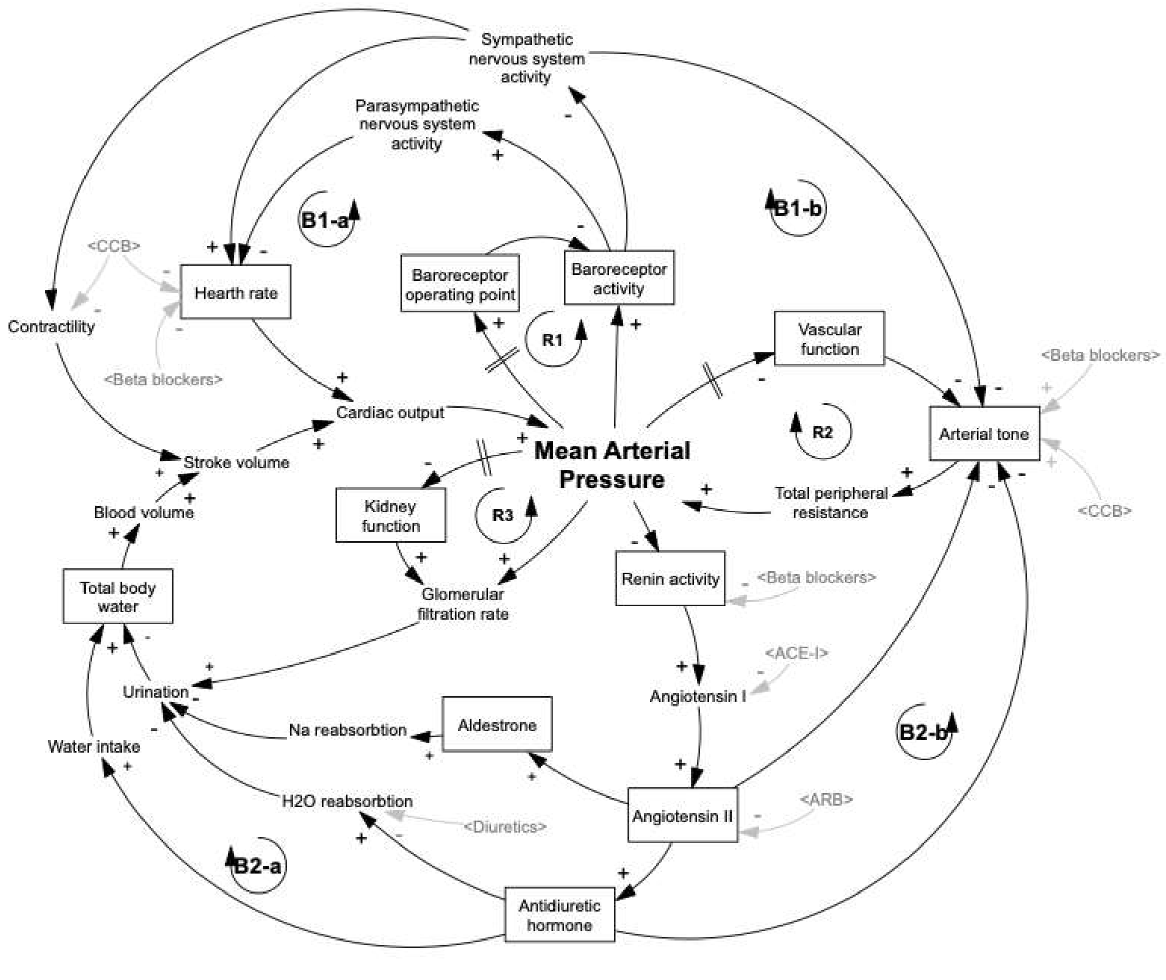

Figure 4.1. Causal loop diagram of the model.

Balancing feedback loops B2-a and B2-b include mechanisms of the renal system. The kidneys also detect changes in blood pressure. With higher blood pressure, the perfusion pressure in the kidneys increases and causes the kidneys to filter more blood. Also, based on perfusion pressure, specialized cells in the kidney regulate their activity to produce an enzyme called renin. Activation of the renin enzyme triggers the renin-angiotensin-aldosterone system (RAAS).

Loop B2-a represents the effect of the renal system on cardiac output. Through filtration rate and hormones that affect permeability, kidneys reabsorb or remove water from the body. An increase in total body water cause expansion of blood volume, delivering more blood to the heart, and thus also increasing cardiac output. Loop B2-b represents the effect of the renal system on total peripheral resistance. When the renin-angiotensin-aldosterone system is activated it produces hormones that constrict vascular walls, thereby increasing peripheral resistance.

These balancing structures deteriorate with old age, and the body finds balance at higher blood pressure levels. When hypertension is not treated, high blood pressure causes the breakdown process to accelerate. The model includes three main reinforcing feedback structures given R1, R2, and R3, as shown in Figure 4.1.

Loop R1 is called baroreceptor resetting, where receptors become desensitized to elevation in blood pressure. Therefore, the mechanisms that lower blood pressure is not activated. Loop R2 is the arterial stiffening. Due to endothelial dysfunction, vessels remain constricted and lose their elasticity. Arterial stiffening increases total peripheral resistance and further increases blood pressure. Loop R3 is the kidney function loss. It decreases the kidney's ability to remove water from the body and causes a further increase in cardiac output and blood pressure. In Figure 4.1, hypertension medication alternatives and their acting points have been demonstrated in a lighter color. Overall there are five classes of medication: Calcium Channel Blockers (CCB), Angiotensin receptor blockers (ARB), Angiotensin Converting Enzyme Inhibitors (ACE-I), Beta-blockers, and Diuretics.

The diversity in pathophysiology occurs as the strength of the control loops is not identical among patients. Therefore, response to the treatment differentiates by individuals. Pharmacological interventions can be planned at multiple leverage points. Because of inter-patient differentiation, optimal antihypertensive treatment strategies can vary.

4.3. Cardiovascular Sector

The cardiovascular sector of the model includes the mechanisms of the heart and blood vessels. The stock-flow diagram of the cardiovascular sector is shown in Figure 4.2. Stock and flow variables in the cardiovascular sector are given in Table 4.1.

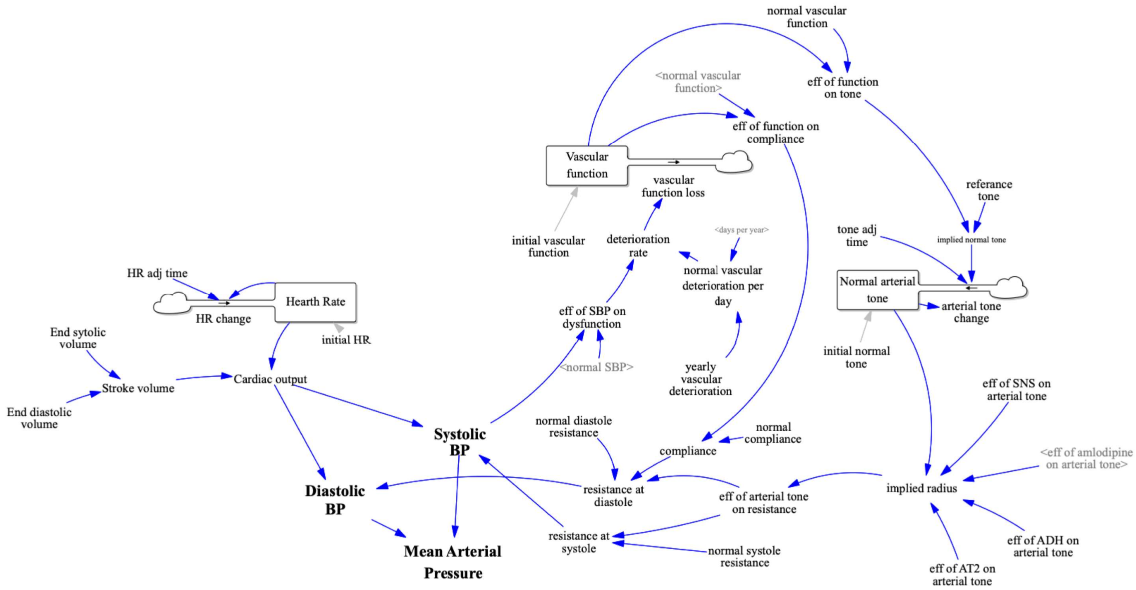

Figure 4.2. Stock flow diagram of cardiovascular sector.

Table 4.1. Stock and flow variables in the cardiovascular sector.

Variable	**Type**	**Unit**
arterial tone change	Bi-flow	1/Day
HR change	Bi-flow	beat/min/Day
vascular function loss	Outflow	1/Day
Hearth Rate	Stock	beat/min
Normal arterial tone	Stock	Dmnl
Vascular function	Stock	Dmnl

The heart's contraction is called systole, and the relaxation of the heart is called diastole. Blood pressure is at its highest in systole and lowest in diastole. *Mean Arterial Pressure (MAP)* is the average force applied by circulating blood against the walls of the arteries in one cardiac cycle. It is calculated with the formulation

$$Mean\ Arterial\ Pressure\ (MAP) \ = \frac{Systolic\ BP + 2 \times Diastolic\ BP}{3}. \tag{4.1}$$

The potential pressure difference in the hearth is the driving force that creates blood flow. In physiology Ohm's law is used to quantify this principle. *Blood pressure* is determined by blood flow and the total resistance of the blood vessels. The blood pressure at the systole is calculated considering the resistance differences and it can be written as

$$Systolic\ BP \ = \ (Cardiac\ output) \times (Resistance\ at\ systole). \tag{4.2}$$

Similarly, the blood pressure at diastole stage is also calculated considering the resistance differences and it can be written as

$$Diastolic\ BP \ = \ (Cardiac\ output) \times (Resistance\ at\ diastole). \tag{4.3}$$

Cardiac output can be explained as the amount of blood pumped by the heart in a minute. It is defined by two factors: hearth rate and stroke volume. *Heart rate* is the number of times the heart contracts in one minute. The volume of blood pumped by the heart in each beat is called *Stroke volume*. The mathematical formulation for cardiac output can be written as

$$Cardiac\ Output \ = \ (Hearth\ rate) \times (Stroke\ volume). \tag{4.4}$$

The heart rate can adapt to daily changes rather quickly. However, it takes longer for the mean resting heart rate to change as it has inertia. The average resting heart rate variability is three beats per week [87]. Therefore, in the model, the heart rate is represented with a stock with a bi-flow and , its formulation can be expressed as

$$Hearth\ Rate(t) \ = (initial\ HR) \times (t - dt) + (HR\ change) \times dt. \tag{4.5}$$

The parasympathetic and sympathetic nervous systems regulate implied heart rate, which will be explained in more detail in the central nervous system sector. The change in heart rate is controlled by the difference in implied and actual heart rate. This change is expressed as

$$HR\ change \ = \frac{(implied\ heart\ rate - Hearth\ Rate)}{HR\ adj\ time}. \tag{4.6}$$

End diastolic volume is the amount of blood filled in the left ventricle during the relaxation stage of the heart right before the contraction. End systolic blood volume is the remaining blood in the left ventricle after the heart has contracted. The difference in the volume before and after the contraction is pumped out of the heart into the arteries. Hence, the *Stroke Volume* can be calculated as

$$Stroke\ Volume \ = \ (End\ Diastolic\ Volume) - (End\ Systolic\ Volume). \tag{4.7}$$

End diastolic volume depends on venous return, the amount of blood carried to the hearth. It is a function of blood volume.

The effect of blood volume will be explained in more detail in the renal sector section. The contractility of the hearth can control end-systolic volume. The sympathetic nervous system acts on the heart to decrease systolic volume by increasing the contractility of the heart. The effects of the sympathetic nervous system will be explained in more detail in the central nervous system sector.

After the cardiac output, the total peripheral resistance is the second factor that directly affects mean arterial pressure. The normal value of the resistance at systole changes with the effect of arterial tone which can be expressed as

$$\begin{aligned} resistance\ at\ systole = {} & (eff\ of\ arterial\ tone\ on\ resistance) \\ & \times (normal\ systole\ resistance). \end{aligned} \tag{4.8}$$

Similar to the systole, the normal value of the resistance at diastole also changes with the effect of arterial tone. The resistance at diastole can be expressed as

$$\begin{aligned} resistance\ at\ diastole = {} & (normal\ diastole\ resistance) \\ & \times (eff\ of\ arterial\ tone\ on\ resistance) \times compliance. \end{aligned} \tag{4.9}$$

Resistance has a positive relationship with the velocity and length of the vessels. Resistance is inversely related to the fourth power of the arterial radius. The Hagen–Poiseuille law in Equation (4.10) is adapted to quantify arterial resistance [83] which can be expressed as

$$Resistance = \frac{8 \times velocity \times length}{\pi \times \Delta\ pressure \times radius^4}. \tag{4.10}$$

The diameter of arteries is determined by smooth muscle constriction. The degree of smooth muscle constriction exhibited at the basal state is referred to as normal arterial tone. Arterial tone given at a given time is defined as implied arterial tone.

The relationship between implied arterial tone, normal arterial tone and other factors effecting it can be expressed as

$$\begin{aligned} Implied\ radius = {} & (Normal\ arterial\ tone) \\ & \times (eff\ of\ SNS\ on\ arterial\ tone) \\ & \times (eff\ of\ AT2\ on\ arterial\ tone) \\ & \times (eff\ of ADH\ on\ arterial\ tone). \end{aligned} \tag{4.11}$$

Sympathetic nervous system activity, angiotensin II and antidiuretic hormones affect the arterial tone. With the action of these mechanisms, arteries respond with vasoconstriction or vasodilation. The effect of the sympathetic nervous system will be explained in more detail in the central nervous system sector. The effect of angiotensin II and antidiuretic hormone will be presented in more detail in the renal sector.

When the arteries constrict and the implied radius decreases, the total peripheral resistance increases as formulated in Equation (4.10). The velocity changes with the number of blood cells, and length changes with an increase in body mass. Hypertension caused by a difference in the velocity and length of the arteries is classified as secondary hypertension. These factors are left out of the scope of this model for simplification. The effect of the radius or arterial tone on resistance is emphasized as

$$eff\ of\ arterial\ tone\ on\ resistance\ = \frac{1}{implied\ radius^4}. \tag{4.12}$$

Aging arteries undergo changes in diameter, wall thickness, stiffness, and endothelial function [88]. These age-dependent changes increase the risk of the development and progression of cardiovascular diseases [89].

Alterations in the functional and structural properties of arteries lead to impaired vascular tone and reduced arterial compliance [90, 91]. Arterial tone can be defined as the degree of active constriction of vessels [92]. Arterial compliance refers to the change in area, diameter, or volume of an artery in response to a change in pressure [93].

Whether endothelial dysfunction is a cause or an effect of hypertension is still controversial, and possibly there is a bidirectional relationship [94]. However, emerging evidence indicates that age-dependent changes are accelerated in the presence of hypertension [88]. The severity of hypertension is positively related to the degree of impairment of endothelial function [95].

Vascular function has inertia therefore, it is modeled as a stock variable. As functional loss is irreversible, there is only an outflow from the stock. The relationship of vascular function and its loss over time can be expressed as

$$\begin{aligned} Vascular\ function(t) = (initial\ vascular\ function) \times (t - dt) \\ - (vascular\ function\ loss) \times dt. \end{aligned} \tag{4.13}$$

With aging, vascular function is lost at a certain deterioration rate. Vascular function loss is equal to the deterioration rate, and the deterioration rate is effected by the systolic blood pressure which can be expressed as

$$\begin{aligned} vascular\ deterioration\ rate = (normal\ vascular\ deterioration\ per\ day) \\ \times (eff\ of\ SBP\ on\ dysfunction). \end{aligned} \tag{4.14}$$

The rate of deterioration is increased by elevated blood pressure. The graphical function of the effect of systolic blood pressure on dysfunction is given in Figure 4.3. This function is presented based on the relationship identified in the literature [96, 97].

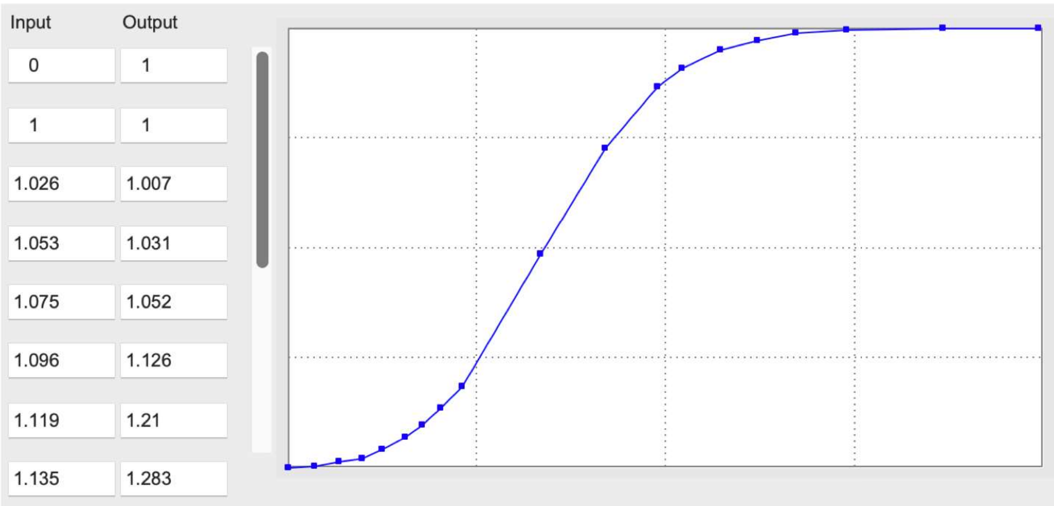

Figure 4.3. Graphical function for the effect of systolic blood pressure on dysfunction.

The graph in Figure 4.3 is drawn by normalizing systolic blood pressure to its reference value which can be computed as

$$eff\ of\ sbp\ on\ dysfunction = f(\frac{Systolic\ BP}{normal\ SBP}). \tag{4.15}$$

Increased vascular smooth muscle tone is one of the primary factors of age-associated blood pressure elevation [98].

The smooth muscle tone or normal arterial tone has inertia and takes a long time to change. Therefore, in the model, normal arterial tone is represented with a stock with a bi-flow. The value of normal arterial tone can be calculated by its initial value and change over time; which can be expressed as

$$\begin{aligned} Normal\ arterial\ tone(t) = initial\ normal\ tone \times (t - dt) \\ + (\ arterial\ tone\ change) \times dt. \end{aligned} \tag{4.16}$$

The change in normal arterial tone is controlled by the difference between a reference value for a healthy person value and the implied value at a given vascular function. The relationship can be formulates as

$$\begin{aligned} arterial\ tone\ change = \frac{reference\ tone \times eff\ of\ function\ on\ tone}{tone\ adj\ time} \\ - \frac{Normal\ arterial\ tone}{tone\ adj\ time}. \end{aligned} \tag{4.17}$$

The effect of vascular function loss on normal arterial tone is represented in graphical function based on literature and expert opinion. The graphical function of the effect of vascular function on normal tone is given in Figure 4.4.

The graph in Figure 4.4 is drawn by normalizing the vascular function to its value which can be calculated as

$$eff\ of\ vascular\ function\ on\ tone = f(\frac{Vascular\ function}{normal\ vascular\ function}). \tag{4.18}$$

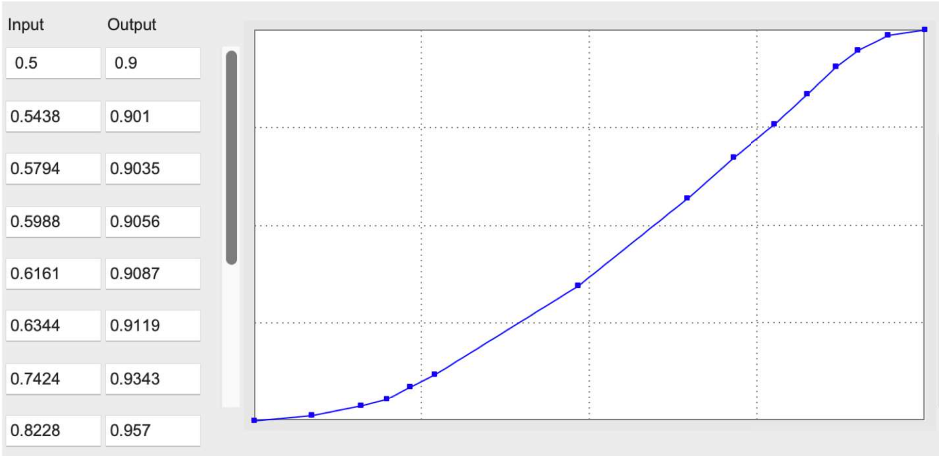

Figure 4.4. Graphical function for the effect of vascular function on normal arterial tone.

Due to the rise in arteriolar resistance, both systolic and diastolic pressure increase. However, diastolic blood pressure tends to decrease later in life. The large artery stiffening in older ages causes to decrease in compliance. As less elastic recoil supports the diastolic pressure, stiff arteries result in lower diastolic pressure with old age [99].

A decrease in compliance reduces resistance at the diastole hence the blood pressure. This effect is formulated in Equation (4.9). The change in compliance is observed over the long term due to vascular function loss.

The relationship of compliance depending on the its normal value and the effect of vascular function can be expressed as

$$compliance = (healthy\ compliance) \times (eff\ of\ function\ on\ compliance). \quad (4.19)$$

The effect of vascular function loss on compliance is represented in graphical function based on literature and expert opinion. The graphical function of the effect of vascular function on compliance is given in Figure 4.5.

The graph in Figure 4.5 is drawn by normalizing the vascular function to its normal value which can be expressed as

$$eff\ of\ vascular\ func.\ on\ compliance = f(\frac{Vascular\ function}{normal\ vascular\ function}). \quad (4.20)$$

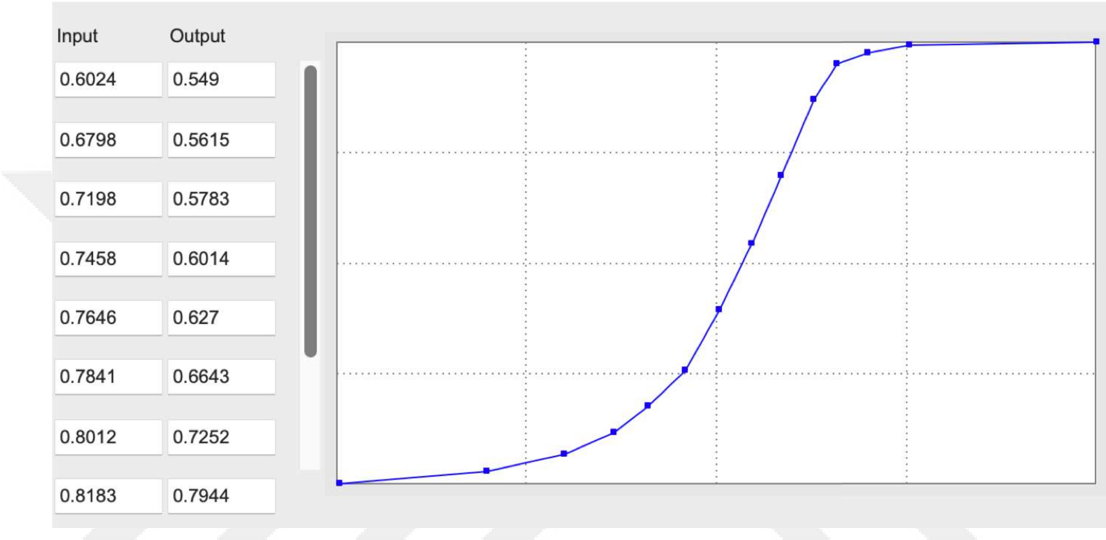

Figure 4.5. Graphical function for the effect of vascular function on compliance.

At the beginning of the simulation the stock variables have initial values. Furthermore some of the formulations use constant values. The constants and initial values used in the cardiovascular sector are given in Table 4.2.

4.4. Central Nervous System Sector

This section examines the blood pressure regulation mechanism controlled by the central nervous system. The central nervous system sector of the model includes the mechanisms of baroreceptors, sympathetic and parasympathetic nervous system activities, and their effects on the cardiovascular sector. Stock, and flow variables in the central nervous system sector are given in Table 4.3.

Table 4.2. Constants and initial values in cardiovascular sector.

Variable name	**Unit**	**Value**
HR adj time	Day	3
normal compliance	Dmnl	1
normal diastole resistance	mmhg*min/ml	0.0133
normal EDV	ml/beat	120
normal ESV	ml/beat	40
normal HR	beat/min	75
normal SBP	mmhg	120
normal systole resistance	mmhg*min/ml	0.02
normal vascular function	Dmnl	1
referance tone	Dmnl	1
reference MAP	mmhg	93.3
tone adj time	Day	60
initial HR	beat/min	75
initial normal tone	Dmnl	1
initial vascular function	Dmnl	1
EDV adjustment time	Day	1
yearly vascular function deterioration	Dmnl/year	0.0035

The central nervous system plays a vital role in regulating blood pressure. This mechanism is triggered by sensors that monitor blood pressure called baroreceptors. Baroreceptors are located on blood vessels. When pressure increases, the arteries stretch and stimulate the nerve fibers that connect to the central nervous system. The activity of these nerve fibers is monitored and compared with a set point for arterial pressure [83]. However, baroreceptors can become desensitized to chronic elevation in pressure and reset to higher pressure [83]. Resetting reduces the firing rate at normal levels of mean arterial pressure. Hence, to reach the previous firing rate, higher blood pressure is required.

Table 4.3. Stock and flow variables in the central nervous system sector.

Variable	**Type**	**Unit**
baroreceptor activity change	Bi-flow	burst/ms/Day
change in baroreceptor operating point	Bi-flow	mmhg/Day
Baroreceptor activity	Stock	burst/ms
Baroreceptor operating point	Stock	mmhg

The resetting can happen in an acute phase, such as exercise or chronic phase hypertension, heart failure, and other disease states [100]. Baroreceptor operating point for mean arterial pressure is modeled as a stock variable due to its intertia. The normal arterial pressure for the baroreceptors has an initial set value called the operating point that can change over time. The change of baroreceptor operating point over time can be expressed as

$$\begin{aligned} Baroreceptor\ operating\ point(t) = {} & (initial\ operating\ point) \times (t - dt) \\ & + (change\ in\ operating\ point) \times dt. \end{aligned} \tag{4.21}$$

The change in baroreceptor operating point is represented with a bi-flow as it can increase or decrease over time through the same mechanism.

The gap between the mean arterial pressure and baroreceptor operating point closes over time. This relationship between the change in baroreceptor operating point and mean arterial pressure can be calculated as

$$\begin{aligned} change\ in\ operating\ point = {} & \frac{Mean\ Arterial\ Pressure}{operating\ point\ adj\ time} \\ & - \frac{Baroreceptor\ operating\ point}{operating\ point\ adj\ time}. \end{aligned} \tag{4.22}$$

An increase in blood pressure increases the baroreceptor firing rate at a given mean arterial pressure. Maximal sensitivity occurs near the normal mean arterial pressure.

The stock-flow diagram of the central nervous system is shown in Figure 4.6.

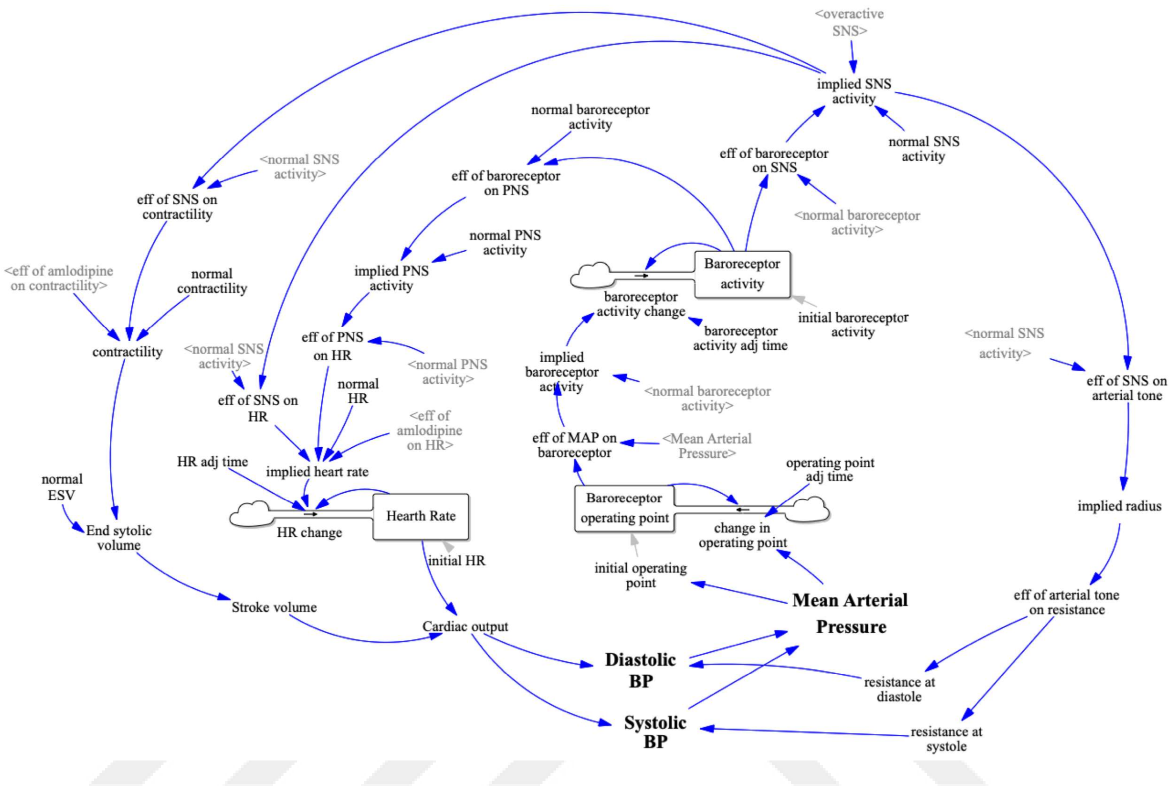

Figure 4.6. Stock flow diagram of the central nervous system sector.

Deviations from this operating point change the baroreceptor firing frequency and result in the activation or deactivation of control systems [83]. The graphical function for the effect of mean arterial pressure on baroreceptor activity is given in Figure 4.7. The effect of mean arterial pressure is represented in a graphical function based on the literature [101,102]. The graph in Figure 4.7 is drawn by normalizing the mean arterial pressure to its reference value. This value can be calculated as

$$eff\ of\ MAP\ on\ baroreceptor = f(\frac{Mean\ Arterial\ Pressure}{Normal\ MAP}). \tag{4.23}$$

Baroreceptor activity is modeled as a stock variable with a bi-flow as it can increase or decrease over time through the same mechanism.

The baroreceptor activity change from its baseline value over time can be calculated as

$$Baroreceptor\ activity(t) = (initial\ baroreceptor\ activity) \times (t - dt) + (baroreceptor\ activity\ change) \times dt. \tag{4.24}$$

The gap between the implied baroreceptor and base activity levels closes over time. This process happens over an adjustment which can be expressed as

$$baroreceptor\ activity\ change = \frac{(implied\ baroreceptor\ activity)}{(baroreceptor\ activity\ adj\ time)} - \frac{(Baroreceptor\ activity)}{(baroreceptor\ activity\ adj\ time)}. \tag{4.25}$$

The baroreceptor activity regulates implied parasympathetic system activity at a given time.

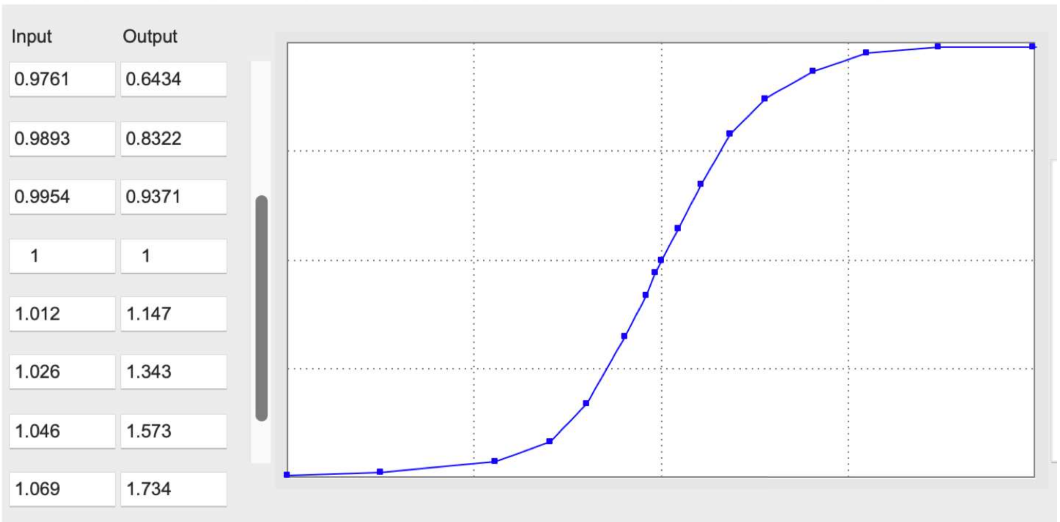

Figure 4.7. Graphical function for the effect of mean arterial pressure on baroreceptor activity.

The implied parasympathetic at a given time depending on its normal value and the baroreceptor activity can be calculated as

$$implied\ PNS\ activity = (normal\ PNS\ activity) \\ \times (eff\ of\ baroreceptor\ on\ PNS). \tag{4.26}$$

The graphical function representing the effect of baroreceptor activity on parasympathetic nervous system activity is given in Figure 4.8. The effect of baroreceptor activity represented in the graphical function is based on expert opinions. The graph in Figure 4.8 is drawn by normalizing baroreceptor activity to its reference value which can be calculated as

$$eff\ of\ baroreceptor\ on\ PNS = f(\frac{Baroreceptor\ activity}{normal\ baroreceptor\ activity}). \tag{4.27}$$

With the activation of the parasympathetic control center, the vagus nerve is stimulated to decrease the heart rate [83]. Studies showed that the heart rate decreased progressively with increased intensity of parasympathetic system activation [103].

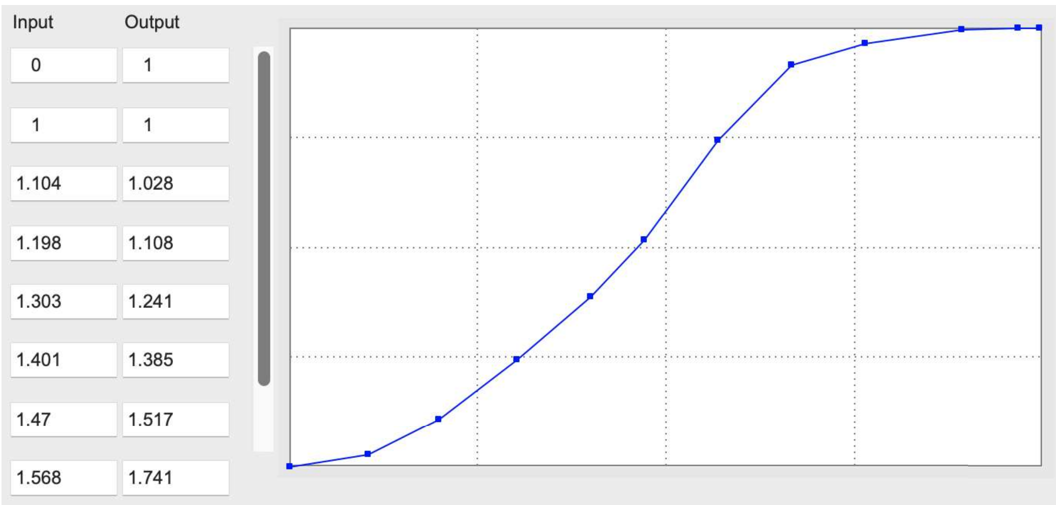

Figure 4.8. Graphical function for the effect of baroreceptor activity on parasympathetic nervous system activity.

The graphical function for the effect of parasympathetic nervous system activity on heart rate is given in Figure 4.9. The effect of nervous system activity on heart rate is represented by findings in the literature [103, 104].

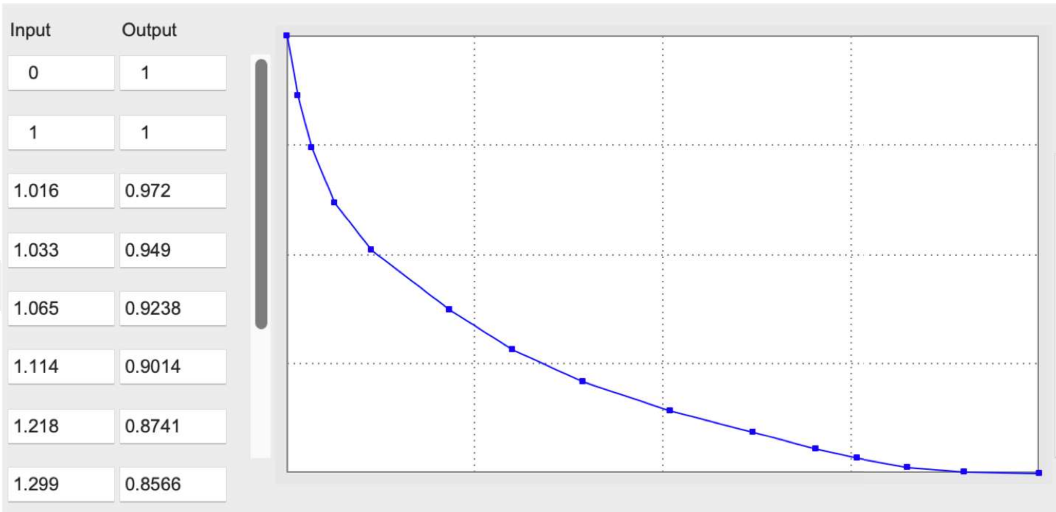

Figure 4.9. Graphical function for the effect of parasympathetic nervous system activity on heart rate.

The graph in Figure 4.9 is drawn by normalizing baroreceptor activity to its reference value which can be calculated as

$$eff\ of\ PNS\ on\ HR = f(\frac{implied\ PNS\ activity}{normal\ PNS\ activity}). \tag{4.28}$$

Similarly to the parasympathetic system, baroreceptor activity regulates the implied sympathetic system activity. The implied sympathetic at a given time depending on its normal value and the baroreceptor activity can be calculated as

$$\begin{aligned} implied\ SNS\ activity = (&normal\ SNS\ activity) \\ &\times (eff\ of\ baroreceptor\ on\ SNS). \end{aligned} \tag{4.29}$$

The graphical function for the effect of baroreceptor activity on sympathetic nervous system activity is given in Figure 4.10. The effect of baroreceptor activity represented in the graphical function is based on expert opinions. The graph in Figure 4.10 is drawn by normalizing baroreceptor activity to its reference value which can be calculated as

$$eff\ of\ baroreceptor\ on\ SNS = f(\frac{Baroreceptor\ activity}{normal\ baroreceptor\ activity}). \tag{4.30}$$

At higher levels of blood pressure, the activity of the sympathetic control center is inhibited. However, when blood pressure drops below a certain level, the sympathetic nervous system acts to increase the heart rate. However, in certain types of hypertension, the central nervous system becomes over-active and appears to seek a higher blood pressure level [105]. Therefore, the activity of the sympathetic nervous system is included in the model.

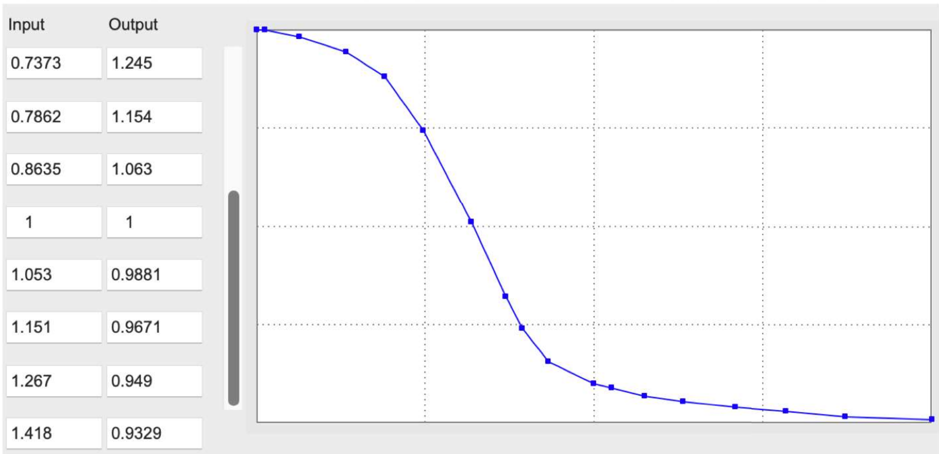

Figure 4.10. Graphical function for the effect of baroreceptor activity on sympathetic nervous system activity.

The sympathetic nervous system works opposite to the parasympathetic system. It has a positive chronotropic effect on the heart, meaning that it can act to increase the heart rate.

The graphical function for the effect of sympathetic nervous system activity on heart rate is given in Figure 4.11. The effect of nervous system activity on heart rate is represented by findings in the literature [103, 104]. The graph in Figure 4.11 is drawn by normalizing baroreceptor activity to its reference value which can be calculated as

$$eff\ of\ SNS\ on\ HR = f(\frac{implied\ SNS\ activity}{normal\ SNS\ activity}). \tag{4.31}$$

Both parasympathetic and sympathetic systems stimulate SA and AV nodes in the heart to regulate heart rate. Moreover, the sympathetic nervous system also has nerve endings at the left ventricle of the heart; hence it also controls the contractility of the heart [106].

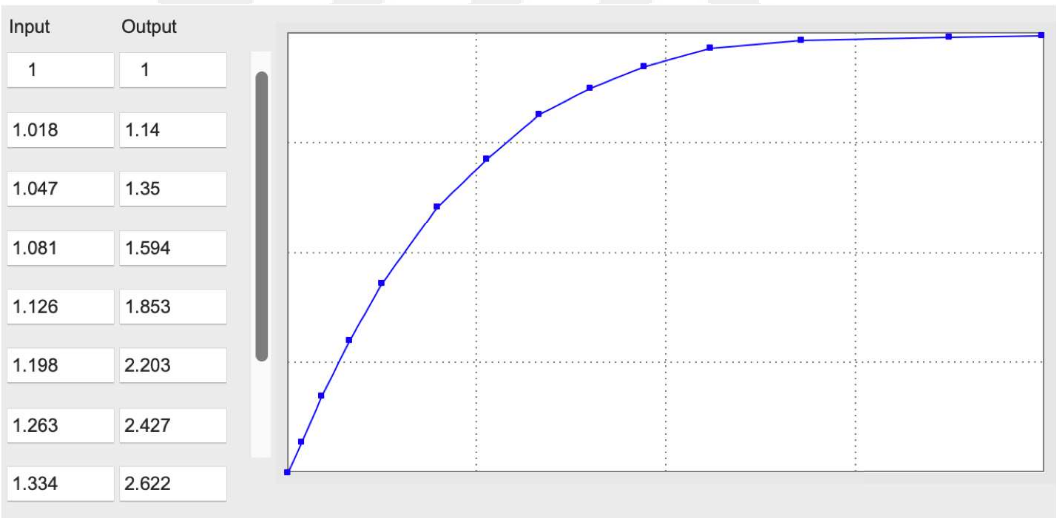

Figure 4.11. Graphical function for the effect of sympathetic nervous system activity on heart rate.

The graphical function for the effect of sympathetic nervous system activity on contractility is given in Figure 4.12. The graph in Figure 4.12 is drawn by normalizing baroreceptor activity to its reference value which can be calculated as

$$eff\ of\ SNS\ on\ contractility = f(\frac{implied\ SNS\ activity}{normal\ SNS\ activity}). \tag{4.32}$$

As a result of increased contractility, the heart's ability to pump blood increases, more blood is ejected at the end of systole, and end-systolic volume decreases, as given in Equation (4.33). With decreased end-systolic volume, the hearth has more space for blood carried from the body. As a result, cardiac output increases, leading to an elevation in blood pressure.

$$End\ systolic\ volume = \frac{1}{contractility} \times normalESV. \tag{4.33}$$

Sympathetic nervous system activity plays an important role in vasomotor function and regulation of arterial tone.

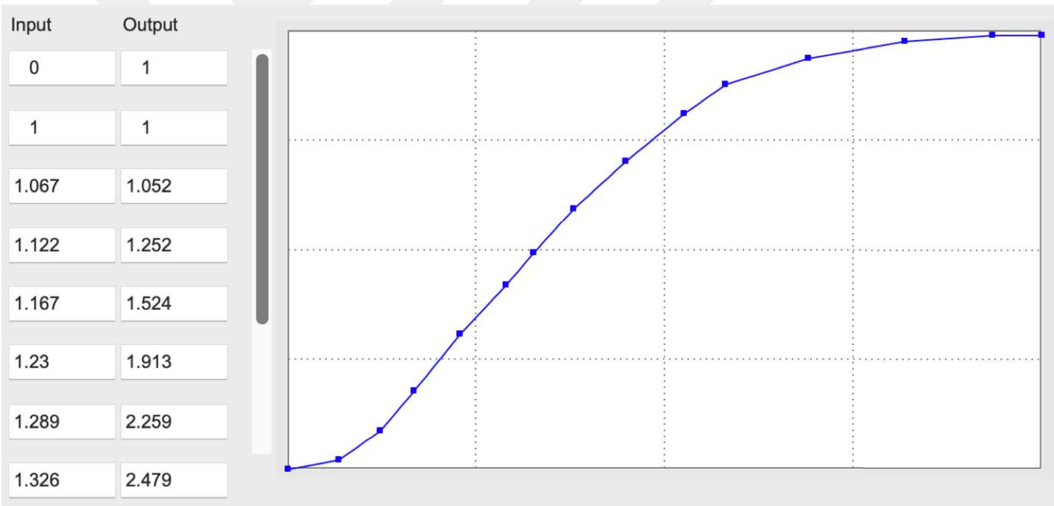

Figure 4.12. Graphical function for the effect of sympathetic nervous system activity on contractility.

The graphical function for the effect of sympathetic nervous system activity on arterial tone is given in Figure 4.13. Findings in the literature [107] represent the effect of nervous system activity on heart rate. The graph in Figure 4.13 is drawn by normalizing baroreceptor activity to its reference value which can be calculated as

$$eff\ of\ SNS\ on\ tone = f(\frac{implied\ SNS\ activity}{normal\ SNS\ activity}). \tag{4.34}$$

At the beginning of the simulation the stock variables have initial values. Furthermore some of the formulations use constant values. The constant and initial values used in the central nervous system sector are given in Table 4.4.

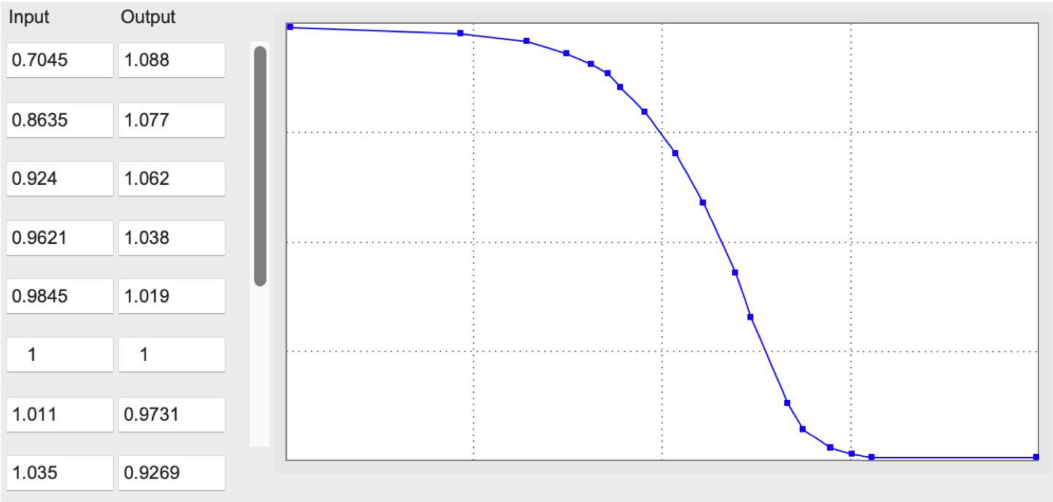

Figure 4.13. Graphical function for the effect of sympathetic nervous system activity on arterial tone.

Table 4.4. Constants and initial values in central nervous system sector.

Variable name	**Unit**	**Value**
normal contractility	Dmnl	1
operating point adj time	Day	3
baroreceptor activity adj time	Day	3
normal baroreceptor activity	burst/ms	1000
normal PNS activity	Dmnl	1
normal SNS activity	Dmnl	1
initial baroreceptor activity	burst/ms	1000

4.5. Renal Sector

This section examines blood pressure regulation mechanisms controlled by the renal system. The renal sector of the model includes two control mechanisms: fluid regulation and hormonal regulation. These two functions of the renal system are explained under two sub-sections.

4.5.1. Fluid Regulation

The fluid regulation structure of the model includes the mechanisms of glomerular filtration, dynamics of total body water and salt, and other fluid volumes, including extracellular and blood volumes. The stock-flow diagram of the renal sector responsible for fluid regulation is given in Figure 4.14. Stock and flow variables in the renal sector responsible for fluid regulation are shown in Table 4.5.

Table 4.5. Stock and flow variables in the renal sector for fluid regulation.

Variable	**Type**	**Unit**
Na intake	Inflow	mEq/Day
water intake	Inflow	L/Day
kidney function loss	Outflow	Dmnl/Day
Na removal	Outflow	mEq/Day
water removal	Outflow	L/Day
Kidney function	Stock	Dmnl
Total body salt	Stock	mEq
Total body water	Stock	L

Physiologic changes associated with aging also affect the kidneys [108]. Longitudinal studies show that renal function declines with age. In the model, the kidney function is included as a stock variable. As the functional loss of the kidney is irreversible, there is only an outflow from the stock.

The kidney function at a given time can be expressed as

$$Kidney\ function(t) = (initial\ kidney\ function) \times (t - dt) - (kidney\ function\ loss) \times dt. \tag{4.35}$$

With aging, kidney function is lost at a certain rate. This average kidney function loss is accelerated by elevated blood pressure. Systolic blood pressure was found to be the highest risk factor for the decline in kidney function [108].

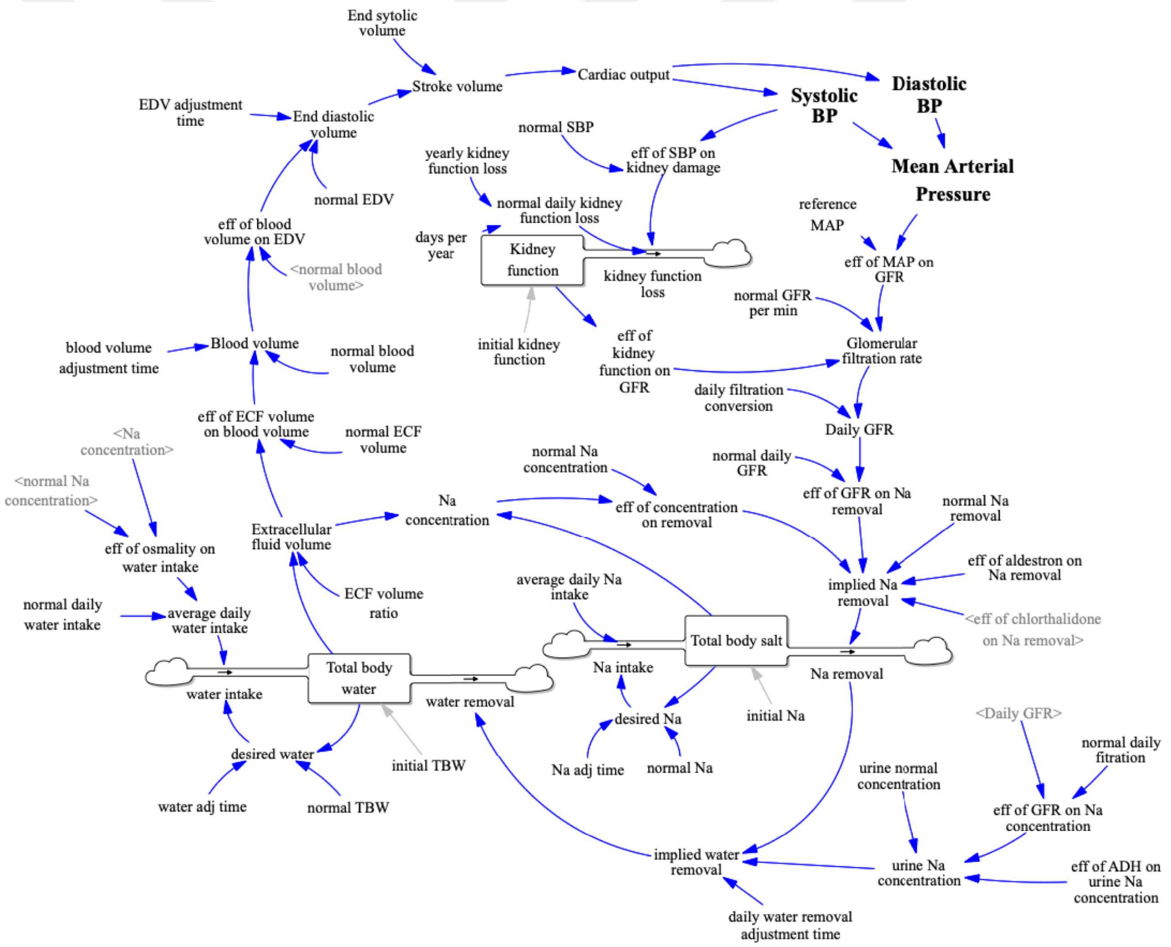

Figure 4.14. Stock flow diagram of renal volume control.

Kidney function loss at a given time can be expressed as

$$\begin{aligned} kidney\ function\ loss = {} & (normal\ daily\ kidney\ function\ loss) \\ & \times (eff\ of\ SBP\ on\ kidney\ damage). \end{aligned} \tag{4.36}$$

The graphical function for the effect of systolic blood pressure on kidney damage is given in Figure 4.15. This function is formed based on the relationship identified in the literature [109–111]. The graph in Figure 4.15 is drawn by normalizing systolic blood pressure to its reference value which can be calculated as

$$eff\ of\ SBP\ on\ kidney\ damage = f(\frac{Systolic\ Blood\ Pressure}{Normal\ SBP}). \tag{4.37}$$

Glomerular filtration rate (GFR) is the milliliter of plasma that flows over one minute. Also, GFR is the primary indicator of the kidney's function.

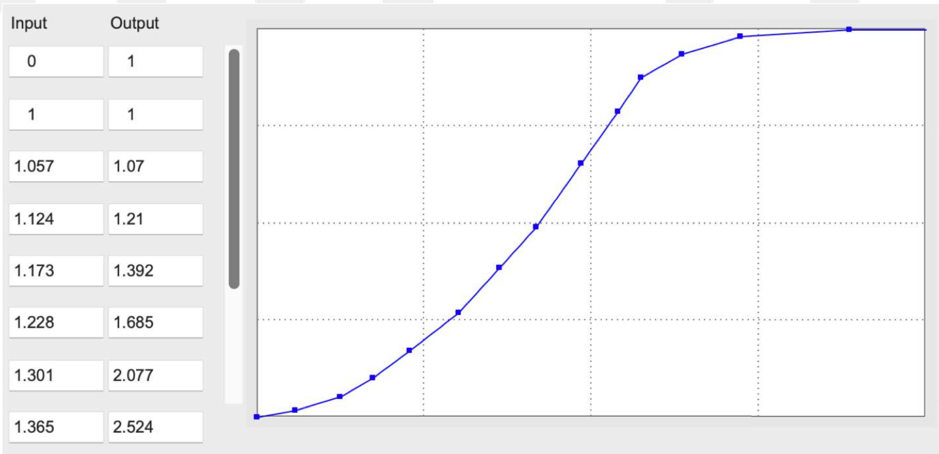

Figure 4.15. Graphical function for the effect of systolic blood pressure on kidney damage.

The maximum level of glomerular filtration that can be achieved depends on the functionality of the kidney. The graphical function for the effect of kidney function on GFR is given in Figure 4.16. This function is formed based on the relationship identified in the literature [68].

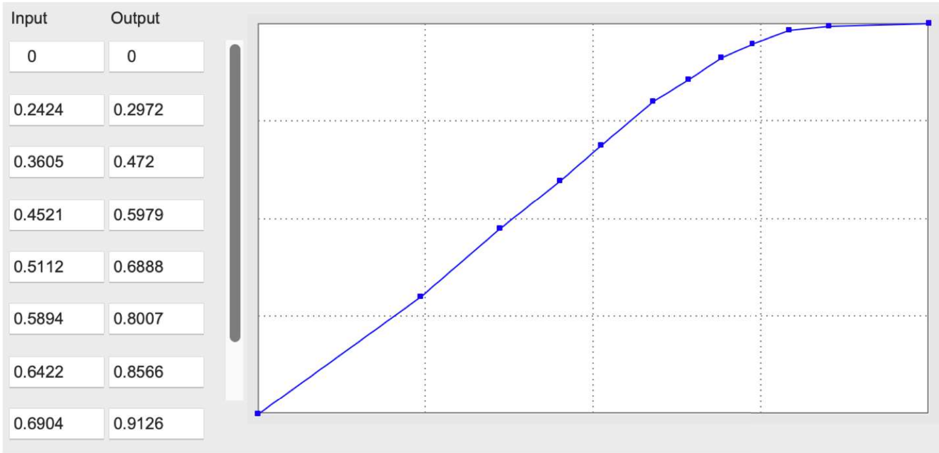

Figure 4.16. Graphical function for the effect of kidney function on glomerular filtration rate.

The main factor that controls GFR per unit of time is arterial pressure. With higher blood pressure, more fluids are filtered in the kidney. Therefore, GFR at a given time can be expressed as

$$\begin{aligned} Glomeruler\ filtrationrate &= (normal\ GFR\ per\ min) \\ &\times (kidney\ function) \times (eff\ of\ MAP\ on\ GFR). \end{aligned} \tag{4.38}$$

The kidney has the ability to auto-regulate, which is a homeostatic mechanism to protect the kidney from injury. Auto-regulation allows kidneys to maintain the GFR over a wide range of renal perfusion pressures. Therefore, GFR is constant while mean arterial pressure is in the range of 75mmHg and 165 mmHg [84]. The graphical function for the effect of mean arterial pressure on GFR is given in Figure 4.17. The graph in Figure 4.17 is drawn by normalizing mean arterial pressure to its reference value which can be calculated as

$$eff\ of\ MAP\ on\ GFR = f(\frac{Mean\ Arterial\ Pressure}{normal\ MAP}). \tag{4.39}$$

Urine output plays a vital role in hypertension regulation. Urine removal includes the removal of two main components: sodium and water. The body's sodium regulation plays a critical role in determining the amount of water removed from urine. Therefore, first, the body salt regulation mechanism will be explained, and later the water regulation will be discussed. Total body salt is modeled as a stock variable as it has inertia. The total body salt can be adjusted with an inflow of sodium intake and an outflow of sodium removal. The formulation for the total body salt at a given time can be expressed as

$$\begin{aligned} Total\ body\ salt(t) &= initial\ Na \times (t - dt) \\ &\quad + (Na\ intake - Na\ removal) \times dt. \end{aligned} \tag{4.40}$$

Daily sodium intake is regulated by two mechanisms: daily average consumption and control mechanism of the body to increase the desire to consume higher salt. The sodium intake cannot be subzero; therefore, a maximum function is used.

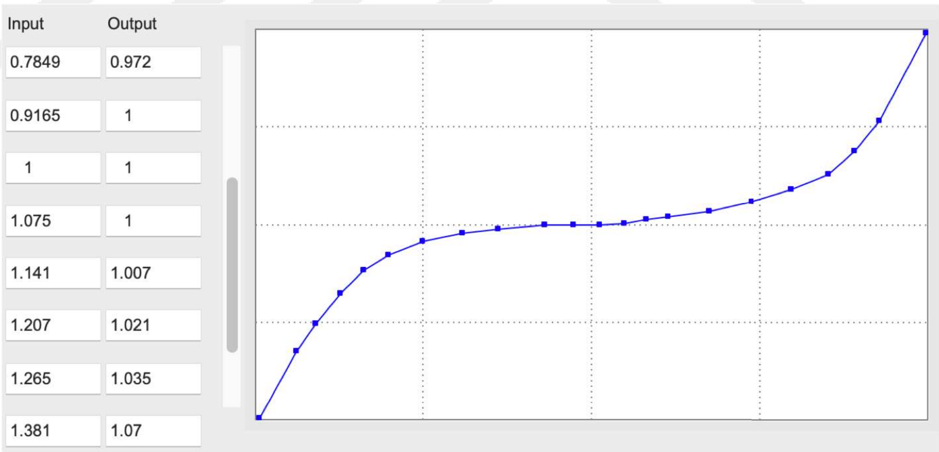

Figure 4.17. Graphical function for the effect of mean arterial pressure on glomerular filtration rate.

Based on the explained relationship the sodium intake can be formulated as

$$Na\ intake = MAX(desired\ Na + average\ daily\ Na\ intake). \tag{4.41}$$

Desired sodium is the amount the patient requires to keep the total body sodium levels at an average level. This mechanism enables the body to remain balanced and recover lost ions. This relationship is formulated as

$$desired\ Na = (Total\ body\ salt - normal\ TBW)/(Na\ adj\ time). \tag{4.42}$$

The implied Na removal depends on the effects of GFR and sodium concentration in the body. Depending on the normal Na removal and the effect of GFR the implied Na removal can be expressed as

$$\begin{aligned} implied\ Na\ removal = {} & (normal\ Na\ removal) \\ & \times (eff\ of\ GFR\ on\ Na\ removal) \\ & \times (eff\ of\ concentration\ on\ Na\ removal). \end{aligned} \tag{4.43}$$

With higher GFR, the sodium amount filtered in the kidney increases. This relationship is linear which can be calculated as

$$eff\ of\ GFR\ on\ Na\ removal = f(\frac{Daily\ GFR}{normal\ daily\ GFR}). \tag{4.44}$$

Also, the concentration of filtered sodium in the kidneys increases with higher sodium concentration in the body. This relationship is linear which can be calculated as

$$eff\ of\ concentration\ on\ removal = f(\frac{Na\ concentration}{normal\ Na\ concentration}). \tag{4.45}$$

Total body water is modeled as a stock variable as it has inertia. Total body water can be adjusted with an inflow of water intake and an outflow of water removal. The formulation for total body water at a given time can be expressed as

$$\begin{aligned} Total\ body\ water(t) = {} & (initial\ TBW) \times (t - dt) \\ & + (water\ intake - water\ removal) \times dt. \end{aligned} \tag{4.46}$$

Daily water intake is regulated by the daily average water consumption of a person which is Daily water intake is regulated by a person's daily average water consumption, which is assumed to be constant in the absence of osmolality's effect. The body's control mechanism increases the desire to intake higher water to recover lost fluids. As water intake cannot be subzero, a maximum function is used while formulating this relationship as

$$\begin{aligned} Na\ intake = MAX(desired\ Na + average\ daily\ Na\ intake) \\ \times (eff\ of\ osmality\ on\ water\ intake). \end{aligned} \tag{4.47}$$

Desired water is the amount of water a patient requires to keep the total body water levels at an average level. This mechanism allows the body to remain in homeostasis and to recover lost water. The relationship between desired water and total body water can be expressed as

$$desired\ water = (Total\ body\ water - normal\ TBW)/(water\ adj\ time). \tag{4.48}$$

Daily average water intake can be increased or decreased by osmolality, representing the body's overall sodium concentration. Average daily water intake depending on its normal value and osmolality can be formulated as

$$\begin{aligned} average\ daily\ water\ intake = (normal\ daily\ water - intake) \\ \times (eff\ of\ osmolality\ on\ water\ intake). \end{aligned} \tag{4.49}$$

Higher osmolality stimulates the hypothalamus, increasing thirst feeling and the average daily water consumption.

The graphical function for the effect of osmolality on water intake is given in Figure 4.18. This function is formed based on the relationship identified in the literature [81].

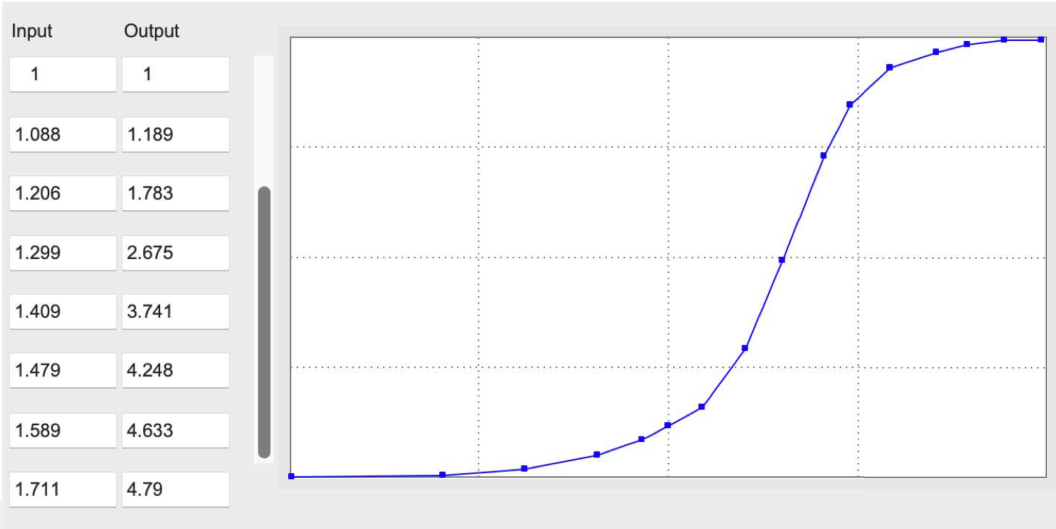

Figure 4.18. Graphical function for the effect of osmolality on water intake.

The graph in Figure 4.18 is drawn by normalizing sodium concentration to its reference value which can be calculated as

$$eff\ of\ osmolality\ on\ water\ intake = f(\frac{Na\ concentration}{normal\ Na\ concentration}). \tag{4.50}$$

As given in Equation (4.49), the implied water removal is regulated by Na removal and urine sodium concentration. Higher sodium excretion causes the body to remove more water with delay. The relationship between water removal and sodium concentration can be expressed as

$$\begin{aligned} water\ removal &= implied\ water\ removal = \\ &= \frac{DELAY1(Na\ removal,\ daily\ water\ removal\ adj.\ time)}{(urine\ Na\ concentration)}. \end{aligned} \tag{4.51}$$

The urine concentration plays a role in determining the amount of water removed from the body. The urine concentration is regulated by the ADH hormone and GFR. With higher GFR, the sodium amount filtered in the kidney increases, increasing the sodium concentration in the urine. The urine Na concentration can be calculated as

$$\begin{aligned} urine\ Na\ concentration = {} & (urine\ normal\ concentration) \\ & \times (eff\ of\ ADH\ on\ urine\ Na\ concentration) \\ & \times (eff\ of\ GFR\ on\ Na\ concentration). \end{aligned} \tag{4.52}$$

The graphical function for the effect of GFR on urine concentration is given in Figure 4.19. This function is formed based on the relationship identified in the literature [68].

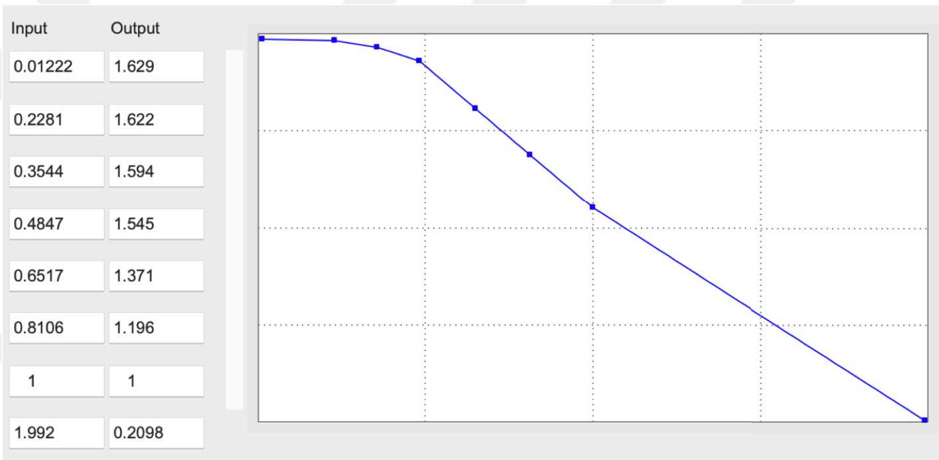

Figure 4.19. Graphical function for the effect of GFR on urine Na concentration.

The graph in Figure 4.19 is drawn by normalizing GFR to its reference value as which can be calculated as

$$eff\ of\ GFR\ on\ urine\ Na\ concentration = f(\frac{Daily\ GFR}{normal\ Daily\ GFR}). \tag{4.53}$$

Two-thirds of the total body water is intracellular, and one-third is extracellular fluids. The fluids in the cardiovascular system are considered in this second compartment. The graphical function for the effect of extracellular fluid volume on blood volume is given in Figure 4.20. This function is formed based on the relationship identified in the literature [30].

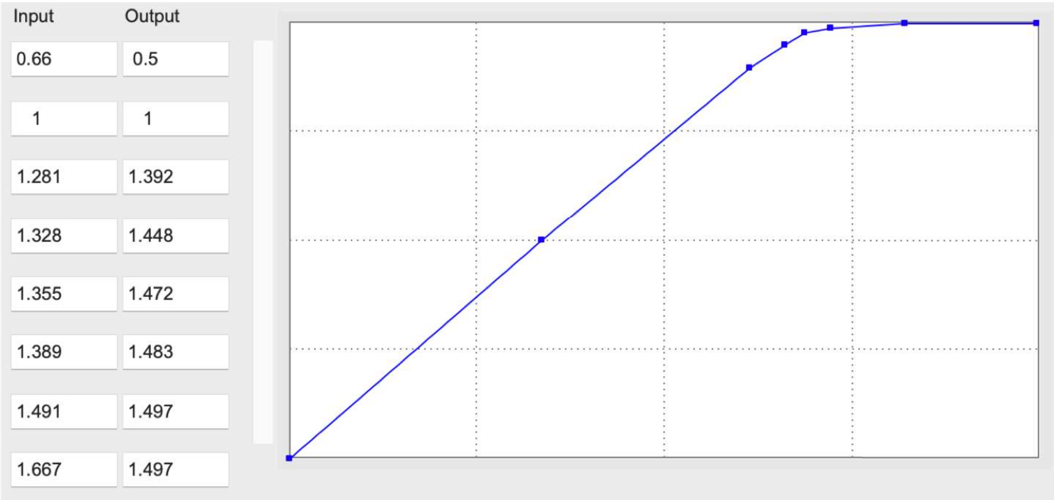

Figure 4.20. Graphical function for the effect of extracellular fluid volume on blood volume.

The graph in Figure 4.20 is drawn by normalizing extracellular fluid volume to its reference value which can be calculated as

$$eff\ of\ ECF\ on\ blood\ volume = f(\frac{Extracellular\ fluid\ volume}{normal\ ECF}). \tag{4.54}$$

When extracellular increases, the blood volume increases. However, after a saturation point, blood volume does not increase with an increase in extracellular volume and causes edema. Furthermore, the conversion of extracellular fluids into blood volume is delayed. The *blood volume* over time can be expressed as

$$\begin{aligned} blood\ volume = {} & DELAY1(normal\ blood\ volume \\ & \times eff\ of\ ECF\ volume\ on\ blood\ vol., blood\ vol.\ adjustment\ time). \end{aligned} \tag{4.55}$$

End diastolic volume depends on venous return, the amount of blood carried to the heart. It is a function of blood volume. The graphical function for the effect of blood volume on end-diastolic volume is given in Figure 4.21. This function is formed based on the relationship identified in the literature [30].

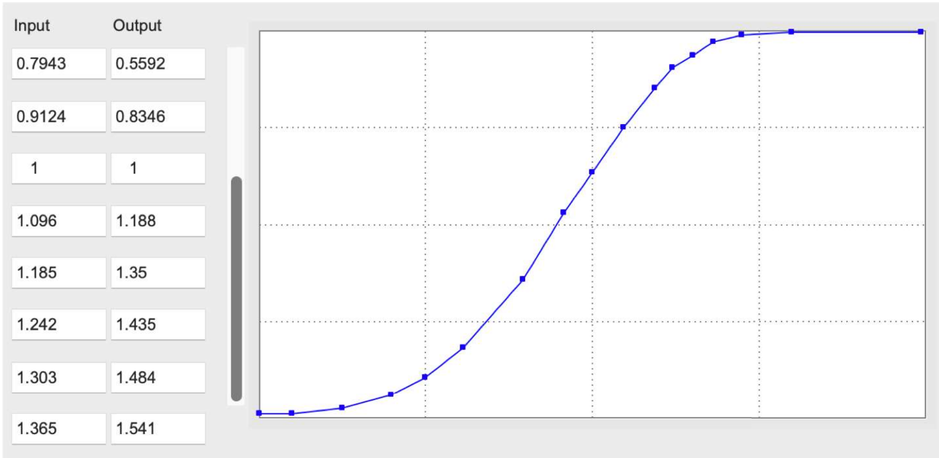

Figure 4.21. Graphical function for the effect of blood volume on end diastolic volume.

The graph in Figure 4.21 is drawn by normalizing extracellular fluid volume to its reference value which can be calculated as

$$eff\ of\ blood\ volume\ on\ EDV = f(\frac{blood\ volume}{normal\ blood\ volume}). \tag{4.56}$$

An increase in blood volume increases end-diastolic volume increases. However, after a saturation point, the end-diastolic volume does not increase with blood volume expansion. Yet, this increase is observed with a time delay which can be expressed as

$$\begin{aligned} End\ diastolic\ volume = DELAY1(&normal\ EDV \\ &\times eff\ of\ blood\ volume\ on\ EDV, EDV\ adjustment\ time). \end{aligned} \tag{4.57}$$

The difference in the volume before and after the contraction is pumped out of the heart into the arteries. End diastolic volume is the amount of blood filled in the heart before the contraction. As more blood is delivered to the heart, cardiac output increases, elevating the blood pressure. Furthermore some of the formulations use constant values. The constant and initial values used in the renal sector responsible for fluid regulation are given in Table 4.6.

Table 4.6. Constant variables for renal sector fluid regulation.

Variable name	**Unit**	**Value**
blood volume adjustment time	Day	3
daily filtration conversion	(ml*Day)/(min*L)	0.694
daily water removal adjustment time	Day	1
ECF volume ratio	Dmnl	0.333
Na adj time	Day	3
normal blood volume	L	5
normal daily fitration	L/Day	180
normal daily GFR	L/Day	180
normal daily water intake	L/Day	2
normal ECF volume	L	14
normal GFR per min	ml/min	125
normal Na	mEq	2160
normal Na concentration	mEq/L	154
normal Na removal	mEq/Day	180
normal TBW	L	42
urine normal concentration	mEq/L	90
water adj time	Day	3
yearly kidney function loss	Dmnl/year	0.008
initial kidney function	Dmnl	1
initial Na	mEq	2160
initial TBW	L	42

4.5.2. Hormonal Regulation

The hormonal regulation structure of the model includes the dynamics of renin, angiotensin II, aldosterone, and antidiuretic hormones and their effects on fluid regulation as well as the total cardiovascular sector.

The stock-flow diagram of the renal sector responsible for hormonal regulation is given in Figure 4.22. The stock and flow variables in the renal system sector responsible for hormonal regulation are given in Table 4.7.

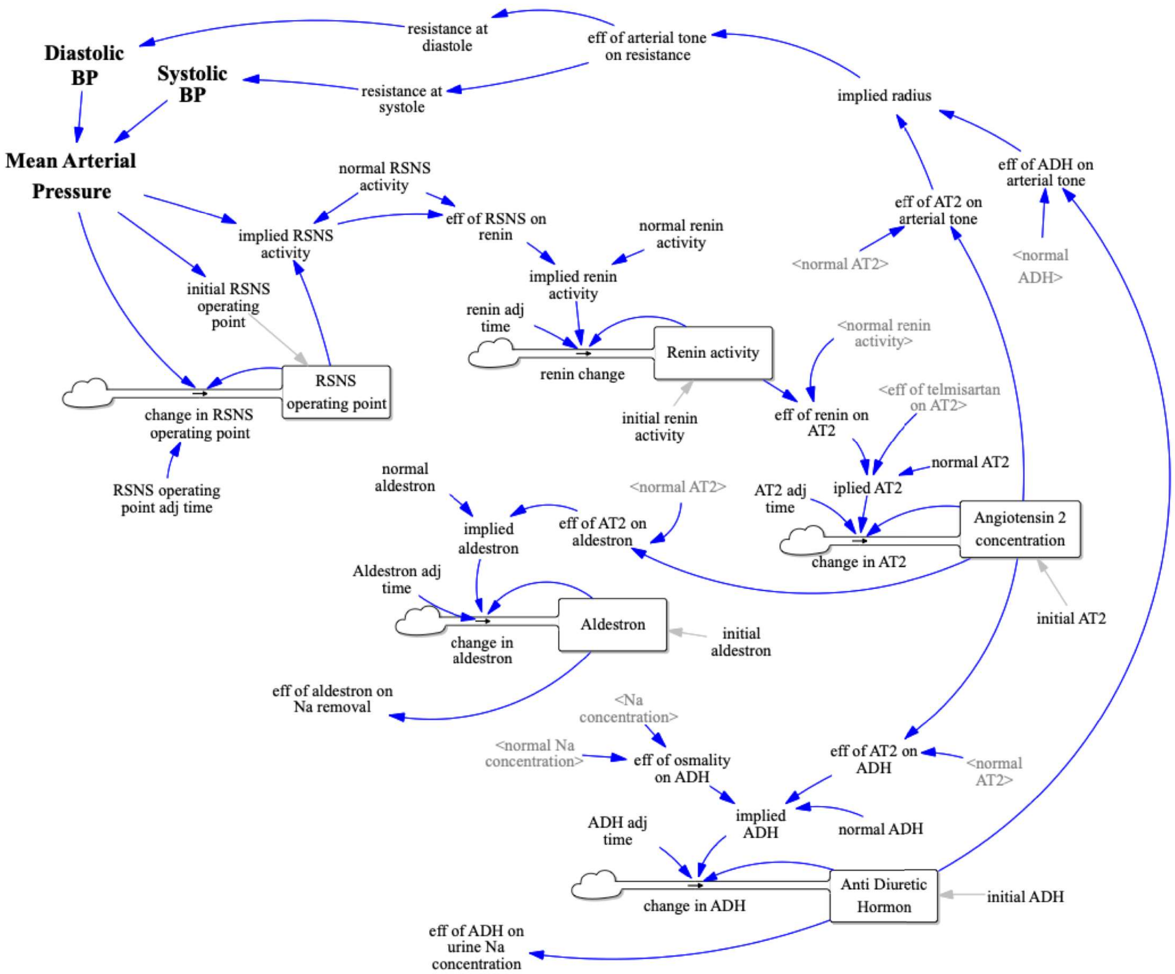

Figure 4.22. Stock flow diagram of the renal hormonal control.

The first response of kidneys to blood pressure change was observed as a change in the glomerular filtration rate. Another regulation mechanism is the change in renin production in the juxtaglomerular cells through renal sympathetic nervous system activity (RSNS) stimulation. Like the baroreceptors, a blood pressure increase in the kidney arteries stimulates the nerve fibers that connect to RSNS. The activity of these nerve fibers is monitored and compared with the operating point for the corresponding arterial pressure which can be expressed as

$$\begin{aligned} implied\ RSNS\ activity = & \frac{Mean\ Arterial\ Pressure}{RSNS\ operating\ point} \\ & \times (normal\ RSNS\ activity). \end{aligned} \tag{4.58}$$

However, RSNS can become desensitized to chronic elevation in pressure and reset to higher pressure [112], similar to the central nervous system behavior. This resetting reduces the RSNS activity at normal levels of mean arterial pressure. Therefore, to reach the previous response, higher blood pressure levels are required.

Table 4.7. Stock and flow variables in the renal sector for hormonal regulation.

Variable	**Type**	**Unit**
change in ADH	Bi-flow	pg/ml/Day
change in aldosterone	Bi-flow	ng/ml/Day
change in AT2	Bi-flow	pg/(ml*Day)
change in RSNS operating point	Bi-flow	mmhg/Day
renin change	Bi-flow	pg/ml/hr/Day
Aldosterone	Stock	ng/ml
Angiotensin 2 concentration	Stock	pg/ml
Anti Diuretic Hormon	Stock	pg/ml
Renin activity	Stock	pg/ml/hr
RSNS operating point	Stock	mmhg

RSNS operating point is modeled as a stock variable with a bi-flow. The normal arterial pressure where the RSNS responds has an initial set value that can change over time. The RSNS operating point at a given time can be expressed as

$$\begin{aligned} RSNS\ operating\ point(t) = {} & (initial\ normal\ MAP) \times (t - dt) \\ & + (change\ in\ RSNS\ operating\ point). \end{aligned} \tag{4.59}$$

The mean arterial pressure and operating point gap close over time. This relationship on RSNS operating point can be expressed as

$$\begin{aligned} change\ in\ RSNS\ operating\ point = {} & \frac{Mean\ Arterial\ Pressure}{normal\ MAP\ adjtime} \\ & - \frac{Normal\ MAP}{normal\ MAP\ adj\ time}. \end{aligned} \tag{4.60}$$

The RSNS activity regulates the implied renin activity at a given time. Therefore, implied renin at a given time is formulated as

$$implied\ renin\ activity = normal\ renin\ activity \times eff\ of\ RSNS\ on\ renin. \tag{4.61}$$

The graphical function for the effect of RSNS on renin activity is given in Figure 4.23. Findings in the literature represent the effect of the RSNS on renin activity [43, 68].

The graph in Figure 4.23 is drawn by normalizing mean arterial pressure to its reference value which can be calculated as

$$eff\ of\ RSNS\ on\ renin = f(\frac{impled\ RSNS\ activity}{normal\ RSNS\ activity}). \tag{4.62}$$

Renin activity is modeled as a stock variable as it has inertia. The stock can be adjusted via a bi-flow as renin activity can increase or decrease through a similar mechanisms.

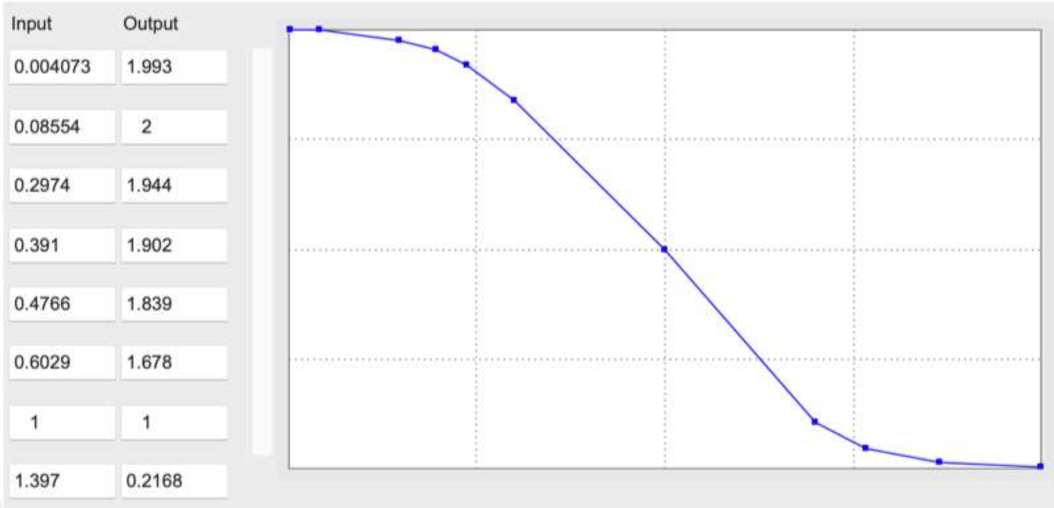

Figure 4.23. Graphical function for the effect of RSNS on renin activity.

The change in renin activity over time can be expressed as

$$Renin\ activity(t) = initial\ renin\ activity \times (t - dt) + (renin\ change) \times dt. \quad (4.63)$$

The gap between the implied and actual renin activity closes over time. The change in renin activity happens over an adjustment time which can be expressed as

$$renin\ change = \frac{implied\ renin\ activity - Renin\ activity}{renin\ adj\ time}. \quad (4.64)$$

The graphical function for the effect of renin activity on angiotensin II is given in Figure 4.24.

The graph in Figure 4.24 is drawn by normalizing renin activity to its reference value which can be calculated as

$$eff\ of\ renin\ on\ AT2 = f(\frac{Renin\ activity}{normal\ renin\ activity}). \quad (4.65)$$

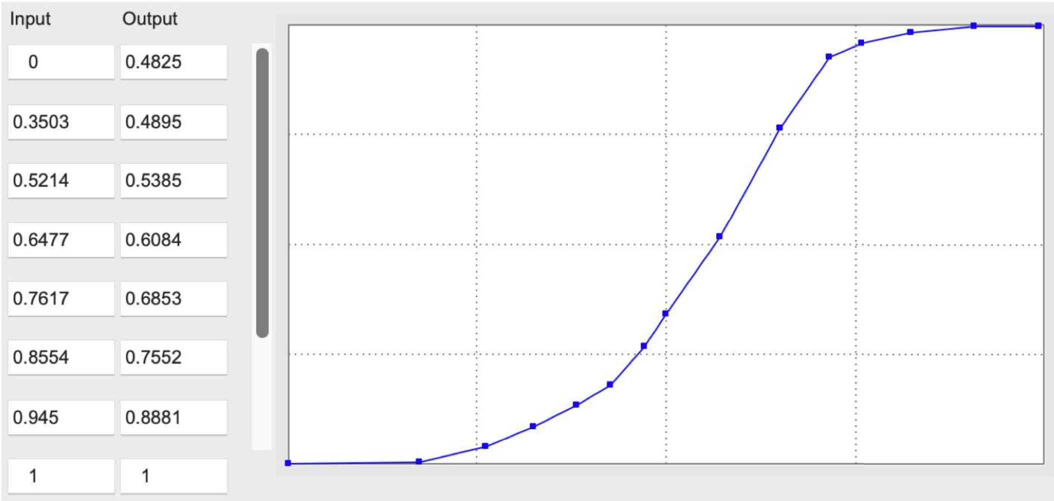

Figure 4.24. Graphical function for the effect of renin activity on angiotensin II.

Implied angiotensin II concentration at a given time is regulated by the renin activity. Therefore, implied angiotensin II concentration at a given time can be expressed as

$$implied\ AT2 = normal\ AT2 \times eff\ of\ renin\ on\ AT2. \tag{4.66}$$

Angiotensin II concentration is modeled as a stock variable as its concentraion in the body has inertia. The concentration can be adjusted with a bi-flow that can increase or decrease the concentration. This relationship can be expressed as

$$Angiotensin\ 2\ concentration(t) = (initial\ AT2) \times (t - dt) + (change\ in\ AT2) \times dt. \tag{4.67}$$

The gap between the implied angiotensin II concentration and actual angiotensin II closes over time. This relationship can be expressed as

$$change\ in\ AT2 = \frac{(implied\ AT2 - Angiotensin\ 2\ concentration)}{AT2\ adj\ time}. \tag{4.68}$$

The graphical function for the effect of Angiotensin II concentration on aldosterone is given in Figure 4.25.

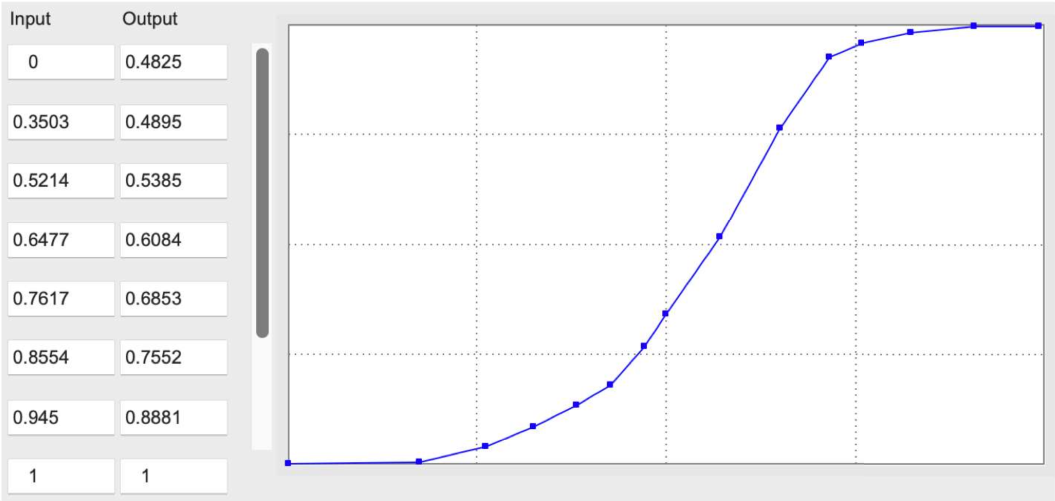

Figure 4.25. Graphical function for the effect of angiotensin II concentration on aldosterone.

The graph in Figure 4.25 is drawn by normalizing angiotensin II concentration to its reference value which can be calculated as

$$eff\ of\ AT2\ on\ aldosterone = f(\frac{Angiotensin\ 2\ concentration}{normal\ AT2}). \tag{4.69}$$

Implied aldosterone concentration at a given time is regulated by the angiotensin II concentration. Therefore, the implied aldosterone depending on the effect of angiotensin II can be calculated as

$$implied\ aldosterone = normal\ aldosterone \times eff\ of\ AT2\ on\ aldosterone. \tag{4.70}$$

Aldosterone concentration is modeled as a stock variable as its concentration in the body has inertia. The aldosterone concentration can be increased or decreased over time through a bi-flow. The relationship between aldosterone concentration and its change over time can be expressed as

$$Aldosterone(t) = (initial\ aldosterone) \times (t-dt) + (change\ in\ aldosterone) \times dt. \tag{4.71}$$

The gap between the implied aldosterone and actual aldosterone concentration closes. This process happens over an adjustment time which can be expressed as

$$change\ in\ aldosterone = \frac{(implied\ aldosterone - Aldosterone)}{(aldosterone\ adj\ time)}. \tag{4.72}$$

The graphical function for the effect of angiotensin II concentration on the antidiuretic hormone is given in Figure 4.26.

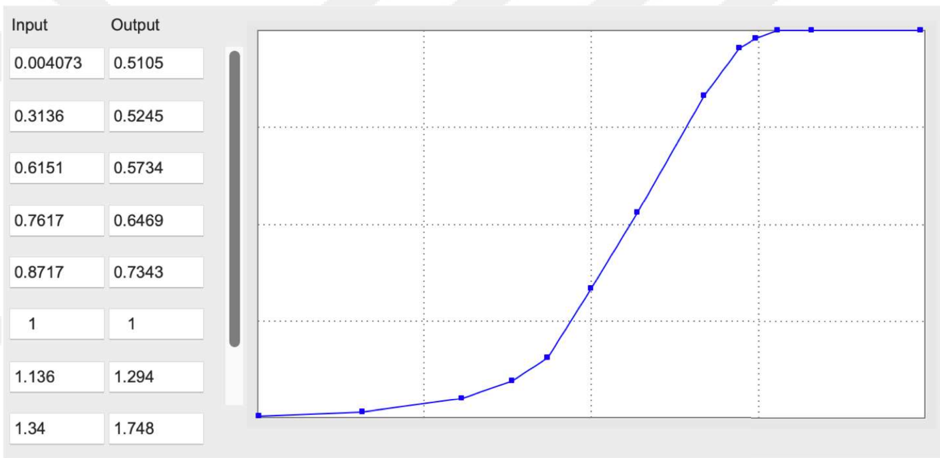

Figure 4.26. Graphical function for the effect of angiotensin II concentration on anti diuretic hormon.

The graph in Figure 4.26 is drawn by normalizing angiotensin II concentration to its reference value can be calculated as

$$eff\ of\ AT2\ on\ ADH = f(\frac{Angiotensin\ 2\ concentration}{normal\ AT2}). \tag{4.73}$$

The angiotensin II concentration regulates implied antidiuretic hormone concentration at a given time.

The implied antidiuretic hormone at a given time is formulated as

$$implied\ ADH = (normal\ ADH) \times (eff\ of\ AT2\ on\ ADH). \tag{4.74}$$

Antidiuretic hormone concentration is modeled as a stock variable as its concentration in the body has inertia. ADH concentration can be increased or decreased over time through a bi-flow which can be expressed as

$$Anti\ Diuretic\ Hormon(t) = (initial\ ADH) \times (t-dt) + (change\ in\ ADH) \times dt. \tag{4.75}$$

The gap between the implied antidiuretic hormone and actual antidiuretic hormone concentration closes over time. This process happens over an adjustment time which can be expressed as

$$change\ in\ ADH = \frac{(implied\ ADH - Anti\ Diuretic\ Hormon)}{ADH\ adj\ time}. \tag{4.76}$$

The graphical function for the effect of angiotensin II concentration on arterial tone is given in Figure 4.27.

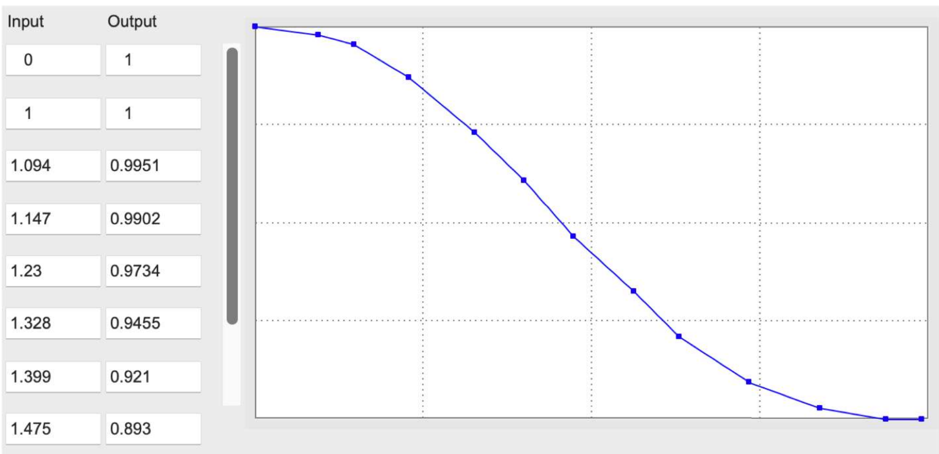

Figure 4.27. Graphical function for the effect of angiotensin II concentration on arterial tone.

The graph in Figure 4.27 is drawn by normalizing angiotensin II concentration to its reference value which can be calculated as

$$eff\ of\ AT2\ on\ arterial\ tone = f(\frac{Angiotensin\ 2\ concentration}{normal\ AT2}) \tag{4.77}$$

The graphical function for the effect of the antidiuretic hormone on arterial tone is given in Figure 4.28.

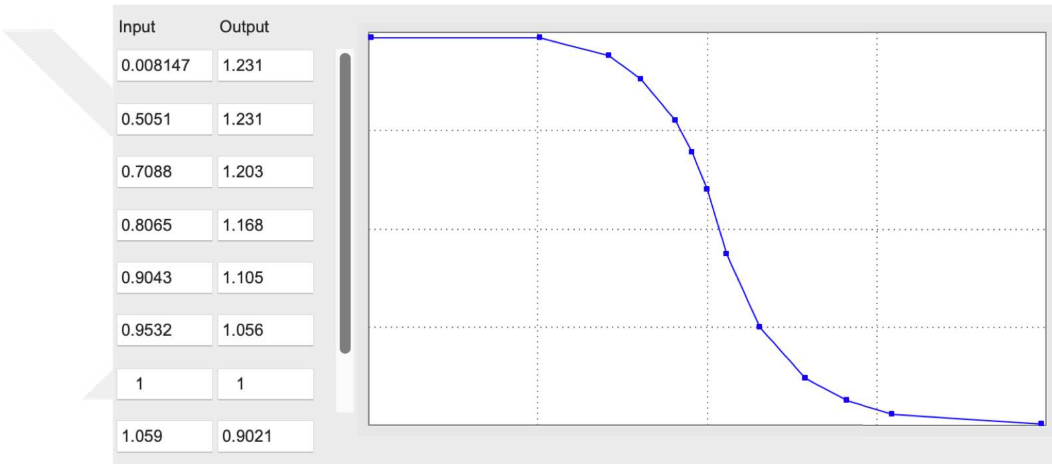

Figure 4.28. Graphical function for the effect of anti diuretic hormone on arterial tone.

The graph in Figure 4.28 is drawn by normalizing antidiuretic hormone concentration to its reference value which can be calculated as

$$eff\ of\ ADH\ on\ arterial\ tone = f(\frac{Anti\ Diuretic\ Hormon}{normal\ AADH}) \tag{4.78}$$

At the beginning of the simulation the stock variables have initial values. Furthermore some of the formulations use constant values. The constants and initial values used in the renal system sector responsible for hormonal regulation are given in Table 4.8.

4.6. Treatment Sector

The treatment sector of the model includes the dynamics of drug dosing, their plasma concentration, and their effects on the body. The stock-flow diagram of the cardiovascular sector is shown in Figure 4.29. Stock and flow variables in the treatment sector are given in Table 4.9.

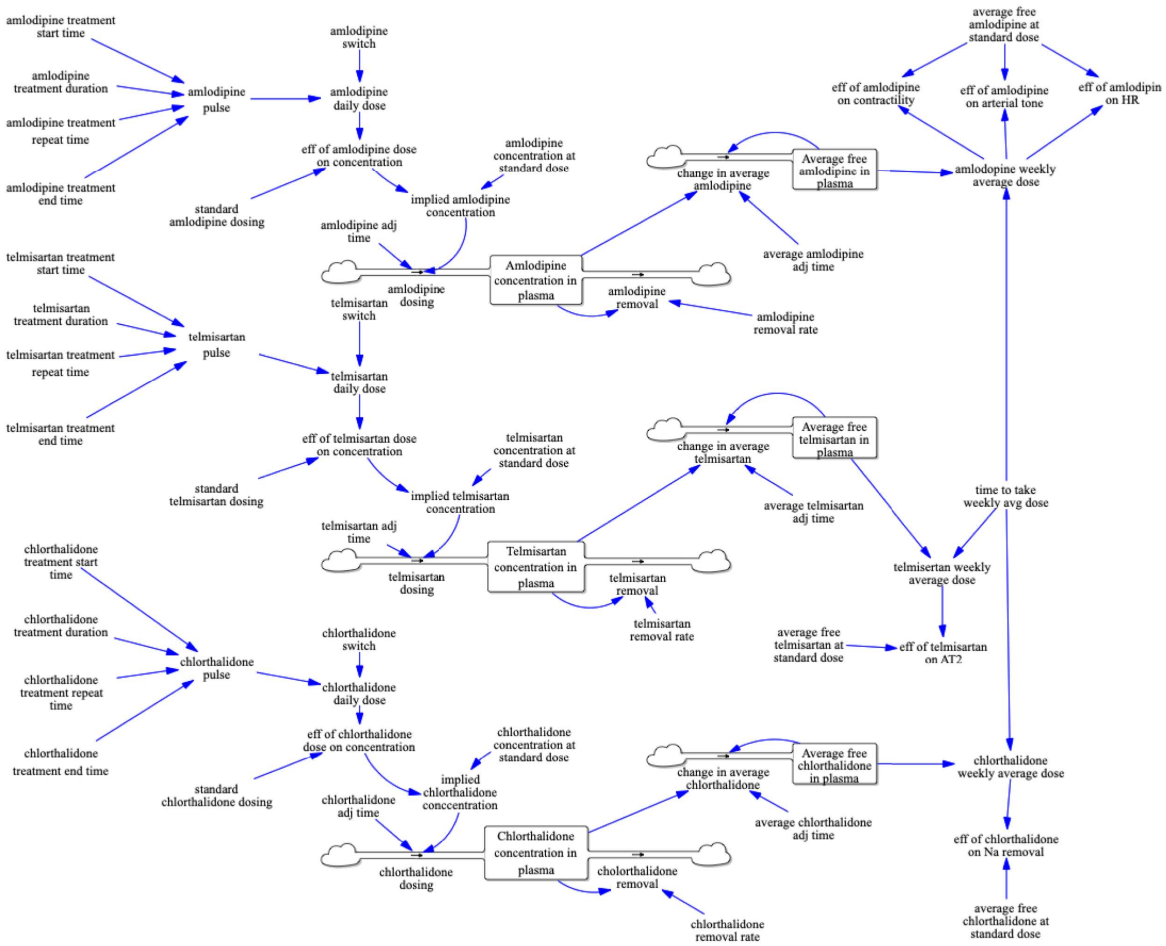

Figure 4.29. Stock flow diagram of the treatment sector.

There are six classes of hypertensive drugs: diuretics, angiotensin-converting enzyme inhibitors (ACE-I), angiotensin II-AT 1 receptor blockers (ARB), beta-blockers, and calcium channel blockers (CCB). This study includes the dynamics of three drugs commonly prescribed in hypertension treatment: amlodipine, telmisartan, and chlorthalidone. These drugs were chosen as their mechanism of action is different from each other. Furthermore, in clinical practice, they are used as combination treatment options to complement each other. Based on the interview with clinical experts, these drugs were found to be suitable for the purpose of the study.

Table 4.8. Constant variables for renal sector hormonal regulation.

Variable name	**Unit**	**Value**
ADH adj time	Day	3
Aldosterone adj time	Day	3
AT2 adj time	Day	3
normal ADH	pg/ml	5
normal aldosterone	ng/ml	250
normal AT2	pg/ml	250
normal renin activity	pg/ml/hr	5.5
normal RSNS activity	Dmnl	1
RAAS operating point adj time	Day	3
renin adj time	Day	3
initial ADH	pg/ml	5
initial aldosterone	ng/ml	250
initial AT2	pg/ml	250
initial renin activity	pg/ml/hr	5.5

Amlodipine is a calcium channel blocker that helps lower blood pressure by decreasing heart rate, contractility, and vasodilating blood vessels. Telmisartan is an Angiotensin II receptor blocker that inhibits this hypertensive enzyme from binding to the receptors. Chlorthalidone is a diuretic that increases sodium removal and excess body water with urination.

Amlodipine concentration in plasma is modeled as a stock variable as it has inertia. The drug concentration can change with an inflow of dosing and an outflow removal. The plasma concentration for amlodipine can be calculated as

$$\begin{aligned} &Amlodipine\ concentration\ in\ plasma(t) = initial\ amlodipine\ concentration \\ &\times (t - dt) + (amlodipine\ dosing - amlodipine\ removal) \times dt. \end{aligned} \tag{4.79}$$

Telmisartan concentration in plasma is modeled as a stock variable as it has inertia. The drug concentration can change with an inflow of dosing and an outflow removal.

Table 4.9. Stock and flow variables in the treatment sector.

Variable	**Type**	**Unit**
change in average amlodipine	Bi-flow	(ng/ml)/Day
change in average chlorthalidone	Bi-flow	(ng/ml)/Day
change in average telmisartan	Bi-flow	(ng/ml)/Day
amlodipine dosing	Inflow	(ng/ml)/Day
chlorthalidone dosing	Inflow	(ng/ml)/Day
telmisartan dosing	Inflow	(ng/ml)/Day
amlodipine removal	Outflow	(ng/ml)/Day
cholorthalidone removal	Outflow	(ng/ml)/Day
telmisartan removal	Outflow	(ng/ml)/Day
Amlodipine concentration in plasma	Stock	ng/ml
Average free amlodipine in plasma	Stock	ng/ml
Average free chlorthalidone in plasma	Stock	ng/ml
Average free telmisartan in plasma	Stock	ng/ml
Chlorthalidone concentration in plasma	Stock	ng/ml
Telmisartan concentration in plasma	Stock	ng/ml

The plasma concentration for telmisartan can be calculated as

$$\begin{aligned} &Telmisartan\ concentration\ in\ plasma(t) = init.\ telmisartan\ concentration \\ &\times (t - dt) + (telmisartan\ dosing - telmisartan\ removal) \times dt. \end{aligned} \tag{4.80}$$

Chlorthalidone concentration in plasma is modeled as a stock variable as it has inertia.

The drug concentration can change with an inflow of dosing and an outflow removal. The plasma concentration for chlorthalidone can be calculated as

$$\begin{aligned} &Chlorthalidone\ concentration\ in\ plasma(t) = chlorthalidone\ concentration \\ &\times (t - dt) + (chlorthalidone\ dosing - chlorthalidone\ removal) \times dt. \end{aligned} \tag{4.81}$$

When a new amlodipine dose is taken daily, the concentration can change from its base value over time by its inflow. The amlodipine dosing changes over an adjustment time which can be expressed as

$$amlodipine\ dosing = \frac{implied\ amlodipine\ concentration}{amlodipine\ adj\ time}. \tag{4.82}$$

When a new telmisartan dose is taken daily, the concentration can change from its base value over time by its inflow. The telmisartan dosing changes over an adjustment time which can be expressed as

$$telmisartan\ dosing = \frac{implied\ telmisartan\ concentration}{telmisartan\ adj\ time}. \tag{4.83}$$

When a new chlorthalidone dose is taken daily, the concentration can change from its base value over time by its inflow. The chlorthalidone dosing changes over an adjustment time which can be expressed as

$$chlorthalidone\ dosing = \frac{implied\ chlorthalidone\ concentration}{chlorthalidone\ adj\ time}. \tag{4.84}$$

After the drug is taken, its concentration in the body can change over time by its outflow. The drugs modeled in this study follow first-order kinetics [113–115] meaning that a constant proportion of the drug is eliminated per unit of time. In drugs with zero order kinetics, the amount of drug eliminated per unit of time is constant.

The amount of amlodipine removed over time depends on its concentration in the body and fractional amlodipine removal rate.

The first-order kinetics of amlodipine removal can be expressed as

$$\begin{aligned} amlodipine\ removal = {} & (Amlodipine\ concentration\ in\ plasma) \\ & \times (amlodipine\ removal\ rate). \end{aligned} \tag{4.85}$$

The amount of telmisartan removed over time depends on its concentration in the body and fractional telmisartan removal rate.

The first-order kinetics of telmisartan removal can be expressed as

$$\begin{aligned} telmisartan\ removal = {} & (Telmisartan\ concentration\ in\ plasma) \\ & \times (telmisartan\ removal\ rate). \end{aligned} \tag{4.86}$$

The amount of chlorthalidone removed over time depends on its concentration in the body and fractional chlorthalidone removal rate.

The first-order kinetics of chlorthalidone removal can be expressed as

$$\begin{aligned} chlorthalidone\ removal = {} & (Chlorthalidone\ concentration\ in\ plasma) \\ & \times (chlorthalidone\ removal\ rate). \end{aligned} \tag{4.87}$$

Based on the dose of amlodipine the concentration implied in the body changes. The implied amlodipine concentration at a given time is calculated by multiplying its concentration at standard dosing to the effect of dosing on concentration. Implied concentrations of amlodipine, can be calculated as

$$\begin{aligned} implied\ amlodipine\ concentration = {} & (amlodipine\ concentration\ at\ std.dose) \\ & \times (eff\ of\ amlodipine\ dose\ on\ concentration). \end{aligned} \tag{4.88}$$

Based on the dose of amlodipine the concentration implied in the body changes.

The implied amlodipine concentration at a given time is calculated by multiplying its concentration at standard dosing to the effect of dosing on concentration. Implied concentrations of amlodipine, can be calculated as

$$\begin{aligned} &implied\ telmisartan\ concentration = (telmisartan\ concentration \\ &\quad at\ std.dose) \times (eff\ of\ telmisartan\ dose\ on\ concentration). \end{aligned} \tag{4.89}$$

Based on the dose of amlodipine the concentration implied in the body changes. The implied amlodipine concentration at a given time is calculated by multiplying its concentration at standard dosing to the effect of dosing on concentration. Implied concentrations of amlodipine, can be calculated as

$$\begin{aligned} &implied\ chlorthalidone\ concentration = (chlorthalidone\ concentration \\ &\quad at\ std.dose) \times (eff\ of\ chlorthalidone\ dose\ on\ concentration). \end{aligned} \tag{4.90}$$

Due to the drug's bioavailability property, the amount of drug taken does not have a linear relationship with the concentration of free drug in the body. The bioavailability, the amount that enters into circulation when the drug is introduced to the body, depends on the drug's characteristics and the route of administration. If the concentration of the drug is low, it can be cleared by the liver before it can enter circulation.

Furthermore, drugs have different plasma binding properties, and not all drug dose is free to bind target receptors. Therefore, increasing the drug dose after a certain point does not increase the free drug concentration, and the drug effectiveness remains constant. The drug doses are formulated with nonlinear graphical functions using fuzzy max and fuzzy min, as given in the Figure 4.30 to represent the free drug concentration in the plasma.

The effect graph of amlodipine is drawn by normalizing the drug dose taken daily to its reference value. The effect of amlodipine concentration based on the normalized doses can be calculated as

$$eff\ of\ amolodipine\ dose\ on\ concentration = f(\frac{amlodipine\ daily\ dose}{std.\ amlodipine\ dose}). \tag{4.91}$$

The effect graph of telmisartan is drawn by normalizing the drug dose taken daily to its reference value. The effect of telmisartan concentration based on the normalized doses can be calculated as

$$eff\ of\ telmisartan\ dose\ on\ concentration = f(\frac{telmisartan\ daily\ dose}{std.\ telmisartan\ dose}). \tag{4.92}$$

The effect graph of chlorthalidone is drawn by normalizing the drug dose taken daily to its reference value.

The effect of chlorthalidone concentration based on the normalized doses can be calculated as

$$eff\ of\ chlorthalidone\ dose\ on\ concentration = f(\frac{chlorthalidone\ daily\ dose}{std.\ chlorthalidone\ dose}). \tag{4.93}$$

Average free concentration of the amlodipine in plasma is modeled as a stock variable due to the inertia of drug concentration in the body. The average free amlodipine concentration has a bi-flow as the concentration can increase or decrease through similar mechanism. The average free concentration of amlodipine concentration based on its flow can be calculated as

$$\begin{aligned} Avg.\ free\ amlodipine\ in\ plasma(t) &= (amlodipine\ concentration) \\ &\times (t - dt) + (change\ in\ avg.\ amlodipine) \times dt. \end{aligned} \tag{4.94}$$

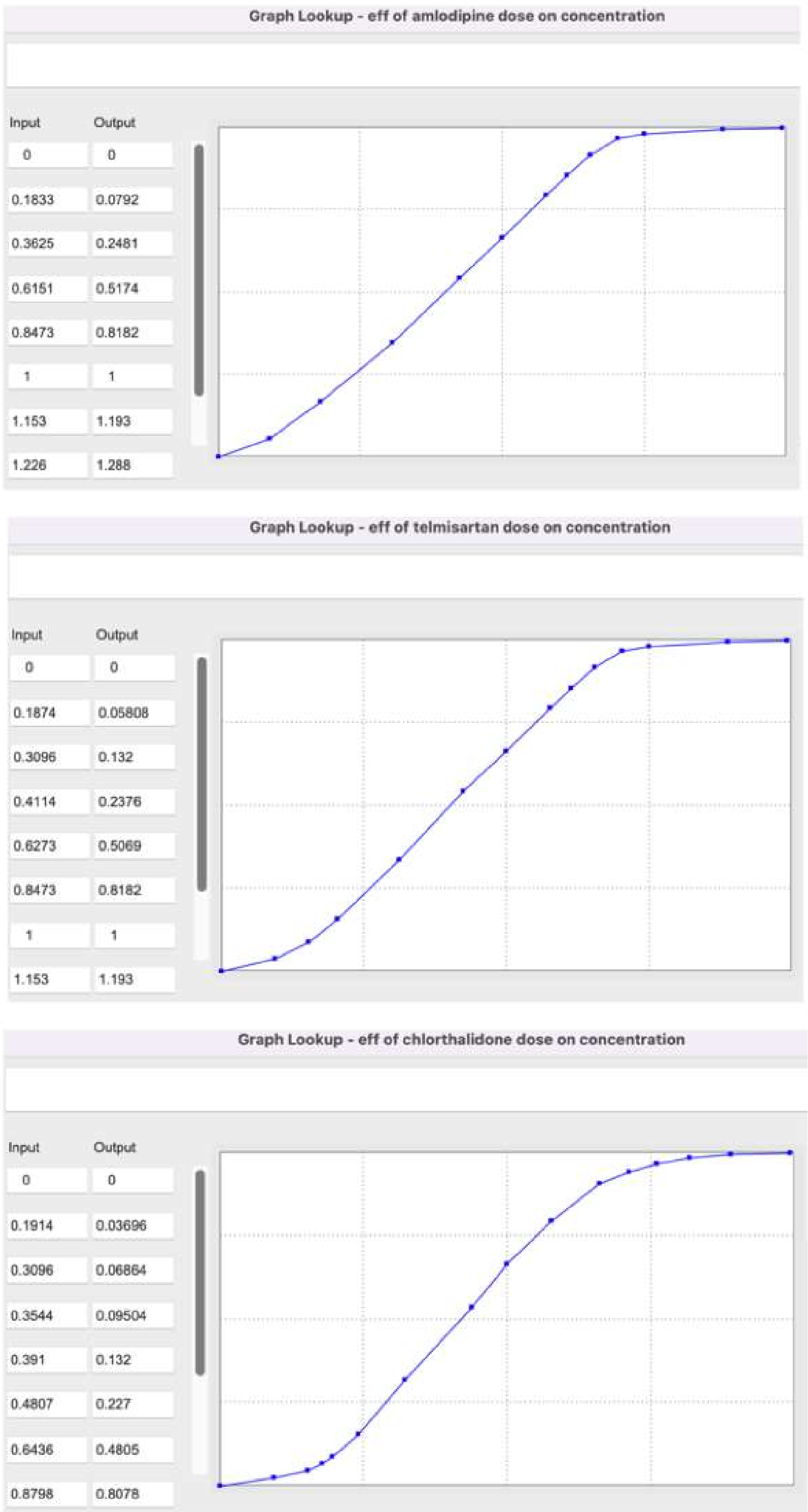

Figure 4.30. Graphical function for the effect of drug doses on concentration.

Average free concentration of the telmisartan in plasma is modeled as a stock variable due to the inertia of drug concentration in the body. The average free telmisartan concentration has a bi-flow as the concentration can increase or decrease through similar mechanism. The average free concentration of telmisartan concentration based on its flow can be calculated as

$$\begin{aligned} Avg.\ free\ telmisartan\ in\ plasma(t) &= (telmisartan\ concentration) \\ &\times (t - dt) + (change\ in\ avg.\ telmisartan) \times dt. \end{aligned} \tag{4.95}$$

Average free concentration of the chlorthalidone in plasma is modeled as a stock variable due to the inertia of drug concentration in the body. The average free chlorthalidone concentration has a bi-flow as the concentration can increase or decrease through similar mechanism. The average free concentration of chlorthalidone concentration based on its flow can be calculated as

$$\begin{aligned} Avg.\ free\ chlorthalidone\ in\ plasma(t) &= (chlorthalidone\ concentration) \\ &\times (t - dt) + (change\ in\ avg.\ chlorthalidone) \times dt. \end{aligned} \tag{4.96}$$

When a new amlodipine dose has been taken every day the amlodipine average daily concentration can change over time by a biflow. This change occurs over an adjustment time which can be expressed

$$\begin{aligned} change\ in\ avg.\ amlodipine &= [(Amlodipine\ concentration\ in\ plasma) \\ &- (Avg.\ free\ amlodipine\ in\ plasma)]/avg.\ amlodipine\ adj\ time. \end{aligned} \tag{4.97}$$

When a new telmisartan dose has been taken every day the telmisartan average daily concentration can change over time by a biflow. This change occurs over an adjustment time which can be expressed

$$\begin{aligned} change\ in\ avg.\ telmisartan &= [(Telmisartan\ concentration\ in\ plasma) \\ &- (Avg.\ free\ telmisartan\ in\ plasma)]/avg.\ telmisartan\ adj\ time. \end{aligned} \tag{4.98}$$

When a new chlorthalidone dose has been taken every day the chlorthalidone average daily concentration can change over time by a biflow. This change occurs over an adjustment time which can be expressed

$$\begin{aligned} change\ in\ avg.\ chlorthalidone = [(&Chlorthalidone\ concentration\ in\ plasma) \\ - (Avg.\ free\ chlorthalidone\ in\ plasma)]/&avg\ chlorthalidone\ adj\ time. \end{aligned} \tag{4.99}$$

The Graphical functions for the effect functions of amlodipine is given in Figure (4.31). The graph is drawn based on normalized dose of amlodipine.

To represent the effects of amlodipine on arterial tone, first, the average weekly free amlodipine concentration was normalized by its standard dose value. The effects of amlodipine at normalized doses to arterial tone can be expressed as

$$eff\ of\ amolodipine\ on\ arterial\ tone = f(\frac{amlodipine\ weekly\ average\ dose}{std.\ free\ amlodipine\ at\ std.\ dose}). \tag{4.100}$$

To represent the effects of amlodipine on contractility, first, the average weekly free amlodipine concentration was normalized by its standard dose value. The effects of amlodipine at normalized doses to contractility can be expressed as

$$eff\ of\ amolodipine\ on\ contractility = f(\frac{amlodipine\ weekly\ average\ dose}{std.\ free\ amlodipine\ at\ std.\ dose}). \tag{4.101}$$

To represent the effects of amlodipine on hearth rate, first, the average weekly free amlodipine concentration was normalized by its standard dose value. The effects of amlodipine at normalized doses to hearth rate can be expressed as

$$eff\ of\ amolodipine\ on\ heart\ rate = f(\frac{amlodipine\ weekly\ average\ dose}{std.\ free\ amlodipine\ at\ std.\ dose}). \tag{4.102}$$

Based on these effect functions of amlodipine in Figure 4.31, it amplodipine effects radius of blood vessels.

Figure 4.31. Graphical function for the effect of amplodipine on the related structures.

The implied value of radius based on the effect of amplodipine and other factors can be calculated as

$$\begin{aligned} Implied\ radius = {} & (Normal\ arterial\ tone) \\ & \times (eff\ of\ SNS\ on\ arterial\ tone) \\ & \times (eff\ of\ AT2\ on\ arterial\ tone) \\ & \times (eff\ of ADH\ on\ arterial\ tone) \\ & \times (eff\ of\ amolodipine\ on\ arterial\ tone). \end{aligned} \tag{4.103}$$

Based on these effect functions of amlodipine in Figure 4.31, it amplodipine effects hearth rate.

Therefore the implied hearth rate based on the effect of amplodipine and other factors can be calculated as

$$\begin{aligned} Implied\ heart\ rate = {} & (normal\ heart\ rate) \\ & \times (eff\ of\ SNS\ on\ heart\ rate) \\ & \times (eff\ of\ PNS\ on\ heart\ rate) \\ & \times (eff\ of\ amolodipine\ on\ heart\ rate). \end{aligned} \tag{4.104}$$

Based on these effect functions of amlodipine in Figure 4.31, it amplodipine effects contractility.

Therefore the implied contractility based on the effect of amplodipine and other factors can be calculated as

$$\begin{aligned} Contractility = {} & (normal\ contractility) \\ & \times (eff\ of\ SNS\ on\ contractility) \\ & \times (eff\ of\ PNS\ on\ contractility) \\ & \times (eff\ of\ amolodipine\ on\ contractility). \end{aligned} \tag{4.105}$$

To represent the effects of telmisartan on Angiotensin II, first, the average weekly free drug concentration was normalized by its standard dose value can be calculated as

$$eff\ of\ telmisartan\ on\ AT2 = f\left(\frac{telmisartan\ weekly\ avg.\ dose}{std.\ free\ telmisartan\ at\ std.\ dose}\right) \tag{4.106}$$

The graphical function for this effect relationship is given in Figure (4.32).

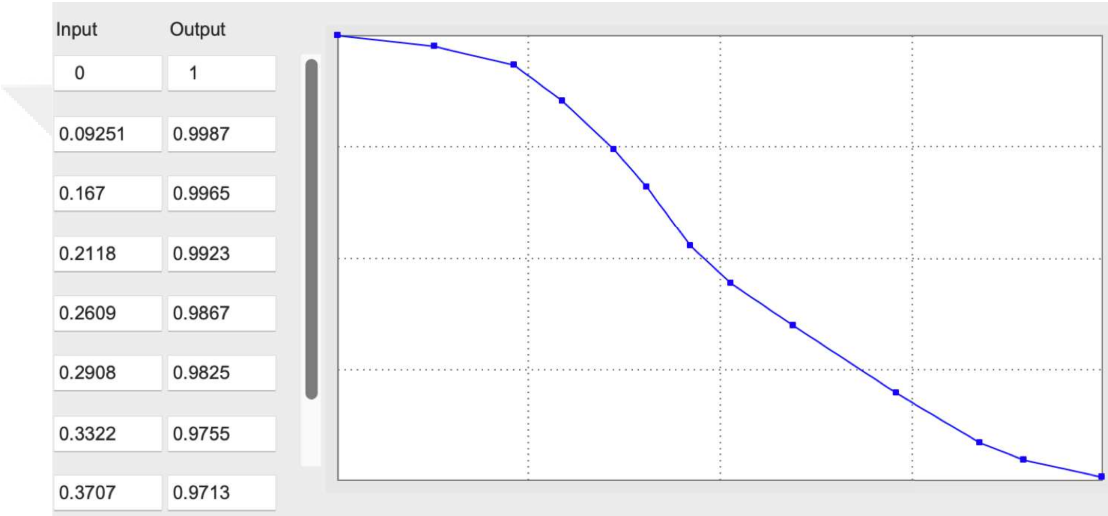

Figure 4.32. Graphical function for the effect of telmisartan on AT2.

Based on these effect functions of telmisartan in Figure 4.32 the implied Angiotensin II values is calculated as

$$Implied\ AT2 = (normal\ AT2) \times (eff\ of\ telmisartan\ on\ AT2). \tag{4.107}$$

To represent the the effects of the chlorthalidone on sodium removal first the average weekly free drug concentration was normalized by its standard dose value as

$$eff\ of\ chlorthalidone\ on\ Na\ removal = f\left(\frac{amlodipine\ weekly\ avg.\ dose}{std.\ free\ amlodipine\ at\ std.\ dose}\right). \tag{4.108}$$

Graphical function for this effect function is given in Figure 4.33. Based on these effect functions of telmisartan in Figure 4.33, the implied Angiotensin II values are calculated as

$$\begin{aligned} Implied\ Na\ removal = {} & (normal\ NA\ removal) \\ & \times (eff\ of\ GFR\ on\ na\ removal) \\ & \times (eff\ of\ chlorthalidone\ on\ na\ removal) \\ & \times (eff\ of\ concentration\ on\ na\ removal). \end{aligned} \tag{4.109}$$

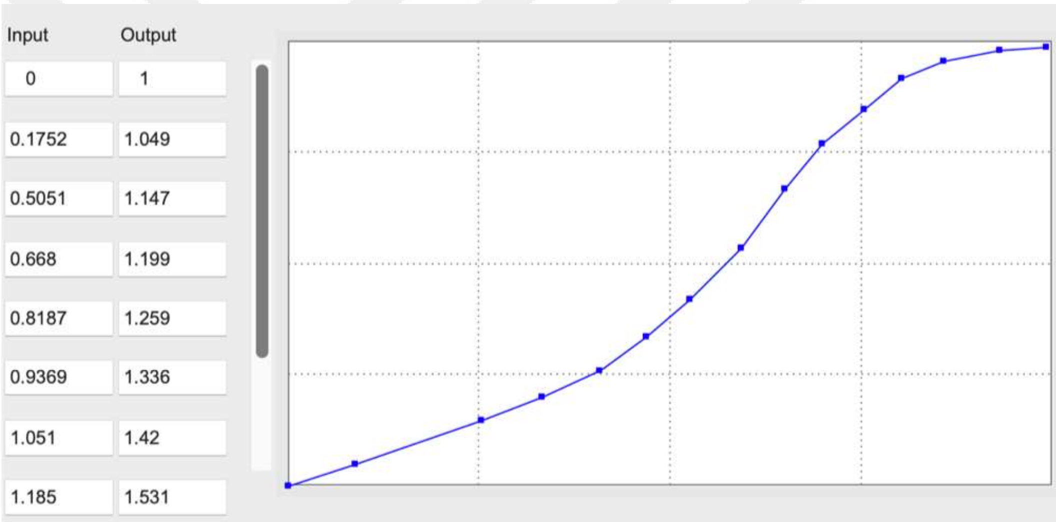

Figure 4.33. Graphical function for the effect of chlorthalidone on Na removal.

After patients start on a hypertensive treatment, they receive their medication daily, every day. Each drug takes its own time to reach its peak concentration, and then it is removed from the body. For drugs with extended clearance longer than one day, time average plasma concentration increases with each drug intake.

Parameters for the drug doses are adjusted to replicate the behavior observed in the pharmacodynamic studies. Simulated amlodipine plasma concentrations and pharmacokinetics in the literature are compared.

Figure 4.34 presents the dynamics of the amlodipine concentration when it is administered once compared with the data in literature [116].

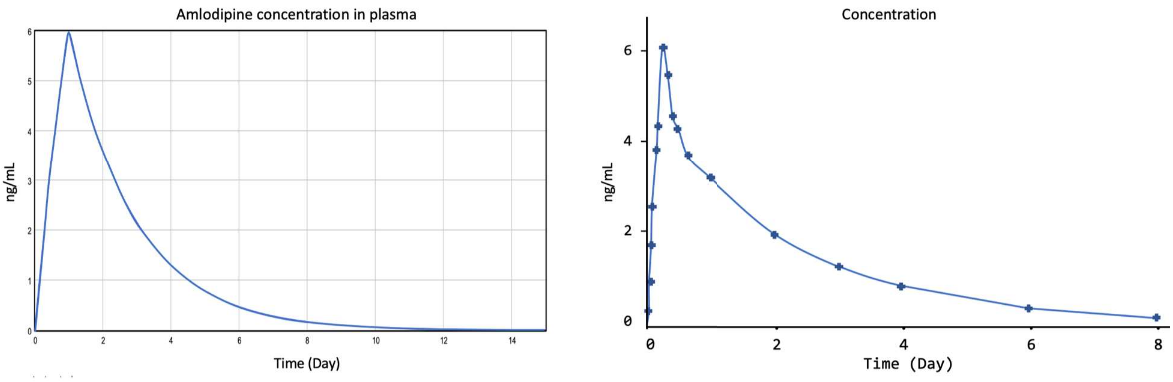

Figure 4.34. Amlodipine plasma concentration in model run, compared to the data in literature (reproduced from [116]).

Whereas, Figure 4.35 presents the dynamics of the amlodipine concentration when it is administered daily compared with the data in literature [117].

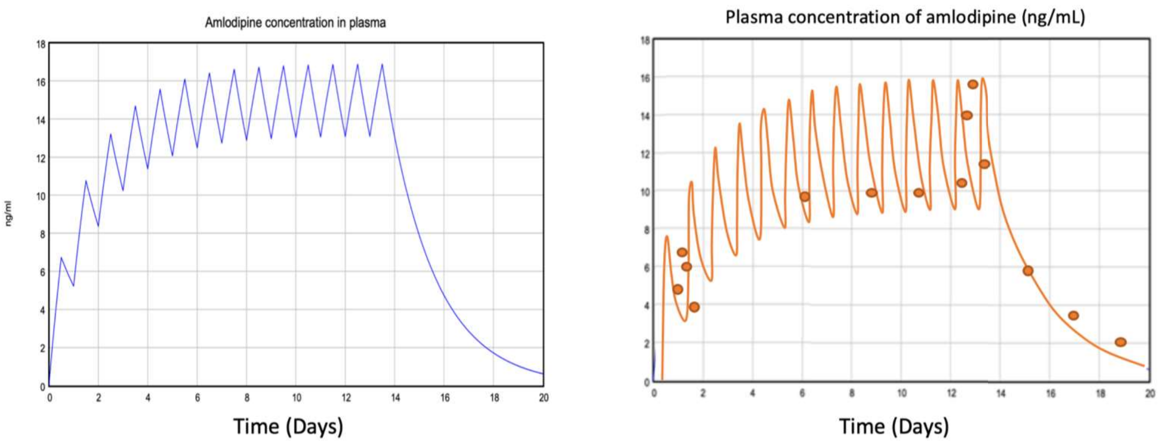

Figure 4.35. Amlodipine long term plasma concentration in model run, compared to the data in literature (reproduced from [117]).

Simulated telmisartan plasma concentrations and pharmacokinetics in the literature [118] are compared in Figure 4.36.

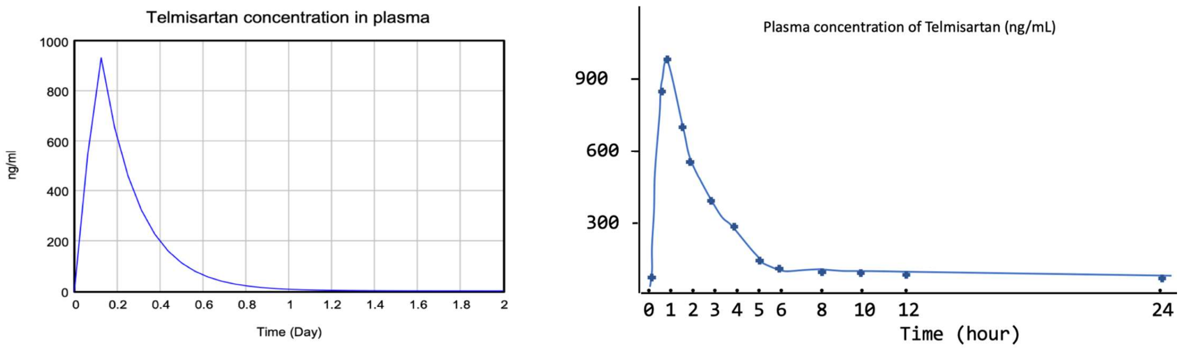

Figure 4.36. Telmisartan plasma concentration in model run, compared to the data in literature (reproduced from [118]).

Simulated chlorthalidone plasma concentrations and pharmacokinetics in the literature [119] are compared in Figure 4.37. As both telmisartan and chlorthalidone clear from the body in less than a day daily concentration of these drugs show the same dynamics every day.

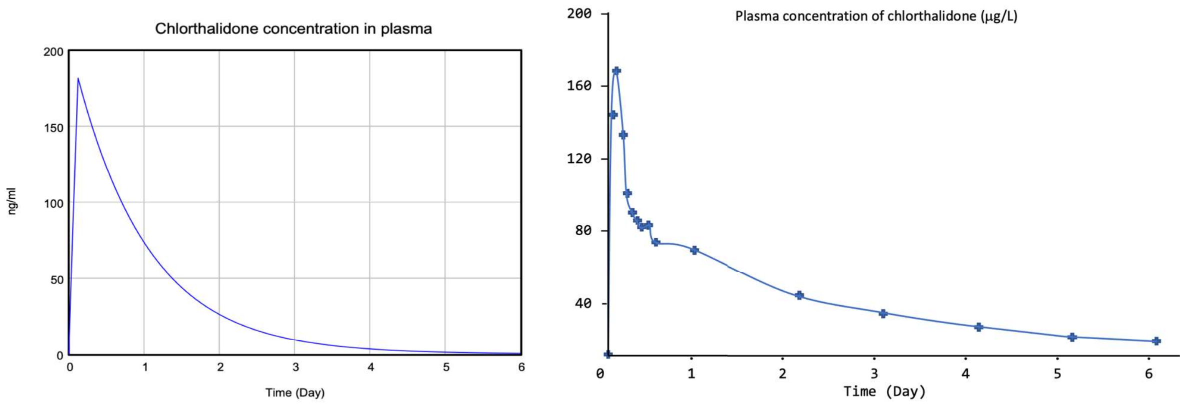

Figure 4.37. Chlorthalidone plasma concentration in model run, compared to the data in literature (reproduced from [119]).

At the beginning of the simulation the stock variables have initial values. Furthermore some of the formulations use constant values. The constant and initial values used in the treatment sector are given in Table 4.10.

Table 4.10. Constant variables for treatment sector.

Variable name	**Unit**	**Value**
amlodipine adj time	Day	2
amlodipine concentration at standard dose	ng/ml	30
amlodipine removal rate	Day	2
average amlodipine adj time	Day	7
average chlorthalidone adj time	Day	7
average free amlodipine at standard dose	ng/ml	25
average free chlorthalidone at standard dose	ng/ml	0.8
average free telmisartan at standard dose	ng/ml	200
average telmisartan adj time	Day	3
chlorthalidone adj time	Day	7
chlorthalidone concentration at standard dose	ng/ml	5
chlorthalidone removal rate	Day	10
standard amlodipine dosing	mg	5
standard chlorthalidone dosing	mg	7
standard telmisartan dosing	mg	40
telmisartan adj time	Day	3
telmisartan concentration at standard dose	ng/ml	800
telmisartan removal rate	Day	1.2
time to take weekly avg dose	Day	7

5. MODEL BEHAVIOR AND VALIDATION

In order to build confidence in the structure of the model, the model behavior is evaluated under extreme conditions [86]. To assess the structure of the model, the following extreme condition tests are conducted: removing aging factors, water loading, sodium loading, hemorrhagic shock, and acute kidney damage. After building confidence in the structural validity of the model, its behavioral validity is tested by comparing it with studies that reflect real-life dynamics.

5.1. Removing Ageing Factors

Under normal circumstances, the human body maintains homeostasis. Therefore, the model is expected to stay in equilibrium when the aging factors are removed and without any disturbances.

To verify this, the model is run by parameter values for a healthy individual and neutralizing the effects of aging as the first step in validation. Hence, the equilibrium run assumes that physiological mechanisms such as kidney and vascular function do not deteriorate over time.

The expected outcome for parameters is to stay constant. Model runs show that parameters remain in healthy equilibrium levels, as seen in Figure 5.1.

When the vascular function is preserved, the resistance does not increase over time, and when kidney function is stable, the total body water is maintained. The sympathetic nervous system is not triggered with stable blood pressure, and the resting heart rate remains in equilibrium. This demonstrates that without the aging and exogenous factors, all other feedback loops balance each other in equilibrium.

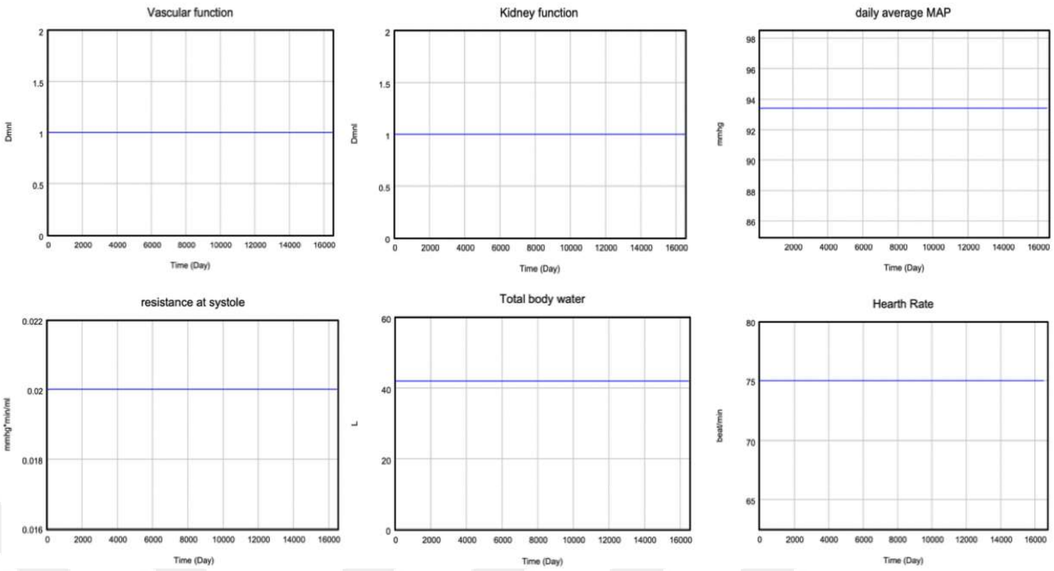

Figure 5.1. Removing ageing factors and equilibrium.

5.2. Water Loading

This test evaluates the effect of increasing total body water to an extreme level by adjusting water intake to ten times the average for one day. Consequently, total body water, extracellular fluid, and blood volume increase, and cardiac output increases with more blood delivered to the heart. As a result of this test, an elevation in blood pressure is expected. This behavior was tested with animal trials and then modeled by calibrating to humans by Guyton *et al.* [84]. Therefore, projections of this study in Figure 5.2 can be compared to findings in the literature [84] given in Figure 5.3. The increase in blood pressure triggers baroreceptors, and the sympathetic nervous system is deactivated. As a result, the arterial tone is increased. However, baroreceptors adjust to higher blood pressure levels due to resetting after a certain point. This causes the sympathetic nervous system to become active despite elevated blood pressure. Hence, the total peripheral resistance starts to increase after the initial drop. For this reason, despite the fluid levels turning back to the initial point, the blood pressure remains elevated for a longer time. In conclusion, the simulation runs align with the expected dynamic behavior for the volume loading test.

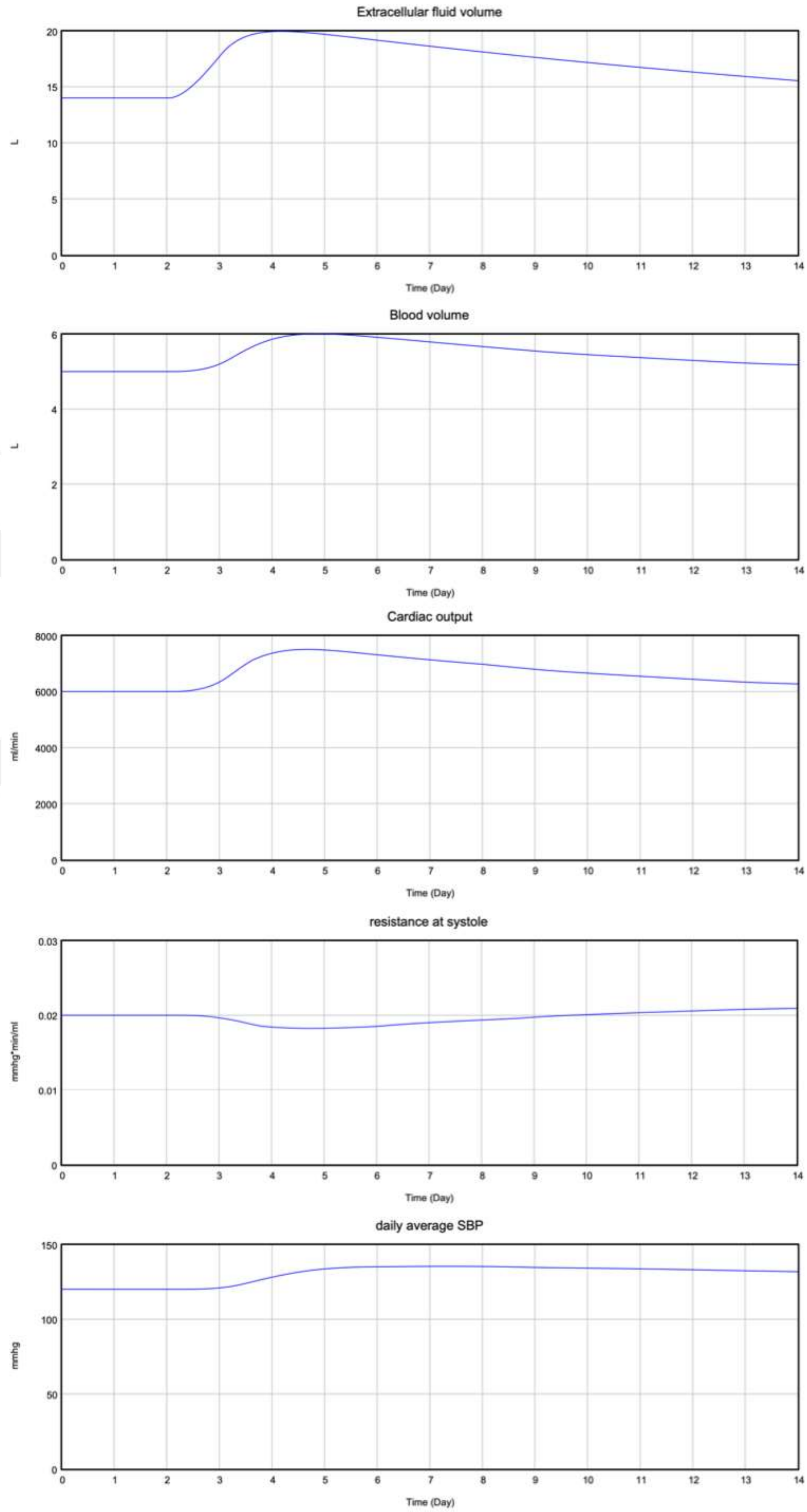

Figure 5.2. Volume loading run and blood pressure dynamics.

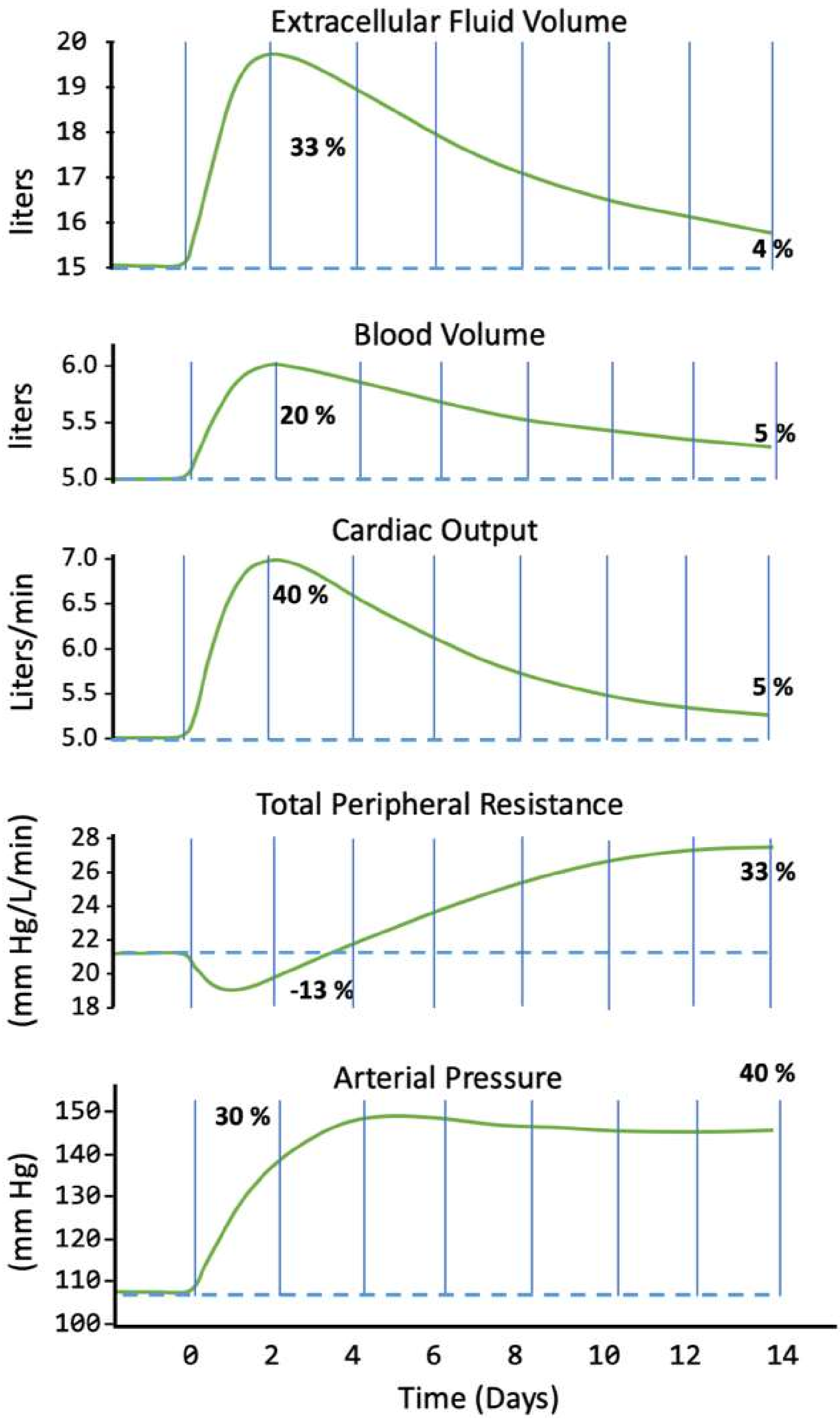

Figure 5.3. Volume loading results from Guyton and Hall model (reproduced from [84]).

5.3. Sodium Loading

This test evaluates the effect of increasing sodium intake to ten times of average daily sodium intake for one day. A high sodium load increases total body salt and osmolality. The expected behavior of this extreme condition test is observing an increase in body volume and blood pressure.

The increased sodium concentration causes water to be retained in the body through the following mechanisms. With the higher osmolality, the antidiuretic hormone secretion increases, causing urine concentration to be higher in salt. Thus, water is reabsorbed and retained in the body, which can be observed as the water removal initially decreases over time.

Higher osmolality also causes thirst and increases the water intake to balance sodium concentration in the body. Therefore, total body water increases, followed by an increase in extracellular fluid volume, blood volume, and cardiac output. These relationships are given in Figure 5.4.

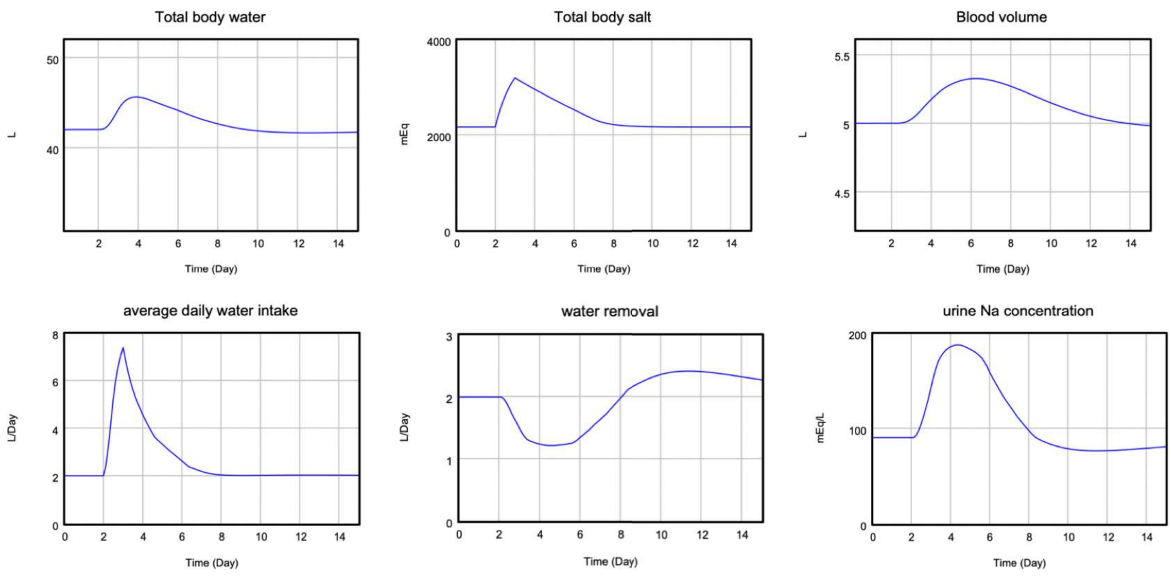

Figure 5.4. Sodium loading and body fluid dynamics.

An increase in blood pressure inhibits central nervous system activities and activates parasympathetic. However, with time the operating point of baroreceptors increases and adjusts to the higher-pressure levels. Therefore, even though the blood pressure is reduced, it remains slightly elevated compared to the initial pressure shown in Figure 5.5.

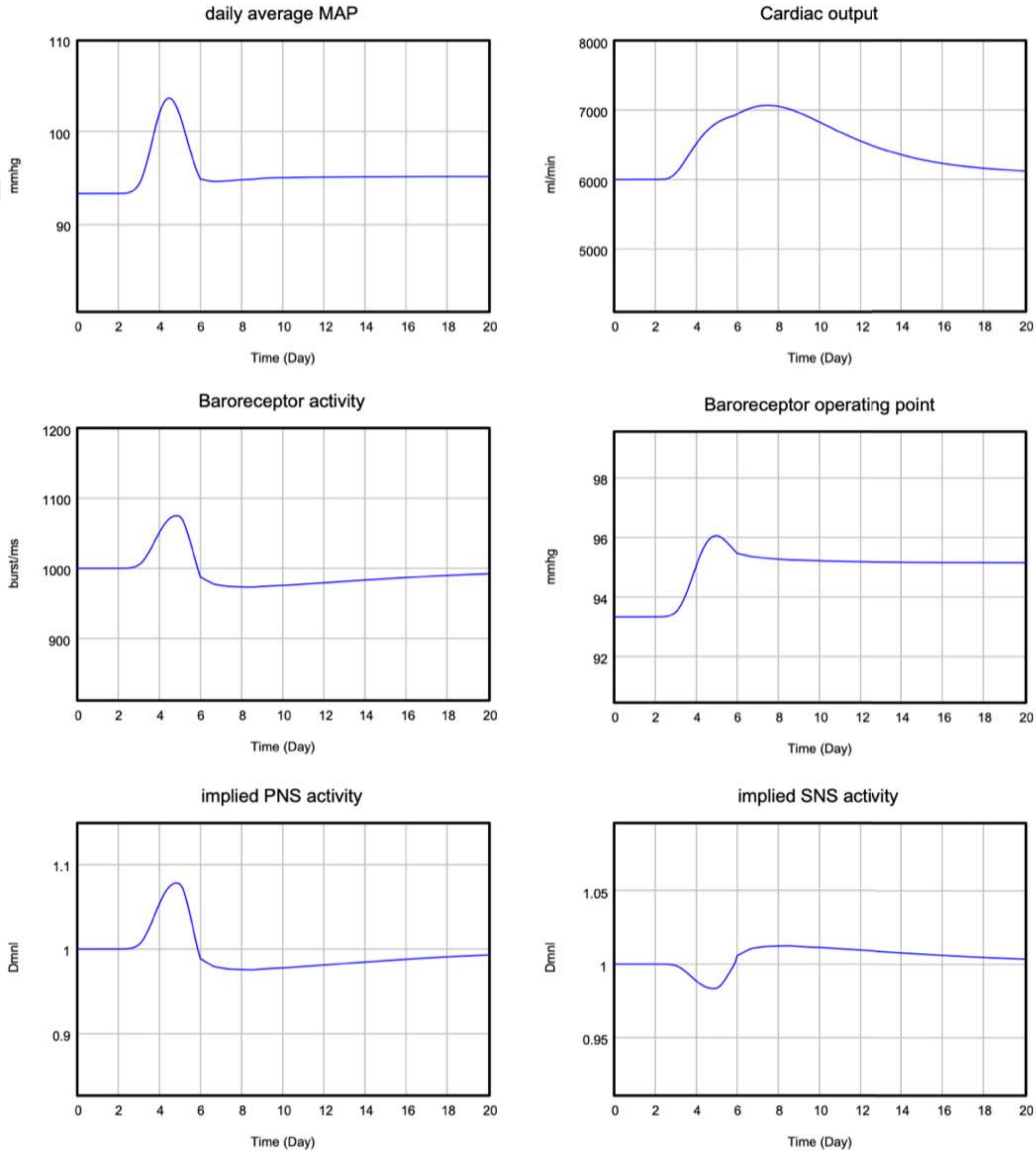

Figure 5.5. Sodium loading blood pressure and SNS activity.

In the Figure 5.5 and, Figure 5.4, it can be seen that even though it takes a long time for fluid levels to return to normal, the blood pressure is regulated quickly as the sympathetic nervous system acts faster than hormonal regulatory mechanisms responsible for fluid regulation. Consequently, total body water, extracellular fluid, and blood volume increase, and cardiac output increases with more blood delivered to the heart similar to water load experiment [84].

Increased blood pressure also inhibits renal sympathetic nervous system activity and renin activity. With a decrease in renin production concentration, angiotensin II in the blood decreases. Angiotensin II is a vasoconstrictor, and with a lower concentration, the arterial smooth muscles relax and reduce peripheral resistance. The antidiuretic hormone is regulated by osmolality and renin. Therefore, antidiuretic hormone production increases initially and decreases later as osmolality acts faster than the hormonal control mechanism.

Furthermore, decreased angiotensin II reduces the release of the aldosterone hormone. With declined aldosterone concentration, epithelial cells of the kidneys are not stimulated, reducing the reabsorption of salt and water. The behavior of these feedback loops that represent the compensation mechanisms of the kidney hormones is given in Figure 5.6.

However, the operating point of baroreceptors increases and adjusts to the higher-pressure levels. Therefore, even though the blood pressure is reduced, it remains slightly elevated compared to the initial pressure.

Later, these findings were compared with animal experiments [120]. Literature shows that with an increased sodium diet, the blood pressure increases, and after the high sodium diet is stopped, blood pressure decreases. It can be concluded that simulation runs align with the expected dynamic behavior for the high sodium diet test. In conclusion, the simulation runs align with the expected dynamic behavior for the sodium loading test.

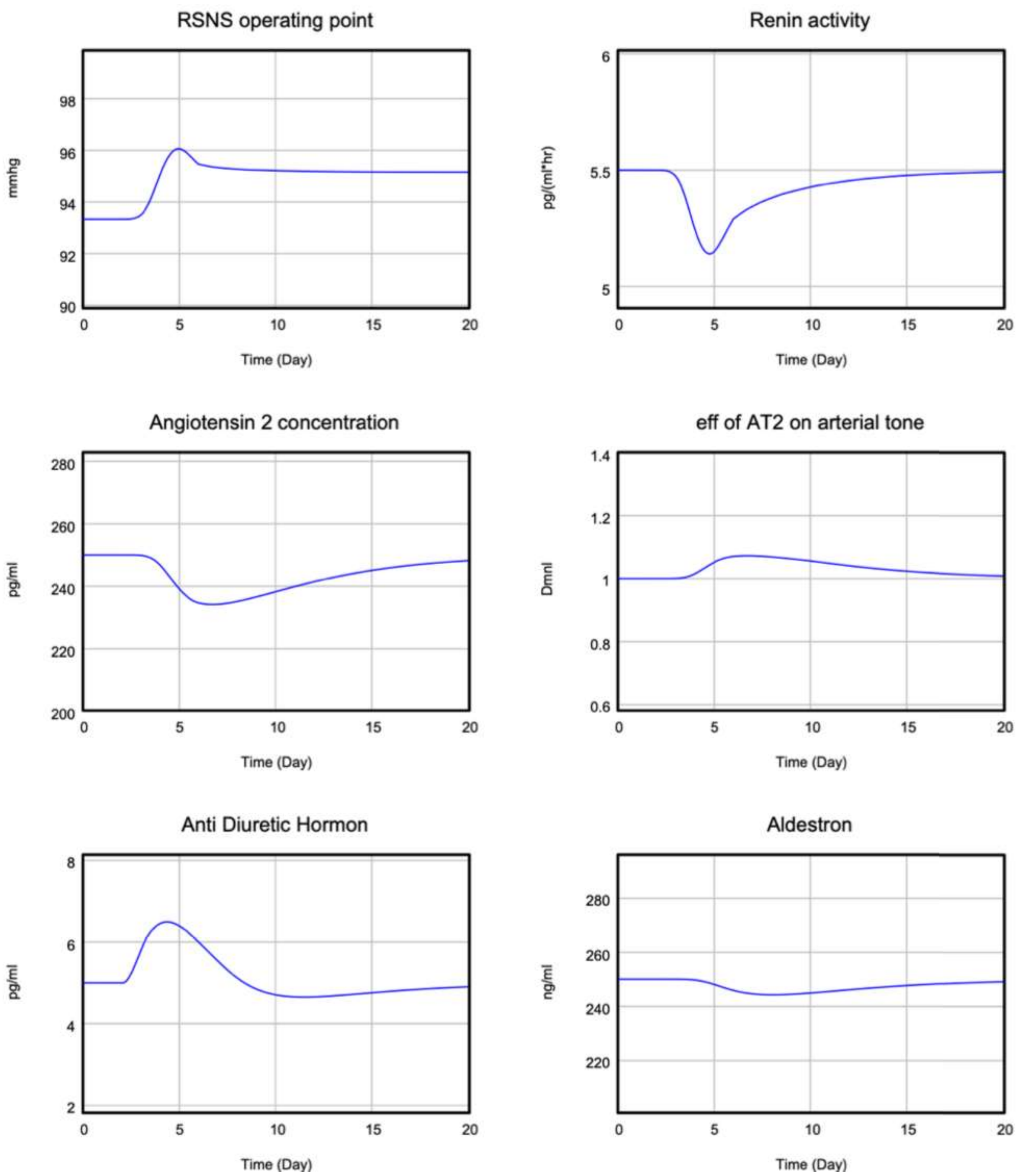

Figure 5.6. RSNS activity after Na load and hormonal control mechanisms.

5.4. Hemorrhagic Shock

This extreme condition test is opposite to the volume loading as hemorrhage or bleeding decreases the cardiac output and blood pressure. The expected outcome of this test is for mean arterial pressure to drop suddenly. As given in Figure 5.7 , the model was able to capture this behavior.

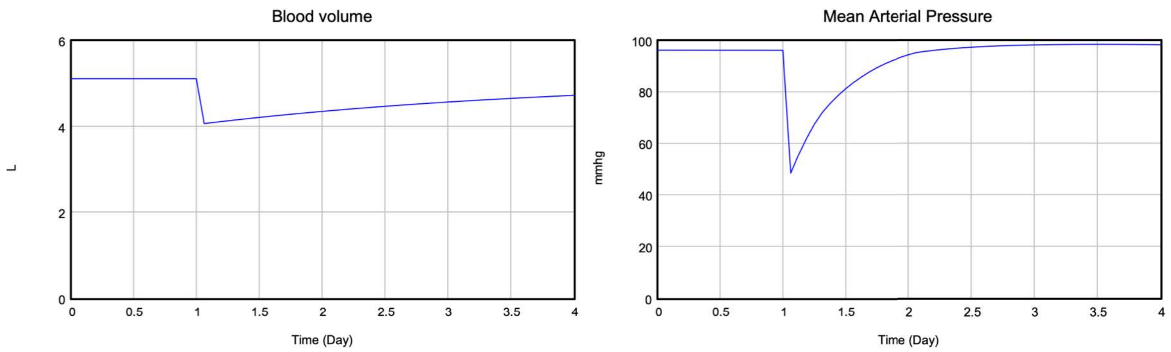

Figure 5.7. Blood loss and sudden drop in blood pressure.

The Figure 5.7 shows that blood volume takes a long time to recover as it is regulated by fluid intake, and adjustment is slower. However, an average blood pressure level is achieved before blood volume can recover. In this case, blood pressure regulation is achieved by the activation of other control mechanisms.

Renin produced in the kidneys gets transformed into angiotensin II. angiotensin II is a potent vasoconstrictor that acts on arterial muscles, increases peripheral resistance, and elevates blood pressure. Angiotensin II also triggers the release of the aldosterone hormone. Aldosterone stimulates the epithelial cells of the kidneys to increase the reabsorption of salt and water.

When blood pressure drops, the central nervous system responds, and the sympathetic nervous system is activated. This increases heart rate and contractility of the heart. As a result, cardiac output is increased. Furthermore, activation of the sympathetic nervous system stimulates blood vessels to constrict. With vasoconstriction, total peripheral resistance increases and boosts blood pressure. This process is demonstrated in Figure 5.8.

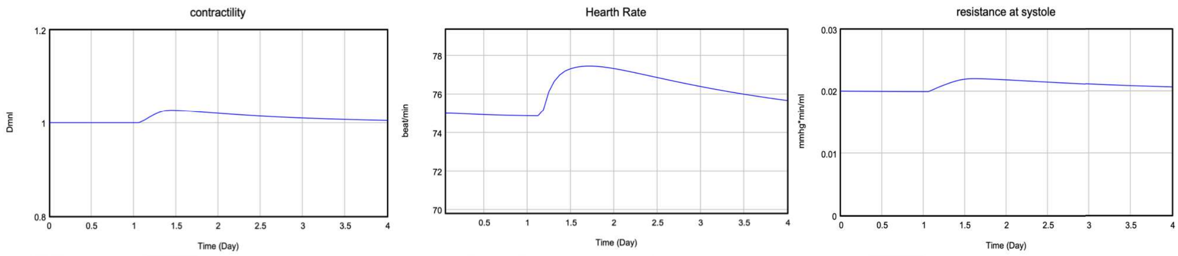

Figure 5.8. Bloos loss compensation mechanisms.

Later, these findings were compared with animal experiments [121]. Literature shows that after a hemorrhagic shock, the heart rate increases, and the blood pressure recovers to its normal values. It can be concluded that simulation runs align with the expected dynamic behavior for the hemorrhagic shock test.

5.5. Acute Kidney Damage

This extreme condition test evaluates the effect of acute kidney damage and 70% kidney function loss in one day. As a result of kidney damage, the glomerular filtration rate and the amount of sodium that can be filtered out of the body decrease. Sodium filtration is slightly increased through control mechanisms; however, this effect is weaker than kidney damage. Therefore, total body salt would accumulate if the patient does not change their sodium intake. The increased total body salt causes water to be retained to regulate sodium concentration in the body. Total body water increases when sodium concentration increases and water removal decreases. As given in Figure 5.9, the model was able to capture this behavior.

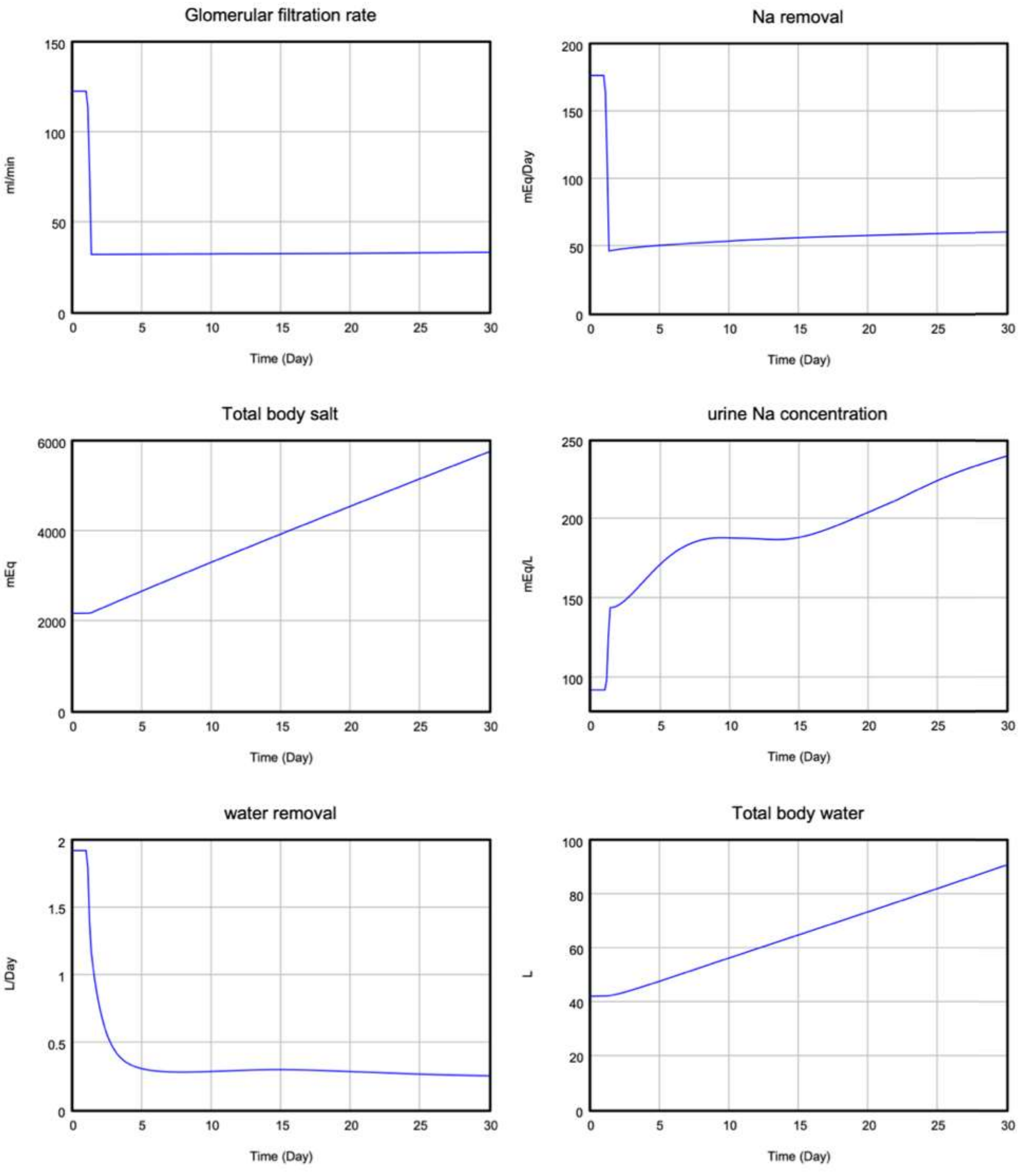

Figure 5.9. Effects of acute kidney damage on water regulation systems.

Consequently, extracellular fluid and blood volume increase, and cardiac output increases as more blood is delivered to the heart. Therefore, as a result of this test, elevation in blood pressure is expected to increase. Even though the total body increase rises over time, the blood volume and stroke volume saturate after a certain value. Excess total water causes edema in the body. This relationship can be seen in Figure 5.10.

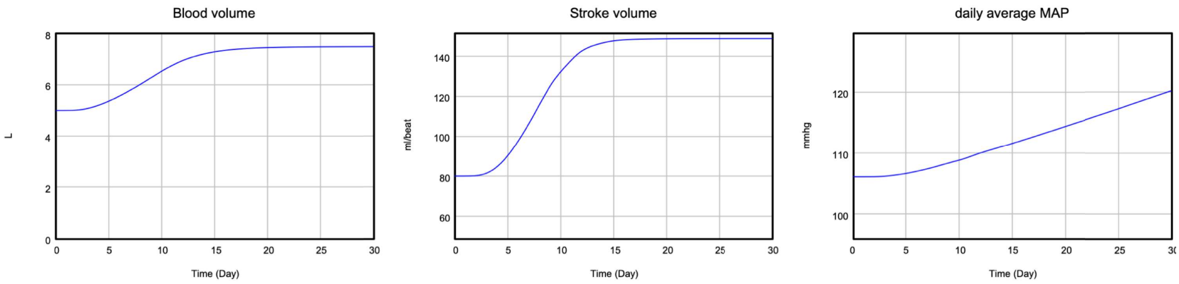

Figure 5.10. Fluid dynamics and blood pressure after kidney damage.

An increase in blood pressure also inhibits renal sympathetic nervous system activity and renin activity with a decreased renin production concentration of angiotensin II in the blood decreases. The arterial smooth muscles relax with a drop in angiotensin II, and peripheral resistance decreases. Furthermore, decreased angiotensin II reduces the release of the aldosterone hormone. With declined aldosterone concentration, epithelial cells of the kidneys are not stimulated, reducing the reabsorption of salt and water. The antidiuretic hormone is regulated by osmolality and renin; therefore, its production increases initially and reduces later as osmolality acts faster than the hormonal control mechanism. The behavior of these feedback loops representing the compensatory mechanisms of kidney hormones is given in Figure 5.11. Similarly, an increase in blood pressure triggers baroreceptors and the nervous system. Then the sympathetic nervous system is deactivated, and the parasympathetic system is activated. As a result, the arterial tone is increased, and the heart rate is reduced in parallel with expectations explained in the literature [122, 123].

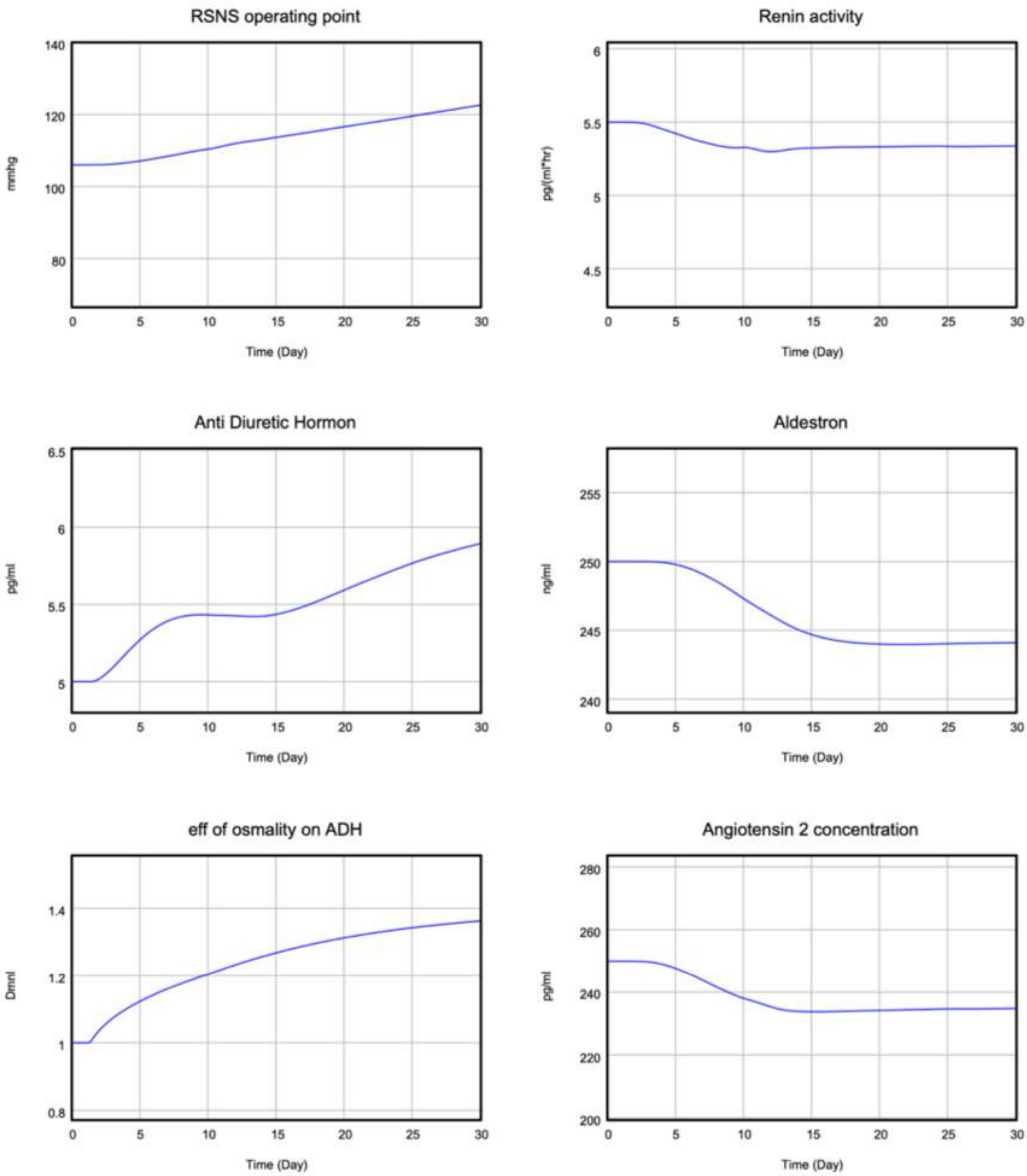

Figure 5.11. Hormonal dynamics after kidney damage.

6. HYPERTENSION DEVELOPMENT DYNAMICS FOR DIFFERENT PROFILES

By definition, in essential hypertension underlying cause of the disease is unknown. However, there are several hypotheses on the pathogenesis of the disease. With the help of the model that covers the relevant sub-systems this study can demonstrate three mechanisms leading to primary hypertension: the over-active nervous system, the over-active renin-angiotensin-aldosterone system (RAAS), and low sodium excretion (salt retention).

In this section, five scenarios are defined to represent inter-patient physiological differences: healthy individual, patient with an over-active nervous system, patient with over-active RAAS, patient with low sodium excretion, and patient with all three pathophysiological mechanisms. Firstly, the blood pressure trends are presented for a healthy individual for the baseline run. Then, three pathogenesis scenarios are analyzed exclusively. Finally, a scenario considering a combination of these pathophysiological mechanisms is simulated.

These scenarios representing patient profiles are summarized in Table 6.1. The columns present the pathophysiological mechanism, and the rows show the scenario. The plus representing the existence of the related pathogenesis mechanism, whereas the minus sign shows the normal function of the corresponding mechanism.

6.1. Healthy Individual: Baseline

First, the model is set to normal values to represent an average person. Then it is run for 16500 days, roughly equal to 45 years, representing a patient's life between 30 and 75 years. The objective of this run is to compare the model's behavior to real-life observations.

Table 6.1. Inter-patient physiological differences for scenario analysis.

Scenario	Overactive SNS	Overactive RAAS	Low sodium excretion
1 (base)	-	-	-
2	+	-	-
3	-	+	-
4	-	-	+
5	+	+	+

Data have been scarce for an individual's blood pressure over the years. Therefore, population data is used to compare the baseline of the model. Simulated blood pressure results are compared with the longitudinal blood pressure data collected for the US National Health and Nutrition Examination Survey [124]. This data focuses on individuals who are not receiving any hypertension treatment.

Average blood pressure measuring in the population is given together with simulation runs in Figure 6.1. The green line presents the diastolic blood pressure. The red line shows the systolic blood pressure of the model projections.

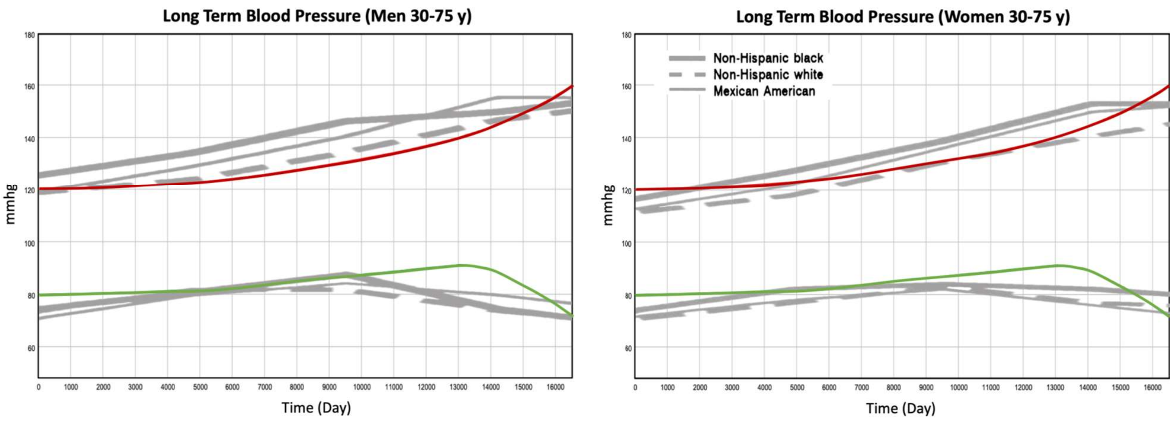

Figure 6.1. Blood pressure dynamics in long term compared to US NHANES data (reproduced from [124]).

The Figure 6.1 shows that the average population's diastolic blood pressure tends to decrease, whereas systolic pressure constantly increases. When the model is set to the baseline parameter for a healthy individual, the projection present similar blood pressure dynamics.

Figure 6.2 shows the dynamics of vascular function and its effects on other factors. Endothelial function is lost with aging, and vascular function decreases over time. Hastening in vascular function loss occurs due to a reinforcing loop between systolic blood pressure and vascular function loss. With vascular function loss, average blood pressure increases, and higher blood pressure causes the deterioration process to accelerate further, increasing blood pressure.

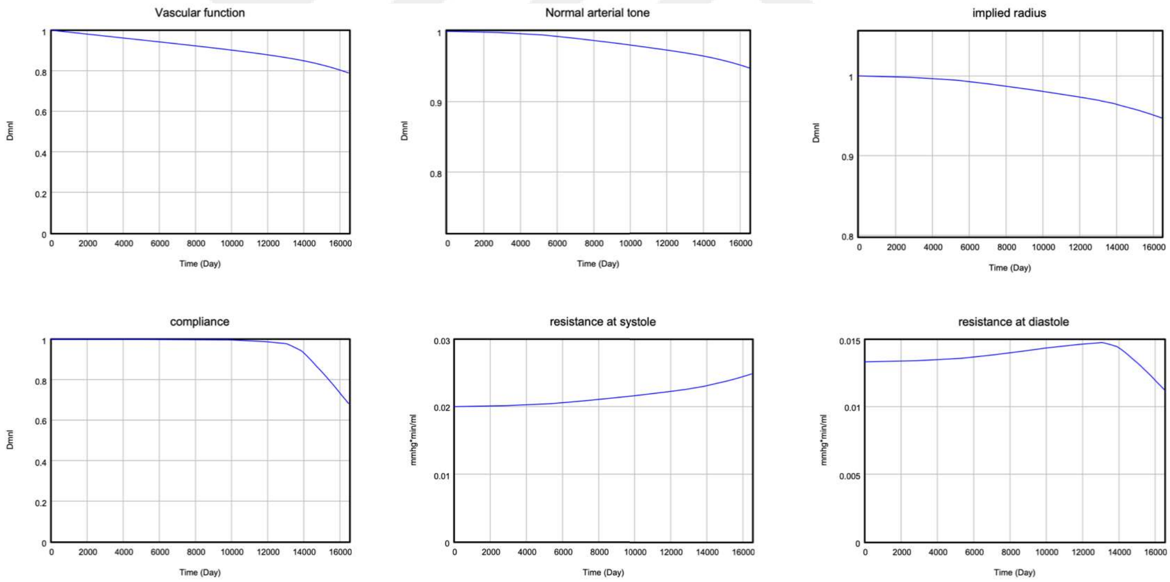

Figure 6.2. Dynamics of vascular factors for a patient over ages 30-75.

There are two effects of vascular function loss on another factor. First, increase in the smooth muscle constriction at the vessels. In a healthy patient, when blood pressure increases parasympathetic nervous system is deactivated, and vascular muscles relax. However, with vascular function loss, vascular muscles remain constricted when the blood pressure rises. This decreases their normal tone, and as the radius of the arteries becomes narrower, the total peripheral resistance increases.

The second effect of vascular function loss is the decline in compliance. As a result, vessels lose their ability to recoil. This effect is observed when the heart is at its diastole state. In Figure 6.2, it can be observed that resistance at systole constantly increases resistance at diastole decreases after a point.

Figure 6.3 shows the dynamics of kidney function and its effects on other factors. Kidney function is lost with aging, and the glomerular filtration rate decreases over time. Therefore, the amount of water and salt that can be filtered out of the body decreases, and extracellular fluid and blood volumes increase. As more blood is delivered to the heart, cardiac output increases, elevating the blood pressure.

Kidney function loss accelerates over time due to a reinforcing loop between systolic blood pressure and kidney function loss. With kidney function loss, average blood pressure increases, and higher blood pressure causes the deterioration process to accelerate further, increasing blood pressure.

In the short term, the baroreceptors are triggered by increased blood pressure. As a result, the sympathetic nervous system is deactivated, and the parasympathetic system is activated. Furthermore, the renal sympathetic nervous system activity is inhibited, leading to a decrease in renin production. These processes aid in keeping the blood pressure under control. However, as this change in blood pressure is slow, the baroreceptors reset and become desensitized to chronic elevation in pressure.

The operating point of baroreceptors and renal sympathetic nervous system increases and adjusts to the higher-pressure levels. Resetting reduces the response of these control systems at high levels of mean arterial pressure. Figure6.4 shows that the operating point of baroreceptors and the renal sympathetic nervous system change over time, and baroreceptor and renin activity remain constant.

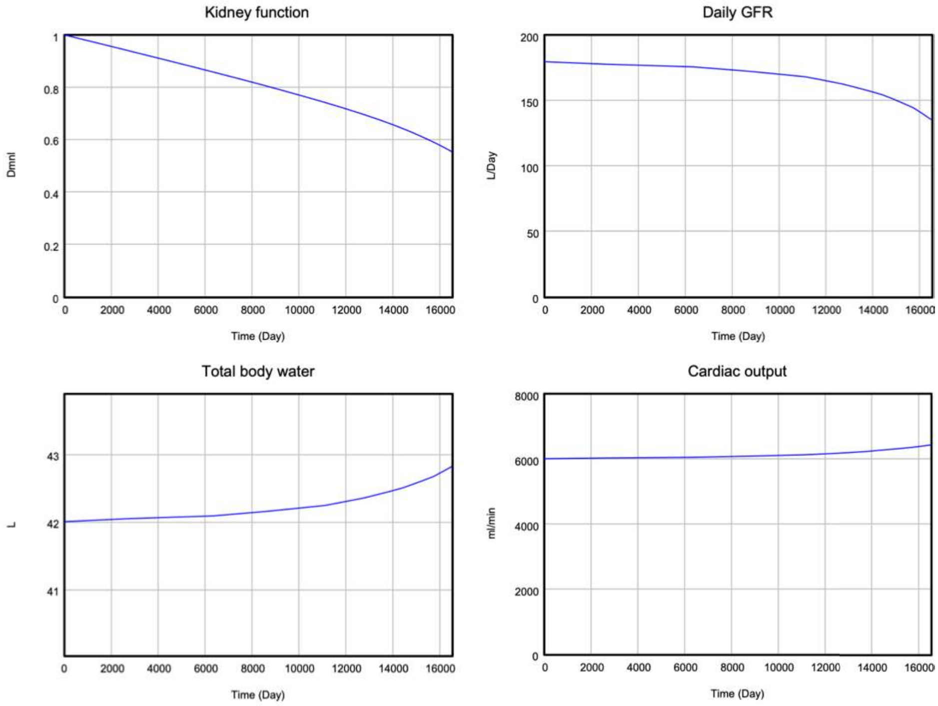

Figure 6.3. Dynamics of renal factors of a patient over ages 30-75.

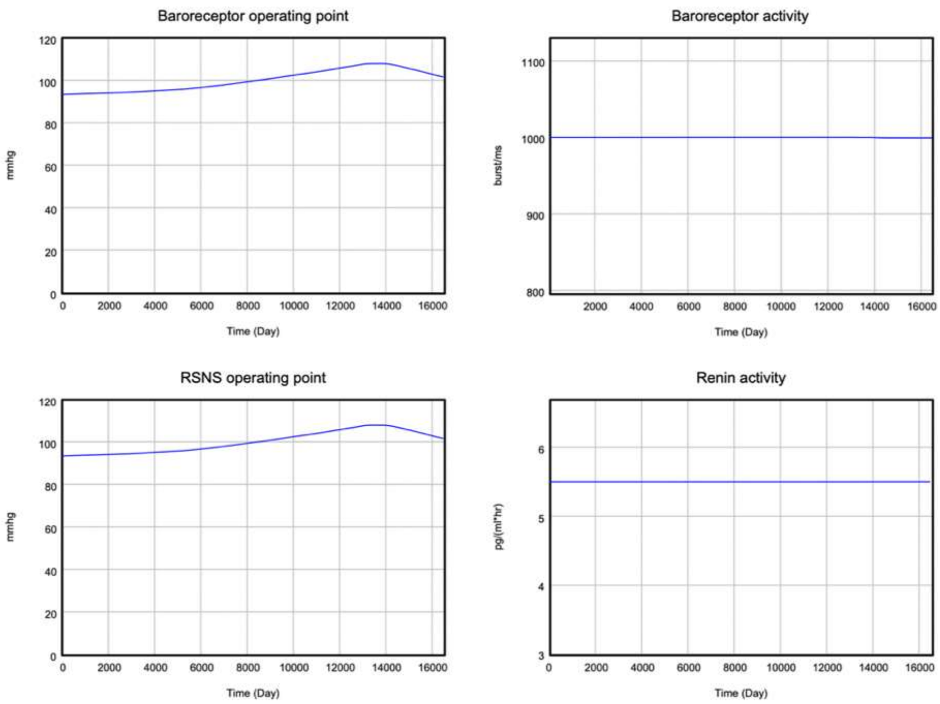

Figure 6.4. Shift of baroreceptor operating point.

It can be concluded that simulation runs align with the expected long-term dynamic behavior. The model can capture increased systolic blood pressure and resistance at systole, decreased compliance and diastolic pressure, and baroreceptor resetting.

Furthermore, even in an extended run, model parameters remain in a realistic value. However, to compare different scenarios, a shorter-term analysis will be used. Therefore, after setting the model to normal values for an average individual, it is run for 3000 days.

6.2. Patient 1: Over-Active Sympathetic Nervous System (SNS)

Chronic stress or mental exhaustion can increase the basal sympathetic nervous system activity through persistent disturbing impulses [125]. To observe the effect of SNS over-activity effects of periodic stress and constant stress are analyzed. In Figure 6.5, the patient is introduced to high stress at different time intervals. In each trial, the intensity of the stimulation is the same; however, the repeating time is different.

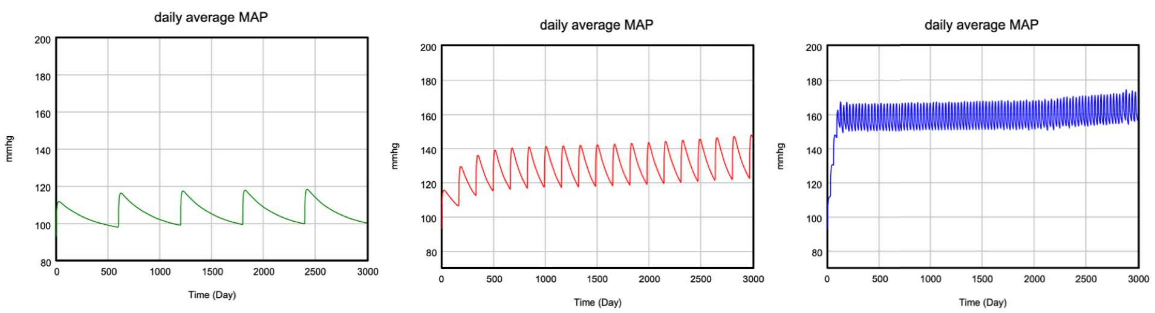

Figure 6.5. Effect of periodic stress on mean arterial pressure.

In the graph on the left, the interval between impulses is long enough for recovery; therefore, arterial pressure can return to its initial value. In the middle graph interval between impulses is not long enough, and the stress response accumulates over time, elevating the blood pressure.

However, after a certain point, blood pressure does not increase further. The right graph can be interpreted as the frequency of the stimulation increasing elevation in blood pressure is higher. Later, the stress factor was removed after a certain point, as given in Figure 6.6. In the left graph, the blood pressure can return to its initial value; however, in trials with higher stress frequency, the bold pressure does not return to its initial value.

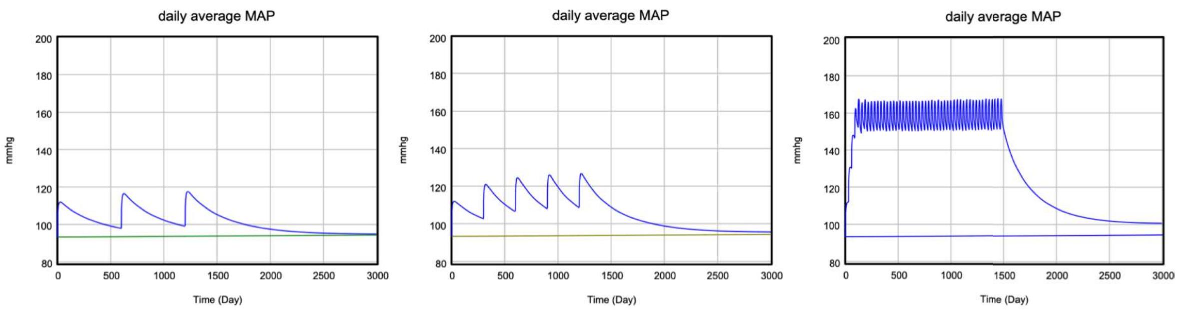

Figure 6.6. Effect of removing periodic stress on mean arterial pressure.

The main reason for blood pressure to sustain high after removing stress factors is due to the damage that occurs in the blood pressure control structures. There is a positive feedback structure with blood pressure and regulatory mechanism. Vascular function loss causes blood vessels to remain constricted and increase blood pressure. Kidney function loss hinders the body's ability to remove salt and water, and the excess volume increases pressure. Higher blood pressure causes even more damage to these mechanisms. In Figure 6.7, the effect of periodic stress on kidney function is given, and in Figure 6.8, the impact of periodic stress on vascular function is presented.

In Figure 6.9, the effect of constant stress is presented. In this scenario, the sympathetic nervous system activity gradually increases for one year and remains constant at the over-active level. Based on the level of overactivity, the blood pressure sets at different severities from bottom to top: baseline, upper normal, hypertension grade 1, hypertension grade 2, and hypertension grade 3.

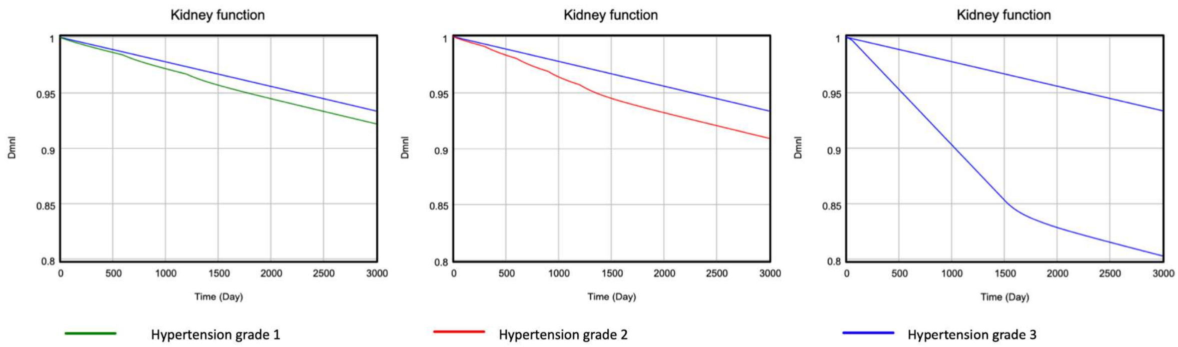

Figure 6.7. Effect of periodic stress on kidney function.

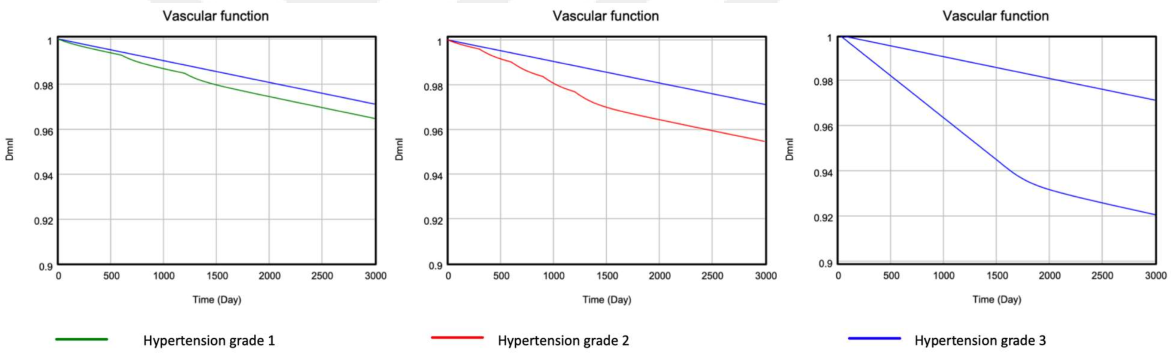

Figure 6.8. Effect of periodic stress on vascular function.

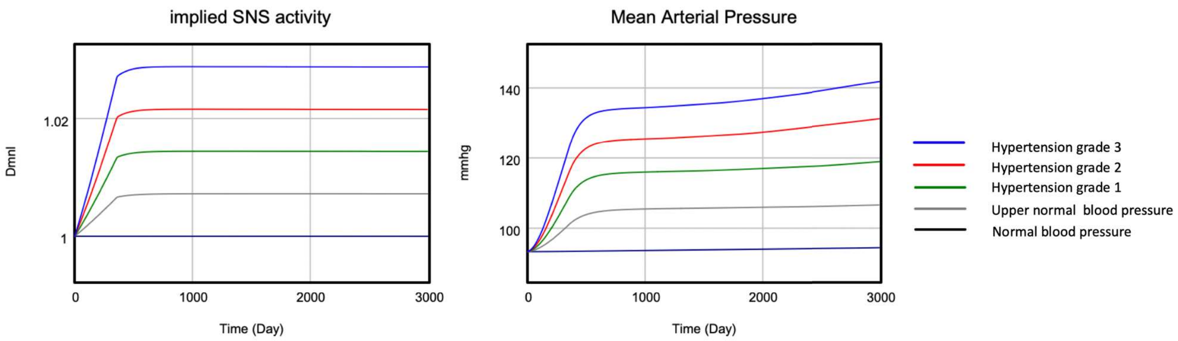

Figure 6.9. Increase in SNS activity and change in mean arterial pressure.

In Figure 6.9, it can be observed that the slope for blood pressure increase over time is low for the less severe blood pressure levels. However, in more severe cases, this increase is more significant. This is the result of the acceleration in the deterioration of control mechanisms.

An over-active sympathetic nervous system leads to an increase in heart rate, contractility, and peripheral resistance. With increased contractility, the blood can pump larger volumes of blood, and cardiac output increases with increased heart rate. Increased sympathetic nervous system activity also constricts vessels and increases total peripheral resistance. Both increases in cardiac output and resistance elevate blood pressure. Figure 6.10 shows different grades of hypertension patients to represent this dynamic.

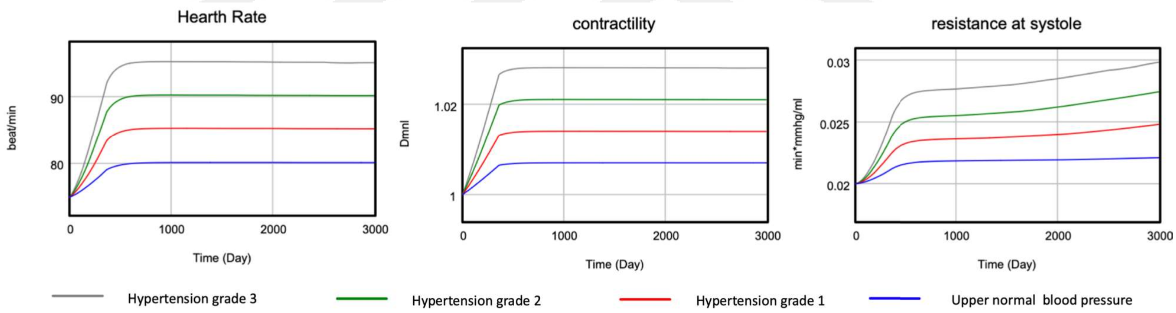

Figure 6.10. Response to increase in SNS activity.

When the sympathetic nervous system is activated, other control mechanisms are activated to bring down mean arterial pressure. In Figure 6.11, it can be observed that GFR increases and end diastolic volume decreases with more sodium filtered out of the body.

However, with a sustained elevation in blood pressure, kidney function deteriorates and with a drop in GFR body cannot bring blood pressure down. Hence for hypertension grade 4 patient a change in dynamic is observed.

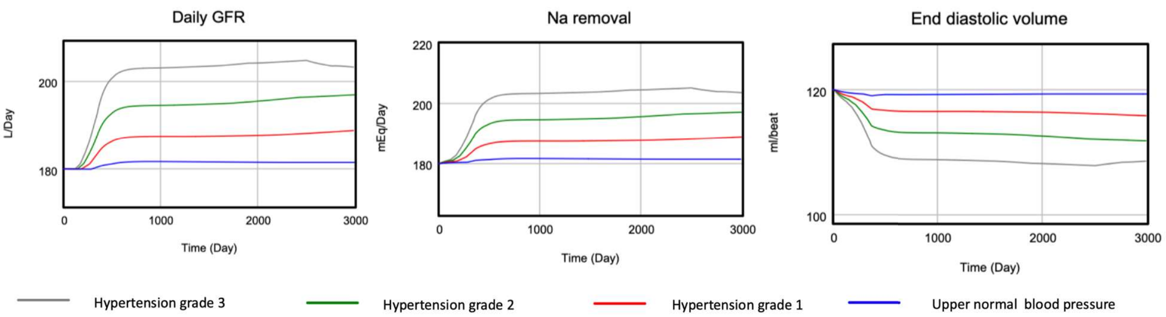

Figure 6.11. Compensation mechanisms to regulate blood pressure in patient with over active SNS.

6.3. Patient 2: Over-Active Renin-Angiotensin Aldosterone System (RAAS)

Renin produced in the kidneys is transformed into angiotensin II. Angiotensin II is a potent vasoconstrictor that acts on arterial muscles, increases peripheral resistance, and elevates blood pressure. Angiotensin II also triggers the release of the aldosterone hormone. Aldosterone stimulates the kidneys' epithelial cells to increase salt and water reabsorption. This feedback loop leading to raised blood volume and high blood pressure is called the renin-angiotensin-aldosterone system (RAAS). Some of the patient groups experience elevated blood pressure because of overactive RAAS [125].

In Figure 6.12, the effect of the increase in RAAS activity is presented. In this scenario, the renin activity gradually increases for one year and remains constant at the over-active level. Based on the level of overactivity, the blood pressure sets at different severities from bottom to top: baseline, upper normal, hypertension grade 1, hypertension grade 2, and hypertension grade 3. An over-active RAAS leads to an increase in renin production, angiotensin II production, aldosterone production and, antidiuretic hormone production. With increased angiotensin II concentration, blood vessels constricts and, increases the total peripheral resistance.

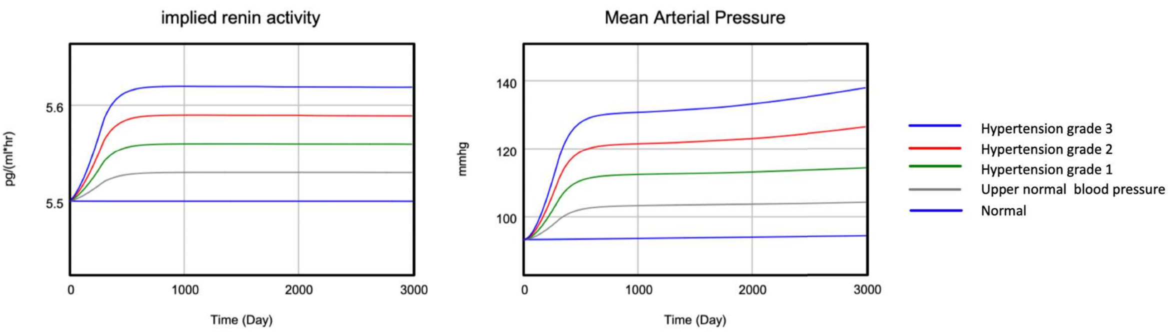

Figure 6.12. Increase in RAAS activity and change in mean arterial pressure.

Due to increase in aldosterone, more salt is reabsorbed in kidneys and, sodium is retained in the body. The increase in antidiuretic hormone affects the urine concentration and, causes more water to be remained in the body. The expansion in total body water increases the cardiac output and increases blood pressure. Figure shows different grades of hypertension patients to represent this dynamic 6.13.

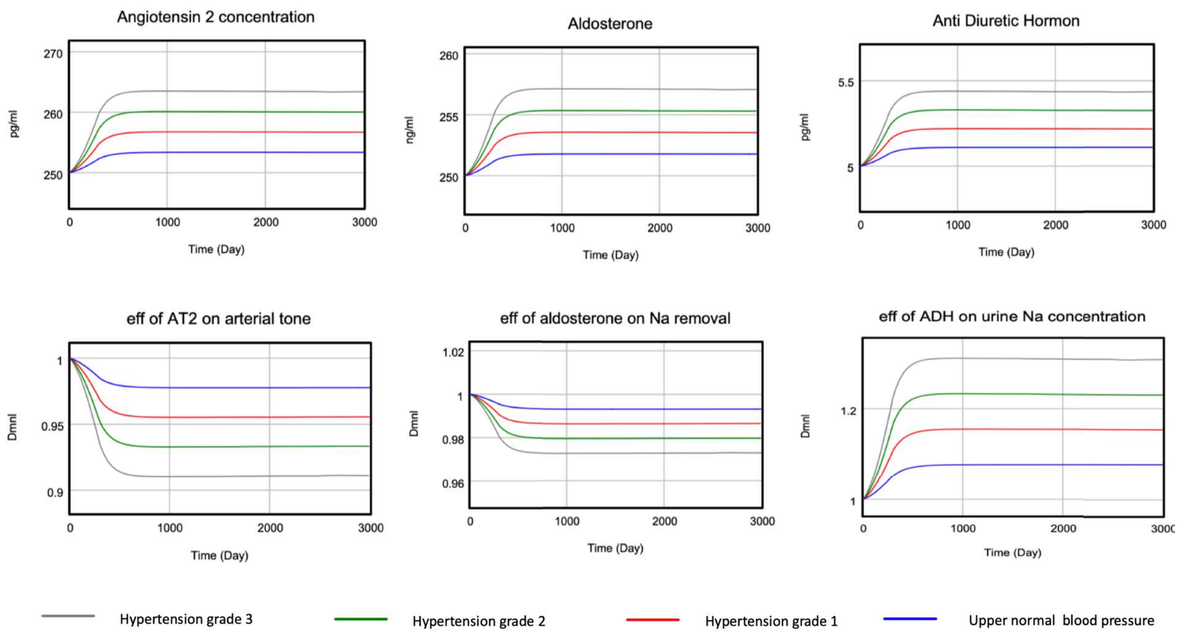

Figure 6.13. Response to increase in RAAS activity.

When the renal sympathetic nervous system activates other control, mechanisms are activated to bring down mean arterial pressure. In Figure 6.14, it can be observed that parasympathetic systems activity increases and sympathetic systems activity is inhibited. As a result of this heart rate is decreased.

However, with a sustained elevation in blood pressure, the baroreceptor operating point resets and cannot bring blood pressure down. Despite the regulatory effects of the central nervous system, blood vessels remain vasoconstriction due to the angiotensin II on arterial tone. Overall, the total peripheral resistance remains high and increases blood pressure.

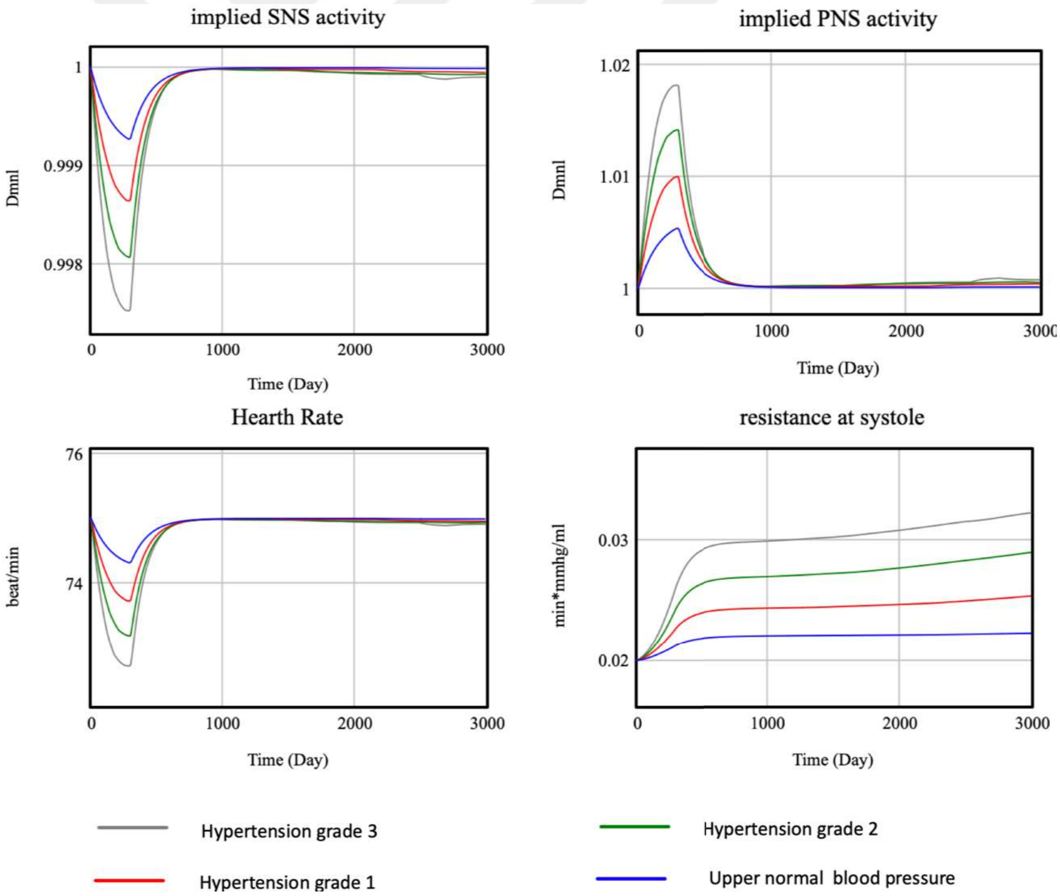

Figure 6.14. Compensation mechanisms to regulate blood pressure in patient with over active RAAS.

6.4. Patient 3: Low Sodium Excretion

In healthy people with high salt intake, glomerular filtration increases, and sodium balance is maintained when blood pressure increases through the pressure-natriuresis mechanism. This hypertension pathogenesis mechanism suggests that high blood pressure occurs as the kidney is not able to excrete the sodium load imposed by the patient's diet [125].

In Figure 6.15, the effect of an increase in salt retention is presented. In this scenario, the salt removal capability gradually decreases for one year and remains constant at a lower level. Based on the level of overactivity, the blood pressure sets at different severities from bottom to top: baseline, upper normal, hypertension grade 1, hypertension grade 2, and hypertension grade 3.

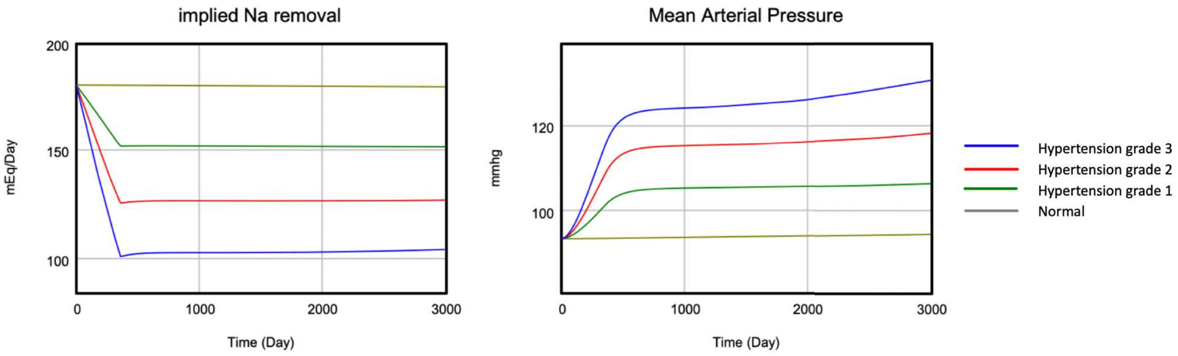

Figure 6.15. Sodium removal and blood pressure.

In Figure 6.15, it can be observed that the slope for blood pressure increase over time is low for the less severe blood pressure levels. However, in more severe cases, this increase is more significant. This is the result of the acceleration in the deterioration of control mechanisms. With a high sodium diet, total body salt increases. Excess sodium in the body causes hypertension through two mechanisms. Firstly, the excess sodium that cannot be removed with glomerular filtration rate capabilities causes more water to be retained in the body. Secondly, higher sodium concentration in the body increases thirst through osmolality control mechanisms, and the water intake increases.

As a consequence of these two feedback loops, extracellular fluid volume and blood volume increase. With more blood delivered to the heart, cardiac output increases, and blood pressure is raised. Figure 6.16 shows different grades of hypertension patients to represent this dynamic.

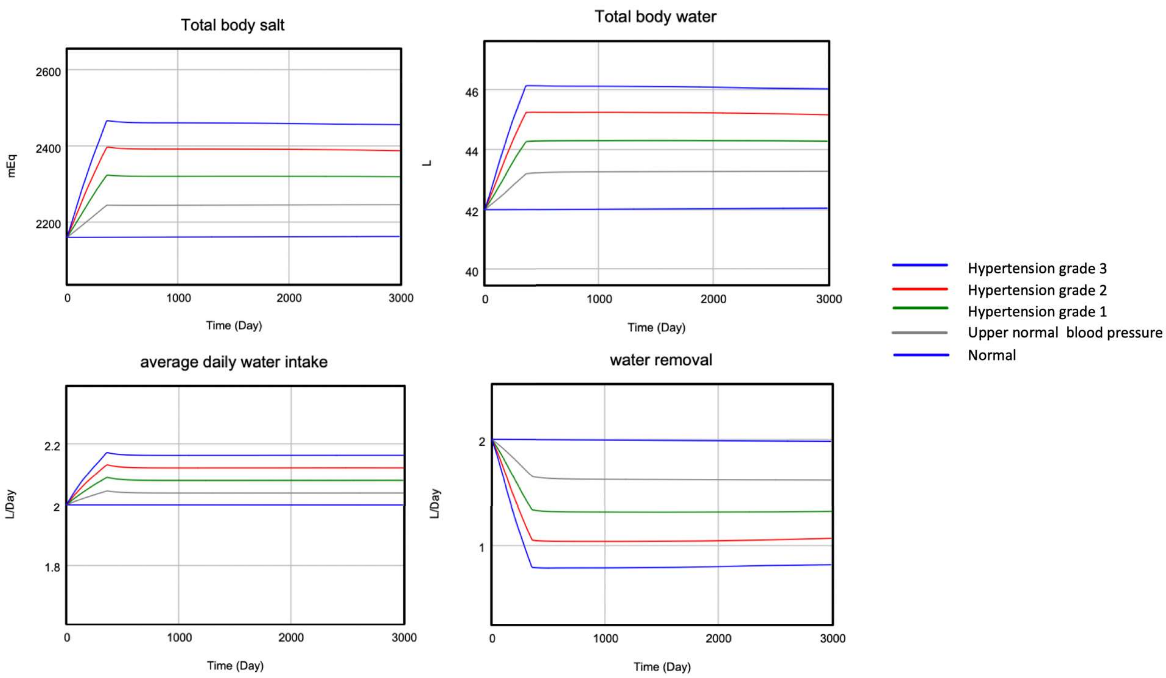

Figure 6.16. Response to increase in salt retention.

Elevation of blood pressure inhibits central and renal sympathetic nervous system activity and activates the parasympathetic system. These processes help in keeping blood pressure under control. However, with aging, the variation in blood pressure is slow; hence baroreceptors reset and become desensitized to chronic elevation in pressure. However, with a persistent high sodium diet, these mechanisms can reset and become desensitized to chronic pressure elevation.

The operating point of baroreceptors and renal sympathetic nervous system increases and adjusts to the higher-pressure levels. Resetting reduces the response of these control systems at high levels of mean arterial pressure.

6.5. Patient 4: Over-Active SNS, Over-Active RAAS and Salt Sensitivity

In this scenario, the sympathetic nervous system and renin activity gradually increases for one year and remains constant at the over-active level. The salt removal capability gradually decreases for one year and remains stable at a lower level. For this scenario analysis, the effects of over-active SNS, over-active RAAS, and salt sensitivity are considered with equal weights.

Figure 6.17 shows different grades of hypertension patients to represent this dynamic, from bottom to top: upper normal, hypertension grade 1, hypertension grade 2, and hypertension grade 3.

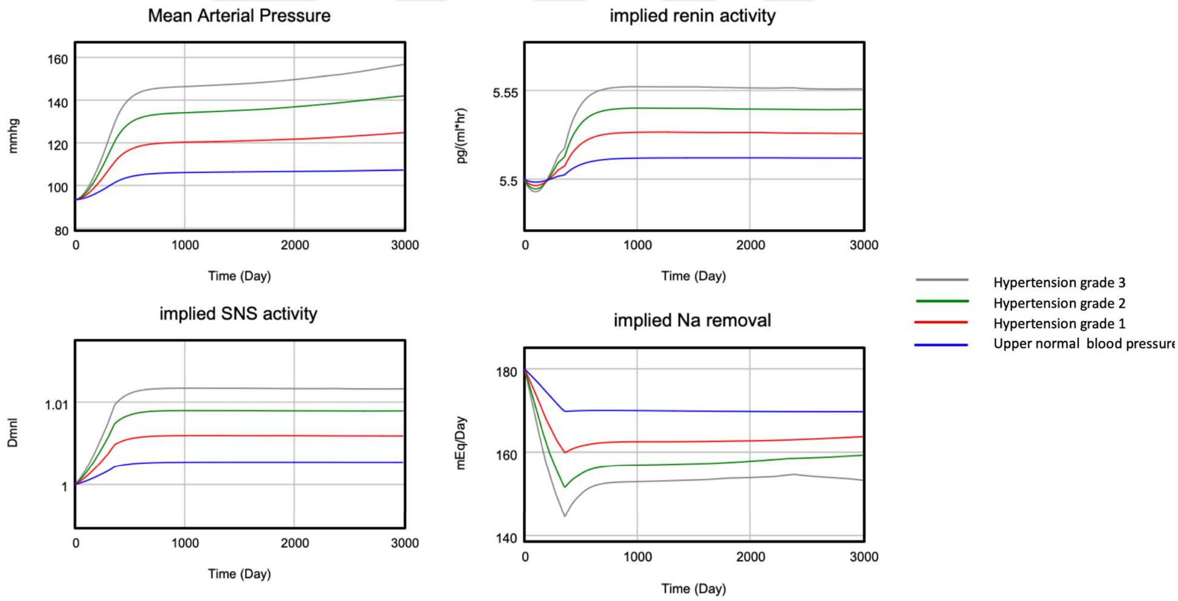

Figure 6.17. Increase in SNS and RAAS activity, decrease in sodium removal and change in mean arterial pressure.

Figure 6.18 blood pressure regulation dynamics that include all pathogenesis are presented with other scenarios for comparison. Even though the dynamics of the parameters responsible for pressure regulation are different, all 4 scenarios result with a hypertension grade 3 in a patient.

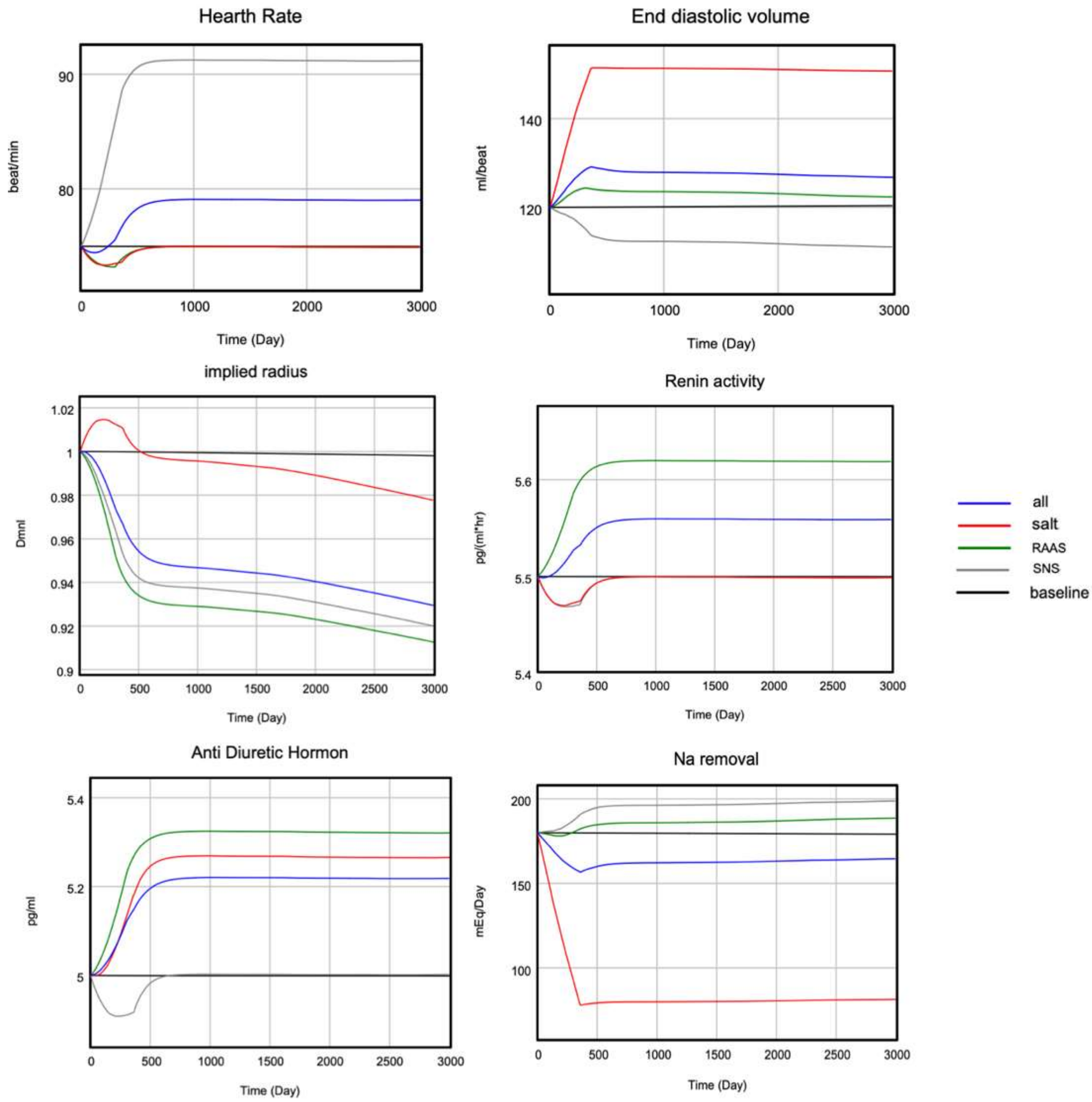

Figure 6.18. Dynamics with co-existence of all three pathogenesis mechanisms.

7. ANALYZING DIFFERENT TREATMENT OPTIONS

In this chapter we explore different treatments options or drug prescription patterns and analyze their effects on the various patient profiles defined in Chapter 6. For each patient, the related pathogenesis starts at time zero, and its impact gradually increases for one year and remains at a constant level after. As the factor causing the elevation in blood pressure changes from its base value, the blood pressure sets to a new equilibrium. After the initial transition, the blood pressure stabilizes at a higher level at day 600, where the individuals are classified as hypertension grade 3 patients.

Treatment option analysis will examine interventions on grade 3 hypertension patients, which is the case where the systolic pressure is higher than 180 mmHg [16]. Treatment option analysis considers that after patients have an established hypertension problem at the time, they visit the doctor at day 900 and receive initial treatment. The treatment varies based on the class of medication and the prescription method. It is assumed that the patient takes their medications daily based on their prescription.

Policies for hypertension treatment are separately examined for four pathogenesis hypotheses: over-active SNS, over-active RAAS, low sodium excretion, and coexistence of all three pathogenesis mechanisms. There are three classes of medication considered for the treatment option analysis: Calcium channel blocker (Amlodipine), Angiotensin Receptor Blocker (Telmisartan), and diuretic (Chlortalidone). The following prescription policies are analyzed for these medications: monotherapy, dual therapy, dual-therapy with adjustment, dual therapy with treatment inertia, gradual increase, and triple therapy.

These policies are briefly explained in Table 7.1. An example for patient 4 is given in Figure 7.1 to represent blood pressure dynamics in each treatment option.

Table 7.1. Descriptions of the treatment options.

Treatment option	**Description**
Mono therapy	At day 900, one medication is prescribed.
Dual therapy	At day 900, two medications are prescribed
Dual therapy with adjustment	At day 900, two medications are prescribed; at day 1500, third medication is added.
Dual therapy with treatment inertia	At day 900, two medications are prescribed; at day 2100, third medication is added.
Gradual increase	At day 900, one medication is prescribed; at day 1200 second medication is added; at day 1500, the third medication is added.
Triple therapy	At day 900, three medications are prescribed.

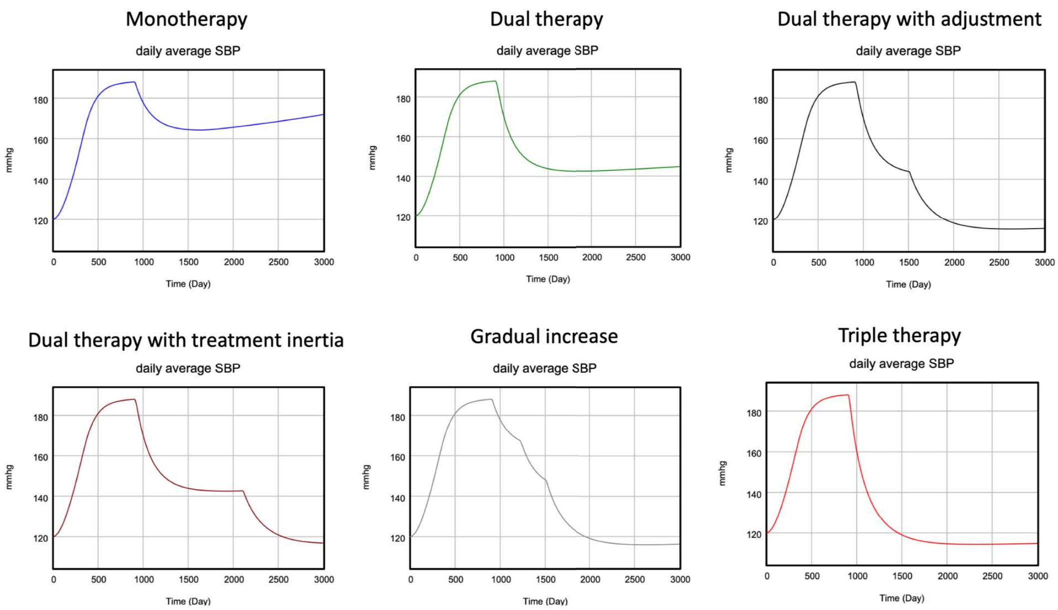

Figure 7.1. Responses of a patient to the different treatment options.

Medical guidelines make recommendations based on cohorts, such as recommending initiating treatment with a combination of two medications and intensifying drugs if it is found to be necessary during follow-up visits [126]. However, in essential hypertension, the underlying pathogenesis of the disease is unknown for individual patients. Therefore, in a standardized treatment where all patients receive diuretics as initial treatment, patients with low sodium excretion and over-active SNS pathophysiology will have different responses. This relationship is demonstrated with an example of the monotherapy given in Figure 7.2.

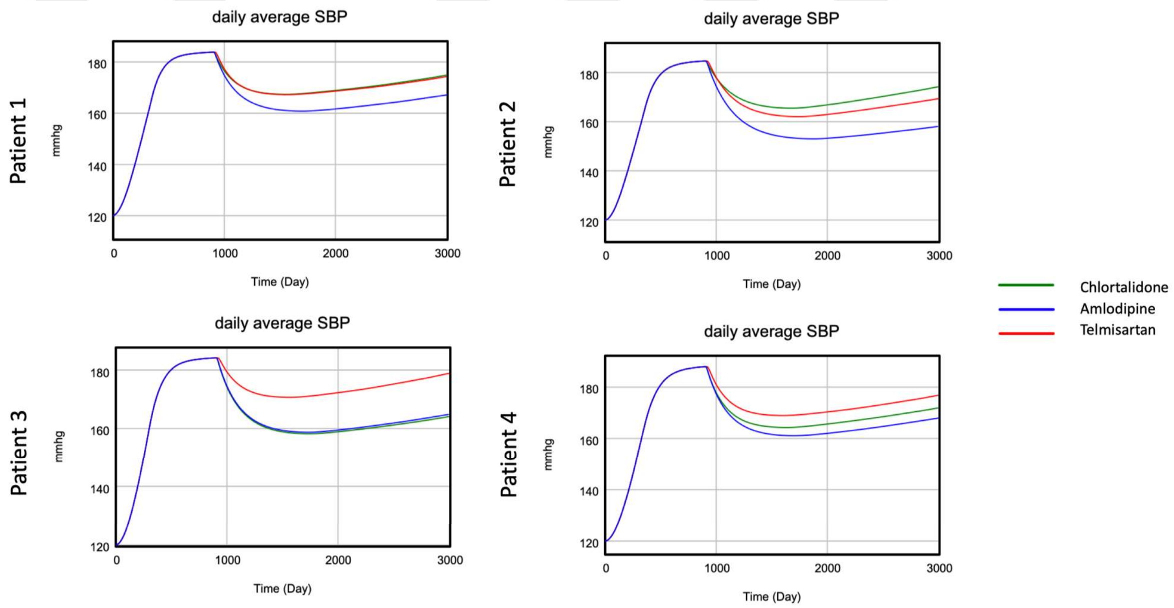

Figure 7.2. Responses of patients to different medications used as monotherapy.

The figure shows that even though all patients receive the same dose at the same time, blood pressure reduction varies. For this reason, a drug's selection can influence the treatment outcome. Furthermore, when a treatment option with gradual increase is used, the order the drugs are prescribed can influence the treatment's performance.

Therapeutic inertia is a significant barrier for patients to achieve blood pressure control. It can occur when a healthcare provider fails to intensify drug therapy in a patient with suboptimal blood pressure. One example of this was when the doctor asked their patients to do a follow-up visit before strengthening the treatment. In treatment option analysis, therapeutic inertia describes when healthcare providers avoid adding combination therapy for a patient with suboptimal blood pressure [13].

In dual therapy with adjustment stategy, at the day 900, the doctor prescribes two of the three medications as initial therapy. If the blood pressure is above the threshold in an annual checkup at day 1500, the treatment is gradually intensified. However, for the treatment with inertia, there is an extended duration before an additional medication is introduced and the therapy is intensified at day 2100. In the gradual increase treatment option, the doctor prescribes one of the three medications as initial therapy.

Later, if the blood pressure is above a certain threshold in the one-year checkup, one more medication is added to the previous treatment plan. This way, the patients start by taking one medication a day and, at the end day they take three medications.

High blood pressure causes damage to blood vessels and kidneys. There is a positive feedback structure with blood pressure and regulatory mechanism. Vascular function loss causes blood vessels to remain constricted and increase blood pressure. Kidney function loss hinders the body's ability to remove salt and water, and the excess volume increases pressure.

World Health Organization developed a list of treatment outcomes and grading system for managing hypertension treatment [126]. On a scale from 1 to 9 rating 7–9 is classified as critical in for decision-making. Based on this grading, coronary artery disease caused by vascular function loss has a rating of 8.1, and end-stage renal disease caused by kidney function loss has a rating 7.8 . Therefore, to assess the performance of the treatment option, the end-organ damage is used as it represents the cumulative effect of high blood pressure on the body.

An example is presented in Figure 7.3 demonstrating kidney function dynamics under different conditions. Considering 4 patient profiles with physiological differences, 6 policies, and prescription orders of 3 medications, a total of 80 runs are simulated. The outcomes of treatment options are compared for the average kidney and vascular function loss at the end of the simulation run.

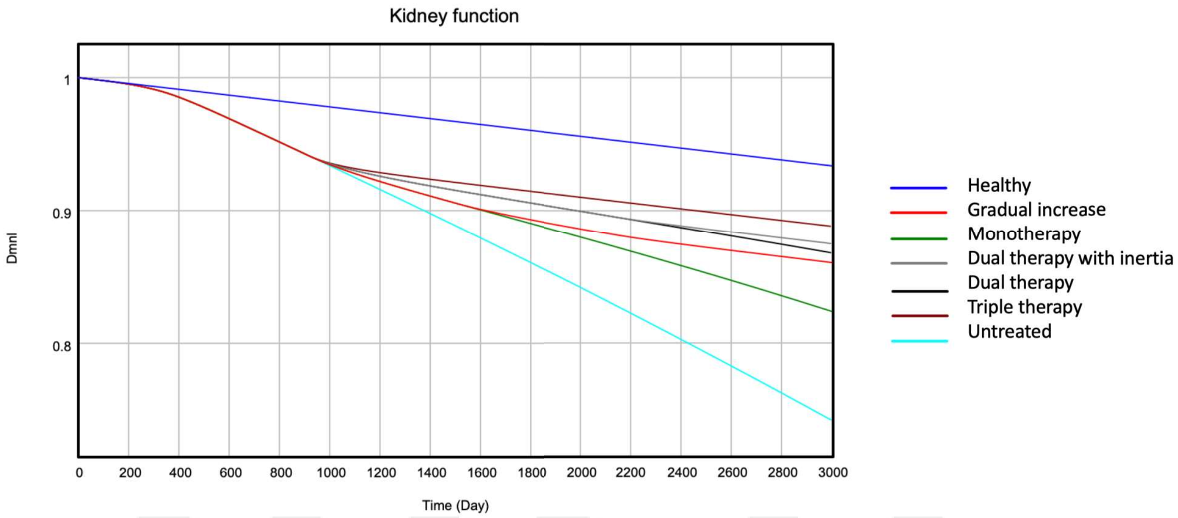

Figure 7.3. Kidney function loss with different treatment options.

The end-organ damage is first assessed by comparing treatment outcomes for each patient profile by taking the untreated run as the baseline. The percent gains from following a specific treatment option are presented in Figure 7.4.

In the heat map, the highest benefit from treatment is represented with green, average with white, and worse with red. Results shows that the triple dose option was the most effective for each patient, and monotherapy was the least effective. Also, adding a third medication to the dual therapy offers benefits.

The sooner an extra medication is initiated, the end organ damage prevention is higher. As expected, faster blood pressure control leads to less organ damage. When treatment outcomes are compared among patients based on the medications and the prescription order, variations in treatment outcomes are observed.

Policy	Drugs	Over-active SNS (Patient 1)	Over-active RAAS (Patient2)	Salt retention (Patient 3)	Combined pathogenesis (Patient 4)
Mono	A	5.54%	6.11%	7.60%	6.07%
Mono	T	4.00%	6.25%	4.55%	5.31%
Mono	C	4.05%	3.28%	5.38%	4.12%
Dual	A & T	10.20%	11.75%	11.57%	11.89%
Dual	T & C	8.96%	10.07%	10.44%	10.60%
Dual	C & A	9.87%	9.58%	11.69%	10.80%
Dual adjusted	A & T, C	11.48%	12.07%	12.10%	12.54%
Dual adjusted	T & C, A	11.21%	11.53%	11.74%	12.20%
Dual adjusted	C & A, T	11.38%	11.43%	12.12%	12.18%
Dual with inertia	A & T, C	10.93%	11.93%	11.87%	12.26%
Dual with inertia	T & C, A	10.26%	10.93%	11.21%	11.56%
Dual with inertia	C & A, T	10.73%	10.67%	11.93%	11.62%
Gradual increase	A, T, C	10.79%	11.24%	11.46%	11.70%
Gradual increase	T, C, A	10.47%	10.99%	10.93%	11.42%
Gradual increase	C, A, T	10.58%	10.55%	11.20%	11.29%
Gradual increase	A, C, T	10.74%	10.93%	11.46%	11.53%
Gradual increase	T, A, C	10.61%	11.25%	11.10%	11.63%
Gradual increase	C, T, A	10.50%	10.60%	11.03%	11.31%
Triple	A & T & C	12.29%	12.48%	12.70%	13.13%

Figure 7.4. Treatment option comparisons with no treatment scenario.

When a monotherapy treatment option is followed, Amlodipine is the most effective drug for a patient with overactive SNS, and Chlortalidone is the least effective. Whereas for a patient with an over-active RAAS, Telmisartan is the most effective drug and Chlortalidone is the least effective. A patient with low sodium secretion benefits most from Amlodipine and least from Telmisartan. For the patient with combined pathogenesis, Amlodipine is the most effective drug, and Chlortalidone is the least effective among monotherapy policies.

In a setting where Chlortalidone is prescribed as monotherapy treatment and is not further intensified, patients with over-active SNS, over-active RAAS, and combined pathogenesis suffer more than those with salt retention. In a setting where Telmisartan is prescribed as a monotherapy treatment, patients with low salt retention benefit least among other patient groups. Among all patient groups, Amlodipine as monotherapy had better outcomes than other monotherapy options.

In a dual therapy treatment option, there are three alternative prescriptions for the three medications. Combining Amlodipine and Telmisartan, Telmisartan and Chlortalidone, and, Chlortalidone and Amlodipine. Based on patient physiology, the best response to these combinations varies; however, Amlodipine and Chlortalidone combination was the most effective for patient 1, patient 2, and patient 4. Whereas patient 3 benefited most from the Chlortalidone and Amlodipine combination. Also, in a treatment option where Telmisartan and Chlortalidone combination is used, a patient with overactive SNS would respond the least in all patient groups. Also, in the dual adjusted therapy treatment option, the responses based on drug initiation orders and responses are identical to the dual therapy.

In dual adjusted therapy, dual therapy with inertia, and gradual increase policies, patients receive three medications at the end of the treatment implementation. However, the performance of the policies varies. In the dual-adjusted therapy treatment option, prevention of end-organ damage is close to the triple therapy, which is the best-case scenario.

Results of dual therapy with inertia outperformed the gradual increase treatment option. This demonstrates at the start of the treatment initiating with an intensified treatment and achieving greater blood pressure reduction offers benefit. After blood pressure is lower than a certain threshold reducing the blood pressure adds less benefit. Hence, starting dual therapy can be as effective as triple therapy has as long as patients receive follow up.

Later, in Figure 7.5, organ damage in hypertension patients is compared with a healthy individual. This represents organ damage caused by the disease in addition to aging. It can be observed that with even with dual therapy, end organ damage can be reduced by around 10%. Due to inter-patient differences in hypertension pathophysiology, patients' responses to antihypertensives and policies change. The medications chosen and their effects on blood pressure management presented variations based on the individual's physiology. This effect is observed in the policies that modify treatment over time, such as dual therapy with adjustment, dual therapy with inertia, and gradual increase. However, the effect of medication orders on the outcome was less significant than the effect of the treatment option.

Policy	Drugs	Over-active SNS (Patient 1)	Over-active RAAS (Patient2)	Salt retention (Patient 3)	Combined pathogenesis (Patient 4)
Untreated	None	-14.15%	-14.28%	-14.36%	-14.79%
Mono	A	-9.39%	-9.04%	-7.85%	-9.61%
Mono	T	-10.72%	-8.92%	-10.46%	-10.27%
Mono	C	-10.68%	-11.46%	-9.75%	-11.28%
Dual	A & T	-5.39%	-4.20%	-4.45%	-4.66%
Dual	T & C	-6.46%	-5.64%	-5.41%	-5.75%
Dual	C & A	-5.68%	-6.06%	-4.34%	-5.59%
Dual adjusted	A & T, C	-4.29%	-3.93%	-4.00%	-4.11%
Dual adjusted	T & C, A	-4.53%	-4.39%	-4.30%	-4.39%
Dual adjusted	C & A, T	-4.38%	-4.48%	-3.98%	-4.41%
Dual with inertia	A & T, C	-4.77%	-4.05%	-4.19%	-4.34%
Dual with inertia	T & C, A	-5.34%	-4.91%	-4.76%	-4.94%
Dual with inertia	C & A, T	-4.94%	-5.13%	-4.14%	-4.89%
Gradual increase	A, T, C	-4.88%	-4.64%	-4.54%	-4.82%
Gradual increase	T, C, A	-5.16%	-4.85%	-5.00%	-5.06%
Gradual increase	C, A, T	-5.07%	-5.23%	-4.76%	-5.17%
Gradual increase	A, C, T	-4.93%	-4.91%	-4.54%	-4.97%
Gradual increase	T, A, C	-5.04%	-4.63%	-4.85%	-4.88%
Gradual increase	C, T, A	-5.14%	-5.19%	-4.91%	-5.16%
Triple	A & T & C	-3.59%	-3.58%	-3.48%	-3.60%

Figure 7.5. Treatment option comparisons with a healthy individual.

Even though the underlying mechanism of the disease is unknown, the patient still can have a good treatment outcome. Avoiding to intensify treatment, such as sticking to monotherapy or delaying the treatment, as in treatment inertia cause worse results than not starting with the best-fit treatment.

Therefore, treatment option analysis can conclude that even though the inter-patient differences and the order of initiating the medicines have an effect, patients still achieve similar outcomes with a close follow-up. Knowing the pathogenesis in a patient and adjusting personalized treatment offers some value; however, it can be compensated with close monitoring and making the adjustments necessary.

8. CONCLUSION

Hypertension treatment is challenging, and the outcome varies by individual patient. This thesis aims to demonstrate the use of simulation modeling to study physiological variations in blood pressure regulation and analyze their effects on hypertension treatment. For this purpose, a system dynamics model is built representing the central nervous system and renal control mechanisms. Furthermore, vascular elasticity and kidney function capabilities are included to capture aging and the long-term effects of hypertension on the body.

The model is initialized for a healthy individual. Later, extreme condition tests are conducted to observe the model behavior when it is disturbed by external factors, including removing aging elements, water loading, sodium loading, blood loss, and acute kidney damage. Extreme condition tests allowed us to compare the results with established models in the literature and assess the model's structure and behavior.

Then, the model is modified to include the effects of three pathogenesis mechanisms of primary hypertension: the over-active nervous system, the over-active renin-angiotensin-aldosterone system (RAAS), and low sodium excretion (salt retention). Pathophysiology variations allowed us to demonstrate that the model can represent different individual patient profiles. Later, the hypertension development is simulated to observe the model behavior for five profiles with inter-patient physiological differences: healthy individual, patient with an over-active nervous system, patient with over-active RAAS, patient with low sodium excretion, and patient that has a combination of all three pathophysiological mechanisms.

Finally, treatment options are analyzed to explore various drug prescription strategies and their outcomes on four identified patient profiles. Treatment option analysis considers patients with established grade 3 hypertension, where their treatment options vary based on the class of medication, the treatment option used while prescribing, and the order in which the medications are initiated. The drugs included for the treatment option analysis were: Calcium channel blockers (Amlodipine), Angiotensin Receptor Blocker (Telmisartan), and diuretics (Chlortalidone). The following prescription policies are analyzed: monotherapy, gradual increase, dual therapy with adjustment, dual therapy with inertia, gradual increase, and triple therapy.

The treatment option analysis evaluates the treatment outcomes by comparing end-organ damage to kidneys and blood vessels at the end of ten years. The end-organ damage is first assessed by comparing treatment outcomes for each patient profile by taking the untreated run as the baseline, presenting the percent gains of following a specific treatment option. Later, organ damage in hypertension patients is compared with a healthy individual showing the harm caused by the disease. In this way, the model helps develop insight into what alternative treatments can be expected for a particular patient.

There are alternative treatment strategies and various factors involved in successfully treating hypertension. Due to inter-patient differences in hypertension pathophysiology, patients are more responsive to some classes of antihypertensive agents than others, and there is no one-fits-all treatment. However, medical guidelines often make recommendations based on cohorts. Yet, in essential hypertension, the underlying pathogenesis of the disease is unknown for individual patients. Therefore, it is not possible to identify patients that are most likely to suffer from a one-fits-all treatment option. Because the system is complex, it is difficult to predict what to expect when a non-standard patient deviates from standard treatment.

In the treatment option analysis, triple therapy was found to be more effective for each patient profile, and monotherapy was least effective and aligned with expectations. For monotherapy and dual therapy, the medications chosen and their effects on blood pressure management presented variations based on the individual's physiology. The policies that modify treatment over time, such as dual therapy with adjustment, dual therapy with inertia, and gradual increase in the order of initiating the medications, changed the treatment outcomes. However, this variation had a narrower range than not intensifying or delaying the treatment.

Therefore, it was concluded that a close follow-up by the doctors plays an important role in a successful treatment. Even though the interpatient differences and the order of starting the medications have an effect, patients still achieve similar outcomes with a close follow-up. Furthermore, targeting lower blood pressure and adding medications to lower blood pressure offers benefits in terms of preventing end-organ damage. Faster blood pressure control leads to less organ damage; therefore, combination therapies as initial therapy offers benefits. These conclusions are in parallel with the recommendations of current medical guidelines, where they recommend initiating two medications and adding a third one in the follow-up visits. The study showed that despite the variations in inter-patient physiologies, the current treatment guidelines perform well where perfect information is unavailable.

This study was able to present the potential benefit of using dynamic simulation models to analyze variations in treatment options for patients with physiological differences and assess the value of personalized treatment. This study used empirical data from the literature to demonstrate treatment outcomes on hypertension patients, and validation tests were conducted while building the model. However, to use such models in a clinical setting, the models need to be calibrated with granular data, such as a longitudinal study that includes biomarkers related to blood pressure control before and after receiving hypertensive treatment. Obtaining such data can be challenging and time-consuming; nonetheless, it holds promise to get closer to individualized treatments.

Furthermore, for better decision-making, a more comprehensive medication portfolio could be analyzed, different dosing strategies could be considered, and more diverse patient profiles could be assessed. This study provides examples of potential patient and treatment profiles and demonstrates an analysis to evaluate different outcomes. However, it has its limitations. The study focuses on three widely recognized essential hypertension pathogenesis: over-active SNS, over-active RAAS, and salt retention. Secondary hypertension is excluded for simplification; comorbidities such as diabetes and obesity are not captured. Furthermore, this study assumes that the side effects are tolerated well. Nonetheless, the comorbidities and possible adverse effects complicate the treatment and impact the doctor's decision-making while prescribing medication.

As a future study, such models could be utilized to assess the cost-effectiveness and value of information. In this study, the model is initialized for a healthy person; however, when the patient already has comorbidities, variations on end-organ damage could be more significant. Furthermore, medical guidelines recommend targeting different blood pressure levels for individuals based on their risk profiles. The intensity of pharmacotherapy and follow-up requirements can change based on the blood pressure targets. Therefore, considering risk profiles, frequency of check-ups, the number of prescribed medications, and comorbidities, the cost-effectiveness of policies can be analyzed.

REFERENCES

1. World Health Organization, "Cardiovascular Diseases (CVDs)", https://www.who.int/news-room/fact-sheets/detail/cardiovascular-diseases-(cvds), accessed in May 1, 2022.

2. Stanaway, J.D., A. Afshin, E. Gakidou, S.S. Lim, D. Abate, K.H. Abate, C. Abbafati, N. Abbasi, H. Abbastabar, F. Abd-Allah, and J. Abdela, "Global, Regional, and National Comparative Risk Assessment of 84 Behavioural, Environmental and Occupational, and Metabolic Risks or Clusters of Risks for 195 Countries and Territories, 1990–2017: A Systematic Analysis for the Global Burden of Disease Study 2017", *The Lancet*, Vol. 392, No. 10159, pp. 1923–1994, 2018.

3. World Health Organization, "Hypertension", https://www.who.int/news-room/fact-sheets/detail/hypertension, accessed in May 1, 2022.

4. Mills, K.T., J.D. Bundy, T.N. Kelly, J.E. Reed, P.M. Kearney, K. Reynolds, J. Chen, and J. He, "Global Disparities of Hypertension Prevalence and Control: A Systematic Analysis of Population-Based Studies From 90 Countries", *Circulation*, Vol. 134, No. 6, pp. 441–450, 2016.

5. Zhou, B., J. Bentham, M. Di Cesare, H. Bixby, G. Danaei, M.J. Cowan, C.J. Paciorek, G. Singh, K. Hajifathalian, J.E. Bennett, and C. Taddei, "Worldwide Trends in Blood Pressure From 1975 to 2015: A Pooled Analysis of 1479 Population-Based Measurement Studies With 19· 1 Million Participants", *The Lancet*, Vol. 389, No. 10064, pp. 37–55, 2017.

6. Virani, S.S., A. Alonso, H. J. Aparicio, E.J. Benjamin, M.S. Bittencourt, C.W. Callaway, A.P. Carson, A.M. Chamberlain, S. Cheng, F.N. Delling, and M.S. Elkind, "Heart Disease and Stroke Statistics—2021 Update: A Report From the

American Heart Association", *Circulation*, Vol. 143, No. 8, pp. e254–e743, 2021.

7. Gaziano, T.A., A. Bitton, S. Anand, and M.C. Weinstein, "The Global Cost of Nonoptimal Blood Pressure", *Journal of Hypertension*, Vol. 27, No. 7, pp. 1472–1477, 2009.

8. World Health Organization, *"The Impact of the Covid-19 Pandemic on Noncommunicable Disease Resources and Services: Results of a Rapid Assessment"*, Geneva: World Health Organization, pp. 22, 2020.

9. Unger, T., C. Borghi, F. Charchar, N.A. Khan, N.R. Poulter, D. Prabhakaran, A. Ramirez, M. Schlaich, G.S. Stergiou, M. Tomaszewski, R.D. Wainford, B. Williams, and A.E. Schutte, "2020 International Society of Hypertension Global Hypertension Practice Guidelines", *Hypertension*, Vol. 75, No. 6, pp. 1334–1357, 2020.

10. Redon, J., J.J. Mourad, R.E. Schmieder, M. Volpe, and T.W. Weiss, "Why in 2016 are Patients With Hypertension Not 100% Controlled? A Call to Action", *Journal of Hypertension*, Vol. 34, No. 8, pp. 1480–1488, 2016.

11. Zhou, B., G. Danaei, G.A. Stevens, H. Bixby, C. Taddei, R.M. Carrillo-Larco, B. Solomon, L.M. Riley, M. Di Cesare, M.L.C. Iurilli, and A.R.-Martinez, "Long-Term and Recent Trends in Hypertension Awareness, Treatment, and Control in 12 High-Income Countries: An Analysis of 123 Nationally Representative Surveys", *The Lancet*, Vol. 394, No. 10199, pp. 639–651, 2019.

12. Geldsetzer, P., J. Manne-Goehler, M.-E. Marcus, C. Ebert, Z. Zhumadilov, C.S. Wesseh, L. Tsabedze, A. Supiyev, L. Sturua, S.K. Bahendeka, and A.M. Sibai, "The State of Hypertension Care in 44 Low-Income and Middle-Income Countries: A Cross-Sectional Study of Nationally Representative Individual-Level Data From 1· 1 Million Adults", *The Lancet*, Vol. 394, No. 10199, pp. 652–662, 2019.

13. Ogedegbe, G., "Barriers to Optimal Hypertension Control", *The Journal of Clinical Hypertension*, Vol. 10, No. 8, pp. 644–646, 2008.

14. Wald, D., M. Law, J.K. Morris, J.P. Bestwick, and N.J. Wald, "Combination Therapy Versus Monotherapy in Reducing Blood Pressure: Meta-Analysis on 11,000 Participants From 42 Trials", *The American Journal of Medicine*, Vol. 122, No. 3, pp. 290–300, 2009.

15. Whelton, P.K., R.M. Carey, W.S. Aronow, D.E. Casey, K.J. Collins, C.D. Himmelfarb, S.M. DePalma, S. Gidding, K.A. Jamerson, D.W. Jones, and E.J. MacLaughlin, "2017 ACC/AHA/AAPA/ABC/ACPM/AGS/APhA/ASH/ASPC/NMA/PCNA Guideline for the Prevention, Detection, Evaluation, and Management of High Blood Pressure in Adults: A Report of the American College of Cardiology/American Heart Association Task Force on Clinical Practice Guidelines", *Journal of the American College of Cardiology*, Vol. 71, No. 19, pp. e127–e248, 2018.

16. Williams, B., G. Mancia, W. Spiering, E.A. Rosei, M. Azizi, M. Burnier, D.L. Clement, A. Coca, G. De Simone, A. Dominiczak, and T. Kahan, "2018 ESC/ESH Guidelines for the Management of Arterial Hypertension: The Task Force for the Management of Arterial Hypertension of the European Society of Cardiology (ESC) and the European Society of Hypertension (ESH)", *European Heart Journal*, Vol. 39, No. 33, pp. 3021–3104, 2018.

17. Hedayati, S., E.F. Elsayed, and R.F. Reilly, "Non-Pharmacological Aspects of Blood Pressure Management: What are the Data?", *Kidney International*, Vol. 79, No. 10, pp. 1061–1070, 2011.

18. Volpe, M., G. Gallo, and G. Tocci, "New Approach to Blood Pressure Control: Triple Combination Pill", *Trends in Cardiovascular Medicine*, Vol. 30, No. 2, pp. 72–77, 2020.

19. Webster, R., A. Salam, H.A. De Silva, V. Selak, S. Stepien, S. Rajapakse, S. Amarasekara, N. Amarasena, L. Billot, A.P. de Silva, and M. Fernando, "Fixed Low-Dose Triple Combination Antihypertensive Medication vs Usual Care for Blood Pressure Control in Patients With Mild to Moderate Hypertension in Sri Lanka: A Randomized Clinical Trial", *Jama*, Vol. 320, No. 6, pp. 566–579, 2018.

20. Wang, N., A. Salam, R. Webster, A. de Silva, R. Guggilla, S. Stepien, J. Mysore, L. Billot, S. Jan, P.K. Maulik, and N. Naik, "Association of Low-Dose Triple Combination Therapy With Therapeutic Inertia and Prescribing Patterns in Patients With Hypertension: A Secondary Analysis of the Triumph Trial", *JAMA Cardiology*, Vol. 5, No. 11, pp. 1219–1226, 2020.

21. Deary, A.J., A.L. Schumann, H. Murfet, S.F. Haydock, R.S.-Y. Foo, and M.J. Brown, "Double-Blind, Placebo-Controlled Crossover Comparison of Five Classes of Antihypertensive Drugs", *Journal of Hypertension*, Vol. 20, No. 4, pp. 771–777, 2002.

22. Hallow, K.M., and Y. Gebremichael, "A Quantitative Systems Physiology Model of Renal Function and Blood Pressure Regulation: Model Description", *CPT: Pharmacometrics & Systems Pharmacology*, Vol. 6, No. 6, pp. 383–392, 2017.

23. Harrison, D.G., "The Mosaic Theory Revisited: Common Molecular Mechanisms Coordinating Diverse Organ and Cellular Events in Hypertension", *Journal of the American Society of Hypertension*, Vol. 7, No. 1, pp. 68–74, 2013.

24. Page, I.H., "The Mosaic Theory of Arterial Hypertension: Its Interpretation", *Perspectives in Biology and Medicine*, Vol. 10, No. 3, pp. 325–333, 1967.

25. McLoone, V., *Modelling of Long and Short Term Blood Pressure Control Systems*, Ph.D. Thesis, National University of Ireland, Maynooth (Ireland), 2014.

26. Hajjar, I. and T.A. Kotchen, "Trends in Prevalence, Awareness, Treatment, and

Control of Hypertension in the United States 1988-2000", *Jama*, Vol. 290, No. 2, pp. 199–206, 2003.

27. Brunberg, A., S. Heinke, J. Spillner, R. Autschbach, D. Abel, and S. Leonhardt, "Modeling and Simulation of the Cardiovascular System: A Review of Applications, Methods, and Potentials", *Biomed Tech (Berl)*, Vol. 54, No. 5, pp. 233–44, 2013.

28. Kokalari, I., T. Karaja, and M. Guerrisi, "Review on Lumped Parameter Method for Modeling the Blood Flow in Systemic Arteries", *Journal of Biomedical Science and Engineering*, Vol. 6, pp. 92–99, 2013.

29. Otto, F., "Die Grundform des Arteriellen Pulses", *Zeitung fur Biologie*, Vol. 37, pp. 483–586, 1899.

30. Guyton, A.C., T.G. Coleman, and H.J. Granger, "Circulation: Overall Regulation", *Annual Review of Physiology*, Vol. 34, No. 1, pp. 13–44, 1972.

31. Guyton, A.G., "Physiologic Regulation of Arterial Pressure", *The American Journal of Cardiology*, Vol. 8, No. 3, pp. 401–407, 1961.

32. Guyton, A.C., T.G. Coleman, A.W. Cowley, R.D. Manning, R.A. Norman, and J.D. Ferguson, "A Systems Analysis Approach to Understanding Long-Range Arterial Blood Pressure Control and Hypertension", *Circulation Research*, Vol. 35, pp. 159–176.1974.

33. Guyton, A.C., T.G. Coleman, A.W. Cowley, J.-F. Liard, R.A. Norman, and R.D. Manning, "Systems Analysis of Arterial Pressure Regulation and Hypertension", *Annals of Biomedical Engineering*, Vol. 1, No. 2, pp. 254–281, 1972.

34. Ikeda, N., F. Marumo, M. Shirataka, and T. Sato, "A Model of Overall Regulation of Body Fluids", *Annals of Biomedical Engineering*, Vol. 7, No. 2, pp. 135–166, 1979.

35. Uttamsingh, R.J., M.S. Leaning, J.A. Bushman, E.R. Carson, and L. Finkelstein, "Mathematical Model of the Human Renal System", *Medical and Biological Engineering and Computing*, Vol. 23, No. 6, pp. 525–535, 1985.

36. Montani, J.P., T.H. Adair, R.L. Summers, T.G. Coleman, and A.C. Guyton, "A Simulation Support System for Solving Large Physiological Models on Microcomputers", *International journal of bio-medical computing*, Vol. 24, No. 1, pp. 41–54, 1989.

37. Hall, J.E., A.C. Guyton, M.J. Smith, and T.G. Coleman, "Blood Pressure and Renal Function During Chronic Changes in Sodium Intake: Role of Angiotensin", *American Journal of Physiology-Renal Physiology*, Vol. 239, No. 3, pp. F271–F280, 1980.

38. Osborn, J.W., V.A. Averina, and G.D. Fink, "Current Computational Models do not Reveal the Importance of the Nervous System in Long-Term Control of Arterial Pressure", *Experimental Physiology*, Vol. 94, No. 4, pp. 389–396, 2009.

39. Osborn, J.W., "Hypothesis: Set-Points and Long-Term Control of Arterial Pressure. A Theoretical Argument for a Long-Term Arterial Pressure Control System in the Brain Rather Than the Kidney", *Clinical and Experimental Pharmacology and Physiology*, Vol. 32, No. 5-6, pp. 384–393, 2005.

40. Malpas, S., "Editorial Comment: Montani Versus Osborn Exchange of Views", *Experimental Physiology*, Vol. 94, No. 4, pp. 381–382, 2009.

41. Averina, V.A., H.G. Othmer, G.D. Fink, and J.W. Osborn, "A Mathematical Model of Salt-Sensitive Hypertension: The Neurogenic Hypothesis", *The Journal of Physiology*, Vol. 593, No. 14, pp. 3065–3075, 2015.

42. Averina, V.A., H.G. Othmer, G.D. Fink, and J.W. Osborn, "A New Conceptual Paradigm for the Haemodynamics of Salt-Sensitive Hypertension: A Mathemat-

ical Modelling Approach", *The Journal of Physiology*, Vol. 590, No. 23, pp. 5975–5992, 2012.

43. Karaaslan, F., Y. Denizhan, and R. Hester, "A Mathematical Model of Long-Term Renal Sympathetic Nerve Activity Inhibition During an Increase in Sodium Intake", *American Journal of Physiology-Regulatory, Integrative and Comparative Physiology*, Vol. 306, No. 4, pp. R234–R247, 2014.

44. Karaaslan, F., Y. Denizhan, A. Kayserilioglu, and H.O. Gulcur, "Long-Term Mathematical Model Involving Renal Sympathetic Nerve Activity, Arterial Pressure, and Sodium Excretion", *Annals of Biomedical Engineering*, Vol. 33, No. 11, pp. 1607–1630, 2005.

45. Formanowicz, D., A. Rybarczyk, M. Radom, and P. Formanowicz, "A Role of Inflammation and Immunity in Essential Hypertension—Modeled and Analyzed Using Petri Nets", *International Journal of Molecular Sciences*, Vol. 21, No. 9, pp. 3348, 2020.

46. Podkowińska A., and D. Formanowicz, "Chronic Kidney Disease as Oxidative Stress -and Inflammatory- Mediated Cardiovascular Disease", *Antioxidants*, Vol. 9, No. 8, pp. 752, 2020.

47. Muniyappa, R., H. Chen, M. Montagnani, A. Sherman, and M.J. Quon, "Endothelial Dysfunction Due to Selective Insulin Resistance in Vascular Endothelium: Insights from Mechanistic Modeling", *American Journal of Physiology-Endocrinology and Metabolism*, Vol. 319, No. 3, pp. E629–E646, 2020.

48. Versypt, A.N.F., G.K. Harrell, and A.N. McPeak, "A Pharmacokinetic/Pharmacodynamic Model of Ace Inhibition of the Renin-Angiotensin System for Normal and Impaired Renal Function", *Computers & Chemical Engineering*, Vol. 104, pp. 311–322, 2017.

49. Hallow, K.M., A. Lo, J. Beh, M. Rodrigo, S. Ermakov, S. Friedman, H. de Leon, A. Sarkar, Y. Xiong, R. Sarangapani, and H. Schmidt, "A Model-Based Approach to Investigating the Pathophysiological Mechanisms of Hypertension and Response to Antihypertensive Therapies: Extending the Guyton Model", *American Journal of Physiology-Regulatory, Integrative and Comparative Physiology*, Vol. 306, No. 9, pp. R647–R662, 2014.

50. Pettersen, K.H., S.M. Bugenhagen, J. Nauman, D.A. Beard, and S.W. Omholt, "Arterial Stiffening Provides Sufficient Explanation For Primary Hypertension", *PLOS Computational Biology*, Vol. 10, No. 5, pp. e1003634, 2014.

51. Rachev A., and T. Shazly, "A Two-Dimensional Model of Hypertension-Induced Arterial Remodeling With Account for Stress Interaction Between Elastin and Collagen", *Journal of Biomechanical Engineering*, Vol. 142, No. 4, 2020.

52. Rachev, A., W.R. Taylor, and R.P. Vito, "Calculation of the Outcomes of Remodeling of Arteries Subjected to Sustained Hypertension Using a 3D Two-Layered Model", *Annals of Biomedical Engineering*, Vol. 41, No. 7, pp. 1539–1553, 2013.

53. Acosta, S., C. Puelz, B. Rivière, D.J. Penny, K.M. Brady, and C.G. Rusin, "Cardiovascular Mechanics in the Early Stages of Pulmonary Hypertension: A Computational Study", *Biomechanics and Modeling in Mechanobiology*, Vol. 16, No. 6, pp. 2093–2112, 2017.

54. Colebank, M.J., M. Qureshi, S. Rajagopal, R.A. Krasuski, and M.S. Olufsen, "A Multiscale Model of Vascular Function in Chronic Thromboembolic Pulmonary Hypertension", *American Journal of Physiology-Heart and Circulatory Physiology*, Vol. 321, No. 2, pp. H318–H338, 2021.

55. Lee, K.J., C. Park, J. Oh, and B. Lee, "Non-Invasive Detection of Intracranial Hypertension Using a Simplified Intracranial Hemo-and Hydro-Dynamics Model", *Biomedical Engineering Online*, Vol. 14, No. 1, pp. 1–12, 2015.

56. Bateman, G.A., S.A. Stevens, and J. Stimpson, "A Mathematical Model of Idiopathic Intracranial Hypertension Incorporating Increased Arterial Inflow and Variable Venous Outflow Collapsibility", *Journal of Neurosurgery*, Vol. 110, No. 3, pp. 446–456, 2009.

57. Golse, N., F. Joly, P. Combari, M. Lewin, Q. Nicolas, C. Audebert, D. Samuel, M.-A. Allard, A.S. Cunha, D. Castaing, and D. Cherqui, "Predicting the Risk of Post-Hepatectomy Portal Hypertension Using a Digital Twin: A Clinical Proof of Concept", *Journal of Hepatology*, Vol. 74, No. 3, pp. 661–669, 2021.

58. Benoit, J.N., W.A. Womack, L. Hernandez, and D.N. Granger, ""Forward" and "Backward" Flow Mechanisms of Portal Hypertension: Relative Contributions in the Rat Model of Portal Vein Stenosis", *Gastroenterology*, Vol. 89, No. 5, pp. 1092–1096, 1985.

59. Leete, J., and A.T. Layton, "Sex-Specific Long-Term Blood Pressure Regulation: Modeling and Analysis", *Computers in Biology and Medicine*, Vol. 104, pp. 139–148, 2019.

60. Darabi, N., and N. Hosseinichimeh, "System Dynamics Modeling in Health and Medicine: A Systematic Literature Review", *System Dynamics Review*, Vol. 36, No. 1, pp. 29–73, 2020.

61. Luginbuhl, W.H., B.R. Forsyth, G.B. Hirsch, and M.R. Goodman, "Prevention and Rehabilitation as a Means of Cost Containment: The Example of Myocardial Infarction", *Journal of Public Health Policy*, Vol. 2, No. 2, pp. 103–115, 1981.

62. Homer, J., B. Milstein, D. Labarthe, D. Orenstein, K. Wile, J. Trogdon, and P. Huang, "Peer Reviewed: Simulating and Evaluating Local Interventions to Improve Cardiovascular Health", *Preventing Chronic Disease*, Vol. 7, No. 1, 2010.

63. Hirsch, G., J. Homer, E. Evans, and A. Zielinski, "A System Dynamics Model

for Planning Cardiovascular Disease Interventions", *American Journal of Public Health*, Vol. 100, No. 4, pp. 616–622, 2010.

64. Homer, J., K. Wile, B. Yarnoff, J.G. Trogdon, G. Hirsch, L. Cooper, R. Soler, D. Orenstein, "Using Simulation to Compare Established and Emerging Interventions to Reduce Cardiovascular Disease Risk in the United States", *Preventing Chronic Disease*, Vol. 11, pp. E195, 2014.

65. Hirsch, G., J. Homer, J. Trogdon, K. Wile, and D. Orenstein, "Using Simulation to Compare 4 Categories of Intervention for Reducing Cardiovascular Disease Risks", *American Journal of Public Health*, Vol. 104, No. 7, pp. 1187–1195, 2014.

66. de Andrade, L., C. Lynch, E. Carvalho, C.G. Rodrigues, J.R.N. Vissoci, G.F. Passos, R. Pietrobon, O.K. Nihei, and M.D. de Barros Carvalho, "System Dynamics Modeling in the Evaluation of Delays of Care in St-Segment Elevation Myocardial Infarction Patients Within a Tiered Health System", *PlOS One*, Vol. 9, No. 7, pp. e103577, 2014.

67. Homer, J., G. Hirsch, M. Minniti, and M. Pierson, "Models for Collaboration: How System Dynamics Helped a Community Organize Cost-Effective Care for Chronic Illness", *System Dynamics Review: The Journal of the System Dynamics Society*, Vol. 20, No. 3, pp. 199–222, 2004.

68. Çömez, S., *"Modeling the Dynamics of Vicious Cycles Involved Inheart-Respiratory Failure"*, M.S. Thesis, Boğaziçi University, Fen Bilimleri Enstitüsü, 2019.

69. Lich, K.H., Y. Tian, C.A. Beadles, L.S. Williams, D.M. Bravata, E.M. Cheng, H.B. Bosworth, J.B. Homer, and D.B. Matchar, "Strategic Planning to Reduce the Burden of Stroke Among Veterans: Using Simulation Modeling to Inform Decision Making", *Stroke*, Vol. 45, No. 7, pp. 2078–2084, 2014.

70. Demirezen E.M., and Y. Barlas, "A Simulation Model for Blood Cholesterol Dynamics and Related Disorders", paper presented at the *27th International Conference of the System Dynamics Society*, New Mexico, USA, Vol. 26, p. 30, 2009.

71. Orenstein, D.R., J. Homer, B. Milstein, K. Wile, P. Pratibhu, and R. Farris, "Modeling the Local Dynamics of Cardiovascular Health: Risk Factors, Context, and Capacity", *Preventing Chronic Disease*, Vol. 5, Vol. 2, 2008.

72. Kenealy, T., D. Rees, N. Sheridan, A. Moffitt, S. Tibby, and J. Homer, "A 'Whole of System' Approach to Compare Options for CVD Interventions in Counties Manukau", *Australian and New Zealand Journal of Public Health*, Vol. 36, No. 3, pp. 263–268, 2012.

73. Mehrjerdi, Y.Z., "A Dynamic Systems Approach to Weight Related Health Problems", *International Journal of Quality & Reliability Management*, Vol. 30, No. 5, pp. 571-589, 2013.

74. Recio, A., C. Linares, and J. Díaz, "System Dynamics for Predicting the Impact of Traffic Noise on Cardiovascular Mortality in Madrid", *Environmental Research*, Vol. 167, pp. 499–505, 2018.

75. Loyo, H.K., C. Batcher, K. Wile, P. Huang, D. Orenstein, and B. Milstein, "From Model to Action: Using a System Dynamics Model of Chronic Disease Risks to Align Community Action", *Health Promotion Practice*, Vol. 14, No. 1, pp. 53–61, 2013.

76. Ansah, J.P., S.T.Y. Wei, and T.L.S. Min, "An Evaluation of the Impact of Aggressive Diabetes and Hypertension Management on Chronic Kidney Diseases at the Population Level: A Simulation Analysis", *System Dynamics Review*, Vol. 36, Vol. 4, pp. 497–522, 2020.

77. Ansah, J.P., R.L.H. Inn, and S. Ahmad, "An Evaluation of the Impact of Aggressive Hypertension, Diabetes and Smoking Cessation Management on CVD Outcomes at the Population Level: A Dynamic Simulation Analysis", *BMC Public Health*, Vol. 19, No. 1, pp. 1–13, 2019.

78. Mingjie, Z., and Z. Zhiyuan, "Application of System Dynamics to Cardiovascular System Biofeedback Regulation of BP for Hypertensives", *The 1987 International Conference of the System Dynamics Society*, Shanghai, China, 1987.

79. Incioğlu, F., *A Dynamic Simulation Model For Long-Term Hypertension Progression*, M.S. Thesis, Boğaziçi University, Fen Bilimleri Enstitüsü, 2006.

80. Ozgun, K., *Modeling the Dynamics of Blood Pressure Under the Sleep Apnea Effect*, M.S. Thesis, Boğaziçi University, Fen Bilimleri Enstitüsü, 2019.

81. Karanfil,Ö., and Y. Barlas, "A Dynamic Simulator for the Management of Disorders of the Body Water Homeostasis", *Operations Research*, Vol. 56, No. 6, pp. 1474–1492, 2008.

82. Lilly, L.S., *Pathophysiology of Heart Disease: A Collaborative Project of Medical Students and Faculty*, Lippincott Williams & Wilkins, 2012.

83. Klabunde, R., *Cardiovascular Physiology Concepts*, Lippincott Williams & Wilkins, 2011.

84. Hall, J.E., and M. Hall, *Guyton and Hall Textbook of Medical Physiology e-Book*, Elsevier Health Sciences, 2020.

85. Sterman, J., *Business Dynamics*, Irwin/McGraw-Hill, 2000.

86. Barlas, Y., "Formal Aspects of Model Validity and Validation in System Dynamics", *System Dynamics Review: The Journal of the System Dynamics Society*, Vol. 12, No. 3, pp. 183–210, 1996.

87. Quer, G., P. Gouda, M. Galarnyk, E.J. Topol, and S.R. Steinhubl, "Inter- and Intraindividual Variability in Daily Resting Heart Rate and its Associations With Age, Sex, Sleep, BMI, and Time of Year: Retrospective, Longitudinal Cohort Study of 92,457 Adults", *PLOS One*, Vol. 15, No. 2, pp. e0227709, 2020.

88. Lakatta, E.G., and D. Levy, "Arterial and Cardiac Aging: Major Shareholders in Cardiovascular Disease Enterprises: Part I: Aging Arteries: A "Set Up" for Vascular Disease", *Circulation*, Vol. 107, No. 1, pp. 139–146, 2003.

89. Vlachopoulos, C., K. Aznaouridis, and C. Stefanadis, "PRediction of Cardiovascular Events and All-Cause Mortality With Arterial Stiffness: A Systematic Review and Meta-Analysis", *Journal of the American College of Cardiology*, Vol. 55, No. 13, pp. 1318–1327, 2010.

90. Chen, Z.-W., C.-H. Tsai, C.-T. Pan, C.-H. Chou, C.-W. Liao, C.-S. Hung, V.-C. Wu, Y.-H. Lin, and TAIPAI Study Group, "Endothelial Dysfunction in Primary Aldosteronism", *International Journal of Molecular Sciences*, Vol. 20, No. 20, pp. 5214, 2019.

91. Jani, B., and C. Rajkumar, "Ageing and Vascular Ageing", *Postgraduate Medical Journal*, Vol. 82, No.968, pp. 357–362, 2006.

92. Hainsworth, R., "The Importance of Vascular Capacitance in Cardiovascular Control", *Physiology*, Vol. 5, Vol. 6, pp. 250–254, 1990.

93. McVeigh, G.E., P.K. Hamilton, and D.R. Morgan, "Evaluation of Mechanical Arterial Properties: Clinical, Experimental and Therapeutic Aspects", *Clinical Science*, Vol. 102, No. 1, pp. 51–67, 2002.

94. Dharmashankar, K., and M.E. Widlansky, "Vascular Endothelial Function and Hypertension: Insights and Directions", *Current Hypertension Reports*, Vol. 12, No. 6, pp. 448–455, 2010.

95. Benjamin, E.J., M.G. Larson, M.J. Keyes, G.F. Mitchell, R.S. Vasan, J.F. Keaney, B.T. Lehman, S. Fan, E. Osypiuk, and J.A. Vita, "Clinical Correlates and Heritability of Flow-Mediated Dilation in the Community: The Framingham Heart Study", *Circulation*, Vol. 109, No. 5, pp. 613–619, 2004.

96. Wen, W., R. Luo, X. Tang, L. Tang, H.X. Huang, X. Wen, S. Hu, and B. Peng, "Age-Related Progression of Arterial Stiffness and its Elevated Positive Association With Blood Pressure in Healthy People", *Atherosclerosis*, Vol. 238, No. 1, pp. 147–152, 2015.

97. Namekata, T., K. Suzuki, N. Ishizuka, and K. Shirai, "Establishing Baseline Criteria of Cardio-Ankle Vascular Index as a New Indicator of Arteriosclerosis: A Cross-Sectional Study", *BMC Cardiovascular Disorders*, Vol. 11, No. 1, pp. 1–10, 2011.

98. Wirth, A., S. Wang, M. Takefuji, C. Tang, T.F. Althoff, F. Schweda, N. Wettschureck, and S. Offermanns, "Age-Dependent Blood Pressure Elevation is Due to Increased Vascular Smooth Muscle Tone Mediated by G-Protein Signalling", *Cardiovascular Research*, Vol. 109, No. 1, pp. 131–140, 2016.

99. Sleight, P., "Lowering of Blood Pressure and Artery Stiffness", *The Lancet*, Vol. 349, No. 9056, pp. 955–956, 1997.

100. Andresen, M.C., and M. Yang, "Arterial Baroreceptor Resetting: Contributions of Chronic and Acute Processes", *Clinical and Experimental Pharmacology & Physiology. Supplement*, Vol. 15, pp. 19–30, 1989.

101. Parlow, J., J.-P. Viale, G. Annat, R. Hughson, and L. Quintin, "Spontaneous Cardiac Baroreflex in Humans: Comparison With Drug-Induced Responses", *Hypertension*, Vol. 25, No. 5, pp. 1058–1068, 1995.

102. Chapleau, M.W., G. Hajduczok, and F.M. Abboud, "Mechanisms of Resetting

of Arterial Baroreceptors: An Overview", *The American Journal of the Medical Sciences*, Vol. 295, No. 4, pp. 327–334, 1988.

103. Lohmeier, T.E., E.D. Irwin, M.A. Rossing, D.J. Serdar, and R.S. Kieval, "Prolonged Activation of the Baroreflex Produces Sustained Hypotension", *Hypertension*, Vol. 43, No. 2, pp. 306–311, 2004.

104. Tank, J., A. Diedrich, E. Szczech, F.C. Luft, and J. Jordan, "Baroreflex Regulation of Heart Rate and Sympathetic Vasomotor Tone in Women and Men", *Hypertension*, Vol. 45, No. 6, pp. 1159–1164, 2005.

105. Julius, S., and S. Nesbitt, "Sympathetic Overactivity in Hypertension: A Moving Target", *American Journal of Hypertension*, Vol. 9, No. 4, pp. 113S–120S, 1996.

106. Gordan, R., J.K. Gwathmey, and L.-H. Xie, "Autonomic and Endocrine Control of Cardiovascular Function", *World journal of cardiology*, Vol. 7, No. 4, pp. 204, 2015.

107. Fu, Q., R.P. Shook, K. Okazaki, J.L. Hastings, S. Shibata, C.L. Conner, M.D. Palmer, and B.D. Levine, "Vasomotor Sympathetic Neural Control is Maintained During Sustained Upright Posture in Humans", *The Journal of Physiology*, Vol. 577, No. 2, pp. 679–687, 2006.

108. Lindeman, R.D., J. Tobin, and N.W. Shock, "Longitudinal Studies on the Rate of Decline in Renal Function With Age", *Journal of the American Geriatrics Society*, Vol. 33, No. 4, pp. 278–285, 1985.

109. Collard, D., Brouwer, T.F., R.H.G.O. Engberink, A.H. Zwinderman, L. Vogt, and B.-J.H. van den Born, "Initial Estimated Glomerular Filtration Rate Decline and Long-Term Renal Function During Intensive Antihypertensive Therapy: A Post Hoc Analysis of the SPRINT and ACCORD-BP Randomized Controlled Trials", *Hypertension*, Vol. 75, No. 5, pp. 1205–1212, 2020.

110. Gilmore, J., "Kdoqi Clinical Practice Guidelines and Clinical Practice Recommendations–2006 Updates", *Nephrology Nursing Journal*, Vol. 33, No. 5, pp. 487–489, 2006.

111. Yu, Z., C.M. Rebholz, E. Wong, Y. Chen, K. Matsushita, J. Coresh, and M.E. Grams, "Association Between Hypertension and Kidney Function Decline: The Atherosclerosis Risk in Communities (ARIC) Study", *American Journal of Kidney Diseases*, Vol. 74, No. 3, pp. 310–319, 2019.

112. Heesch, C.M., and C.M. Foley, "CNS Effects of Ovarian Hormones and Metabolites on Neural Control Of Circulation", *Annals of the New York Academy of Sciences*, Vol. 940, No. 1, pp. 348–360, 2001.

113. Meredith, P.A., and H.L. Elliott, "Clinical Pharmacokinetics of Amlodipine", *Clinical Pharmacokinetics*, Vol. 22, No. 1, pp. 22–31, 1992.

114. Stangier,J., C. Su, and W. Roth, "Pharmacokinetics of Orally and Intravenously Administered Telmisartan in Healthy Young and Elderly Volunteers and in Hypertensive Patients", *Journal of International Medical Research*, Vol. 28, No. 4, pp. 149–167, 2000.

115. Carter, B.L., M.E. Ernst, and J.D. Cohen, "Hydrochlorothiazide Versus Chlorthalidone: Evidence Supporting Their Interchangeability", *Hypertension*, Vol. 43, No. 1, pp. 4–9, 2004.

116. Kim, Y., M. Son, D. Lee, H. Roh, H. Son, D. Chae, M.Y. Bahng, and K. Park, "Pharmacokinetic Comparison of 2 Fixed-Dose Combination Tablets Of Amlodipine and Valsartan in Healthy Male Korean Volunteers: A Randomized, Open-Label, 2-Period, Single-Dose, Crossover Study", *Clinical Therapeutics*, Vol. 35, No. 7, pp. 934–940, 2013.

117. Mukherjee, D., J. Zha, R.M. Menon, and M. Shebley, "Guiding Dose Adjustment

of Amlodipine After Co-Administration With Ritonavir Containing Regimens Using a Physiologically-Based Pharmacokinetic/Pharmacodynamic Model", *Journal of Pharmacokinetics and Pharmacodynamics*, Vol. 45, No. 3, pp. 443–456, 2018.

118. Noh, Y.-H., H.-S. Lim, M.J. Kim, Y.H. Kim, H.Y. Choi, H.R. Sung, S.-J. Jin, J. Lim, and K.-S. Bae, "Pharmacokinetic Interaction of Telmisartan With S-Amlodipine: An Open-Label, Two-Period Crossover Study in Healthy Korean Male Volunteers", *Clinical Therapeutics*, Vol. 34, No. 7, pp. 1625–1635, 2012.

119. Jeon, I., S.J. Moon, S.-I. Park, Y. Choi, J. Jung, K.-S. Yu, and J.-Y. Chung, "Pharmacokinetics of a Fixed-Dose Combination of Amlodipine/Losartan and Chlorthalidone Compared to Concurrent Administration of the Separate Components", *Clinical Pharmacology in Drug Development*, Vol. 11, No. 1, pp. 91–99, 2022.

120. Denton, D., R. Weisinger, N.I. Mundy, E.J. Wickings, A. Dixson, P. Moisson, A.M. Pingard, R. Shade, D. Carey, R. Ardaillou, and F. Paillard, "The Effect of Increased Salt Intake on Blood Pressure of Chimpanzees", *Nature medicine*, Vol. 1, No. 10, pp. 1009–1016, 1995.

121. Martini, W.Z., D.S. Cortez, and M.A. Dubick, "Comparisons of Normal Saline and Lactated Ringer's Resuscitation on Hemodynamics, Metabolic Responses, and Coagulation in Pigs After Severe Hemorrhagic Shock", *Scandinavian Journal of Trauma, Resuscitation and Emergency Medicine*, Vol. 21, No. 1, pp. 1–12, 2013.

122. Ku, E., B.J. Lee, J. Wei, and M.R. Weir, "Hypertension in CKD: Core Curriculum 2019", *American Journal of Kidney Diseases*, Vol. 74, No. 1, pp. 120–131, 2019.

123. Bovée, D.M., L. Ren, E. Uijl, M.C.C.-van Groningen, R. van Veghel, I.M. Garrelds, O. Domenig, M. Poglitsch, I. Zlatev, J.B. Kim, and S. Huang, "Renoprotective Effects of Small Interfering RNA Targeting Liver Angiotensinogen in Experimental Chronic Kidney Disease", *Hypertension*, Vol. 77, No. 5, pp. 1600–

1612, 2021.

124. Burt, V.L., P. Whelton, E.J. Roccella, C. Brown, J.A. Cutler, M. Higgins, M.J. Horan, and D. Labarthe, "Prevalence of Hypertension in the US Adult Population: Results From the Third National Health and Nutrition Examination Survey, 1988-1991", *Hypertension*, Vol. 25, No. 3, pp. 305–313, 1995.

125. Saxena, T., A.O. Ali, and M. Saxena, "Pathophysiology of Essential Hypertension: An Update", *Expert Review of Cardiovascular Therapy*, Vol. 16, No. 12, pp. 879–887, 2018.

126. World Health Organization, *Guideline for the Pharmacological Treatment of Hypertension in Adults: WEB ANNEX A: Summary of Evidence*, Geneva: World Health Organization, pp.185, 2021.

APPENDIX A: MODEL EQUATIONS

base renin activity = 1
Units: [pg/(ml*hr)]

overactive RAAS = (RAAS pulse + RAAS pulse train + RAAS ramp + RAAS step + RAAS step up down) * base renin activity
Units: [pg/(ml*hr)]

salt ramp slope = salt hp 1 intensity + salt hp 2 intensity + salt hp 3 intensity + salt hp 4 intensity + Mixed salt
Units: [Dmnl]

mix salt frac= 1.3
Units: [Dmnl]

mix SNS frac= 1.3
Units: [Dmnl]

Mixed RAAS= RAAS base ramp intensity * mixed RAAS switch * mix RAAS frac
Units: [Dmnl]

ramp slope= SNS hp 1 intensity + SNS hp 2 intensity + SNS hp 3 intensity + SNS hp 4 intensity + Mixed SNS
Units: [Dmnl]

Mixed salt= salt base ramp intensity * mixed salt switch * mix salt frac
Units: [Dmnl]

mixed salt switch= 0

Units: [Dmnl] [0,1,1]

RAAS ramp slope= RAAS hp 1 intensity + RAAS hp 2 intensity + RAAS hp 3 intensity + RAAS hp 4 intensity + Mixed RAAS
Units: [Dmnl]

SNS ramp= RAMP(ramp slope , ramp start , SNS ramp finish)*SNS ramp switch
Units: [Dmnl]

mix RAAS frac= 1.3
Units: [Dmnl]

Mixed SNS= SNS base ramp intensity * mixed SNS switch * mix SNS frac
Units: [Dmnl]

mixed SNS switch= 0
Units: [Dmnl] [0,1,1]

mixed RAAS switch= 0
Units: [Dmnl] [0,1,1]

Salt retention= (salt pulse + salt pulse train + salt ramp + salt step + salt step up down)
Units: [Dmnl]

implied Na removal= patient Na removal * eff of aldosterone on Na removal * eff of GFR on Na removal * eff of concentration on removal
Units: [mEq/Day]

patient Na removal= healthy normal na removal * (1 + eff of chlorthalidone on na removal) -retained salt

Units: [mEq/Day]

retained salt= healthy normal na removal * Salt retention / (1+eff of chlorthalidone on na removal)
Units: [mEq/Day]

implied heart rate= normal HR * eff of SNS on HR * eff of PNS on HR - (normal HR*eff of amlodipine on HR*eff of SNS on HR)
Units: [beat/min]

RAAS ramp= RAMP (RAAS ramp slope , RAAS ramp start , RAAS ramp finish) * RAAS ramp switch
Units: [Dmnl]

RAAS ramp switch=0
Units: [Dmnl/Day] [0,1,1]

eff of SNS on HR= WITH LOOKUP (implied SNS activity/normal SNS activity, ([(1, 1)-(2, 3)], (0, 1), (1, 1), (1.01833, 1.13986), (1.04684, 1.34965), (1.08147, 1.59441), (1.12627, 1.85315), (1.19756, 2.2028),(1.26273, 2.42657), (1.33401, 2.62238), (1.39919, 2.74825), (1.47047, 2.84615), (1.56008, 2.93007), (1.67821, 2.96503), (1.87373, 2.97902), (1.99796, 2.98601)))
Units: [Dmnl]

salt pulse start= 0
Units: [Day] [0,30]

salt pulse switch= 0
Units: [Dmnl] [0,1,1]

salt pulse train= SMOOTH (PULSE TRAIN (salt pulse train start , salt pulse train

duration , salt pulse train repeat time, salt pulse train end) , salt pulse smooth time) * salt percent increase * salt pulse train switch
Units: [Dmnl]

salt pulse train duration= 1
Units: [Day] [0,?] salt pulse train end= 1500
Units: [Day] [0,?]

salt pulse train repeat time= 30
Units: [Day [0,?]

salt pulse train start= 1
Units: [Day] [0,?]

salt pulse train switch= 0
Units: [Dmnl] [0,1,1]

salt ramp= RAMP(salt ramp slope , salt ramp start , salt ramp finish) * salt ramp switch
Units: [Dmnl]

salt ramp start= 0
Units: [Day] [0,?]

salt ramp switch= 0
Units: [Dmnl/Day] [0,1,1]

salt step= SMOOTH((STEP(salt percent increase step, salt step start)*salt step switch), salt pulse smooth time)
Units: [Dmnl]

salt step start= 30
Units: [Day]

salt step switch= 0
Units: [Dmnl] [0,1,1]

salt step up down= SMOOTH(((STEP(salt percent increase, salt step up down start) - STEP(salt percent increase, salt step up down end))), salt pulse smooth time)* salt step up down switch
Units: [Dmnl]

RAAS base ramp intensity= 0.000135
Units: [Dmnl] [0,0.0005,5e-06]

RAAS hp 1 intensity= RAAS base ramp intensity* 1* RAAS hp 1 switch ramp
Units: [Dmnl]

arterial tone increase at normal dose= 0.025
Units: [Dmnl] [0,0.1]

RAAS hp 1 percent step= base percent for RAAS step* 1* RAAS hp 1 switch step
Units: [Dmnl]

AT2 decrease in normal dose= 0.025
Units: [Dmnl] [0,0.3]

RAAS hp 1 percent= base percent for RAAS activity increase* 1* RAAS hp 1 switch pulse
Units: [Dmnl]

salt base ramp intensity= 0.00055

Units: [Dmnl] [0,0.0005,5e-06]

RAAS hp 2 intensity= RAAS base ramp intensity * 2 * RAAS hp 2 switch ramp
Units: [Dmnl]

RAAS hp 2 percent= base percent for RAAS activity increase * 2 * RAAS hp 2 switch pulse
Units: [Dmnl]

RAAS hp 2 percent step= base percent for RAAS step * 2 * RAAS hp 2 switch step
Units: [Dmnl]

salt hp 1 percent step= base percent for salt step * salt hp 1 switch step
Units: [Dmnl]

salt hp 1 switch pulse= 0
Units: [Dmnl] [0,1,1]

HR decrease at normal dose= 0.1
Units: [Dmnl] [0,?]

RAAS hp 3 intensity= RAAS base ramp intensity * 3 * RAAS hp 3 switch ramp
Units: [Dmnl]

RAAS hp 3 percent= base percent for RAAS activity increase * 3 * RAAS hp 3 switch pulse
Units: [Dmnl]

RAAS hp 3 percent step= base percent for RAAS step * 3 * RAAS hp 3 switch step
Units: [Dmnl]

salt hp 2 percent step= 2 * base percent for salt step * salt hp 2 switch step
Units: [Dmnl]

salt hp 2 switch pulse= 0
Units: [Dmnl] [0,1,1]

salt hp 2 switch ramp= 0
Units: [Dmnl] [0,1,1]

RAAS hp 4 intensity= RAAS base ramp intensity*4*RAAS hp 4 switch ramp
Units: [Dmnl]

base percent for RAAS activity increase= 1
Units: [Dmnl]

base percent for RAAS step= 0.03
Units: [Dmnl]

base percent for salt retention increase= -0.03
Units: [Dmnl]

base percent for salt step= -0.02
Units: [Dmnl]

eff of amlodipine on contractility= eff of amlodipine on dose on contractility * contractility decrease at normal dose
Units: [Dmnl] [0,0.1]

implied radius= Normal arterial tone * eff of SNS on arterial tone * eff of AT2 on arterial tone * eff of ADH on arterial tone + (Normal arterial tone * (eff of amlodipine on arterial tone/ eff of SNS on arterial tone))

Units: [Dmnl]

implied renin activity= (normal renin activity+overactive RAAS)*(eff of RSNS on renin)
Units: [pg/(ml*hr)]

implied RSNS activity= (Mean Arterial Pressure/RSNS operating point)*(normal RSNS activity)
Units: [Dmnl]

salt hp 4 percent step= 4* base percent for salt step* salt hp 4 switch step
Units: [Dmnl]

salt hp 4 switch pulse= 0
Units: [Dmnl] [0,1,1]

salt hp 4 switch ramp= 0
Units: [Dmnl] [0,1,1]

salt hp 4 switch step= 0
Units: [Dmnl] [0,1,1]

salt percent increase= salt hp 1 percent+ salt hp 2 percent+ salt hp 3 percent+ salt hp 4 percent
Units: [Dmnl]

salt percent increase step= salt hp 1 percent step+ salt hp 2 percent step+ salt hp 3 percent step+ salt hp 4 percent step
Units: [Dmnl]

salt pulse= SMOOTH (PULSE(salt pulse start , salt pulse duration)*salt percent

increase , salt pulse smooth time)*salt pulse switch
Units: [Dmnl]

salt pulse duration= 1
Units: [Day] [0,?]

eff of chlorthalidone on na removal= na removal increase in normal dose* eff of chlorthalidone dose on Na removal
Units: [Dmnl]

salt pulse smooth time= 7
Units: [Day]

RAAS hp 4 percent step= base percent for RAAS step*4*RAAS hp 4 switch step
Units: [Dmnl]

salt hp 1 switch ramp= 0
Units: [Dmnl] [0,1,1]

salt hp 1 switch step= 0
Units: [Dmnl] [0,1,1]

salt hp 2 intensity= salt base ramp intensity * 2 * salt hp 2 switch ramp
Units: [Dmnl]

salt hp 2 percent= 2 * base percent for salt retention increase * salt hp 2 switch pulse
Units: [Dmnl]

contractility decrease at normal dose= 0.05
Units: [Dmnl][0,0.2]

iplied AT2= normal AT2 * eff of renin on AT2 - (normal AT2 * eff of telmisartan on AT2)
Units: [pg/ml]

eff of telmisartan on AT2= AT2 decrease in normal dose * eff of telmisartan dose on AT2
Units: [Dmnl]

salt ramp finish= 360
Units: [Day] [0,?]

salt hp 3 intensity= salt base ramp intensity * 3 * salt hp 3 switch ramp
Units: [Dmnl]

salt hp 3 percent= 3* base percent for salt retention increase* salt hp 3 switch pulse
Units: [Dmnl]

salt hp 3 percent step= 3* base percent for salt step* salt hp 3 switch step
Units: [Dmnl]

eff of amlodipine on arterial tone= arterial tone increase at normal dose* eff of amlodipine dose on arterial tone
Units: [Dmnl][0,0.1]

salt hp 3 switch step= 0
Units: [Dmnl][0,1,1]

eff of amlodipine on HR= eff of amlodipine dose on HR * HR decrease at normal dose
Units: [Dmnl][0,0.2]

salt hp 4 percent= 4 * base percent for salt retention increase * salt hp 4 switch pulse

Units: [Dmnl]

contractility= normal contractility * eff of SNS on contractility - (normal contractility * eff of amlodipine on contractility * eff of SNS on contractility)
Units: [Dmnl]

salt hp 4 intensity= salt base ramp intensity * 4 * salt hp 4 switch ramp
Units: [Dmnl]

salt step up down switch= 0
Units: [Dmnl][0,1,1]

healthy normal na removal= 180
Units: [mEq/Day]

salt hp 2 switch step= 0
Units: [Dmnl][0,1,1]

salt hp 1 intensity= salt base ramp intensity * salt hp 1 switch ramp
Units: [Dmnl]

salt hp 1 percent= base percent for salt retention increase* salt hp 1 switch pulse
Units: [Dmnl]

salt step up down start= 1
Units: [Day]

RAAS hp 4 percent= base percent for RAAS activity increase*4*RAAS hp 4 switch pulse
Units: [Dmnl]

salt hp 3 switch pulse= 0
Units: [Dmnl][0,1,1]

salt hp 3 switch ramp= 0
Units: [Dmnl][0,1,1]

salt step up down end= 720
Units: [Day]

na removal increase in normal dose= 0.2
Units: [Dmnl][0,1]

chlorthalidone daily dose= standard chlorthalidone dosing*chlorthalidone pulse*chlorthalidone switch
Units: [mg]

amlodipine daily dose= standard amlodipine dosing * amlodipine pulse * amlodipine switch
Units: [mg]

telmisartan daily dose= standard telmisartan dosing*telmisartan pulse*telmisartan switch
Units: [mg]

eff of GFR on Na concentration= WITH LOOKUP (Daily GFR/ normal daily fitration, ([(0,0)-(2,2)], (0.01222, 1.62937), (0.236253, 1.6014), (0.484725, 1.54545), (0.651731, 1.37063), (0.810591, 1.1958), (1,1),(1.99593, 0.286713)))
Units: [Dmnl]

SNS hp 4 intensity= SNS base ramp intensity * 4 * SNS hp 4 switch ramp
Units: [Dmnl]

SNS hp 4 percent= 4*base percent for SNS activity increase*SNS hp 4 switch pulse
Units: [Dmnl]

normal daily na consumed= 180
Units: [mEq/Day]

base percent for SNS step= 0.02
Units: [Dmnl]

SNS base ramp intensity= (1e-05)*2.5
Units: [Dmnl][0,0.0005,5e-06]

SNS hp 1 intensity= SNS base ramp intensity * SNS hp 1 switch ramp
Units: [Dmnl]

SNS hp 1 percent= base percent for SNS activity increase * SNS hp 1 switch pulse
Units: [Dmnl]

SNS hp 1 percent step= base percent for SNS step * SNS hp 1 switch step
Units: [Dmnl]

eff of RSNS on renin= WITH LOOKUP (implied RSNS activity/ normal RSNS activity, ([(0,0)-(2,2)], (0.00407332, 1.99301), (0.0855397,2), (0.297352,1.94406), (0.391039,1.9021),(0.476578, 1.83916), (0.602851, 1.67832), (1,1), (1.39715, 0.216783), (1.53564, 0.0979021), (1.73116, 0.034965), (1.99593, 0.00699306)))
Units: [Dmnl]

na loading= (STEP (na loading step height , na load start time) - STEP(na loading step height , na loading end time)) * normal daily na consumed * na intake multiplication factor * na loading switch
Units: [mEq/Day]

SNS ramp switch= 0
Units: [Dmnl/Day] [0,1,1]

SNS hp 2 intensity= SNS base ramp intensity * 2 * SNS hp 2 switch ramp
Units: [Dmnl

SNS hp 2 percent= 2 * base percent for SNS activity increase * SNS hp 2 switch pulse
Units: [Dmnl]

SNS hp 2 percent step= 2 * base percent for SNS step * SNS hp 2 switch step
Units: [Dmnl]

SNS hp 4 percent step= 4 * base percent for SNS step * SNS hp 4 switch step
Units: [Dmnl]

SNS hp 3 intensity= SNS base ramp intensity * 3*SNS hp 3 switch ramp
Units: [Dmnl]

normal SNS= 1
Units: [Dmnl]

SNS hp 3 percent step= 3 * base percent for SNS step * SNS hp 3 switch step
Units: [Dmnl]

overactive SNS= normal SNS * (SNS pulse + SNS pulse train + SNS ramp + SNS step + SNS step up down)
Units: [Dmnl]

SNS hp 3 percent= 3 * base percent for SNS activity increase * SNS hp 3 switch pulse
Units: [Dmnl]

base percent for SNS activity increase= 0.02
Units: [Dmnl]

RAAS hp 2 switch pulse= 0
Units: [Dmnl][0,1,1]

RAAS hp 2 switch ramp= 0
Units: [Dmnl][0,1,1]

RAAS hp 2 switch step= 0
Units: [Dmnl][0,1,1]

RAAS hp 3 switch pulse= 0
Units: [Dmnl][0,1,1]

RAAS hp 3 switch ramp= 0
Units: [Dmnl][0,1,1]

amlodipine pulse= PULSE TRAIN(amlodipine treatment start time , amlodipine treatment duration , amlodipine treatment repeat time, amlodipine treatment end time)
Units: [Dmnl]

chlorthalidone pulse= PULSE TRAIN(chlorthalidone treatment start time , chlorthalidone treatment duration, chlorthalidone treatment repeat time , chlorthalidone treatment end time)
Units: [Dmnl]

amlodipine treatment duration= 0.5
Units: [Day]

amlodipine treatment end time= 3000

Units: [Day]

amlodipine treatment repeat time= 1

Units: [Day]

amlodipine treatment start time= 900

Units: [Day] [300,1500,30]

chlorthalidone treatment start time= 900

Units: [Day] [300,1500,30]

RAAS pulse= SMOOTH (PULSE (RAAS pulse start , RAAS pulse duration) * RAAS percent increase , RAAS pulse smooth time) * RAAS pulse switch

Units: [Dmnl]

RAAS pulse duration= 1

Units: [Day] [0,?]

RAAS pulse smooth time= 7

Units: [Day]

RAAS pulse start= 0

Units: [Day] [0,30]

RAAS pulse switch= 0

Units: [Dmnl][0,1,1]

RAAS pulse train= SMOOTH (PULSE TRAIN(RAAS pulse train start , RAAS pulse train duration , RAAS pulse train repeat time , RAAS pulse train end) , RAAS pulse smooth time) * RAAS percent increase* RAAS pulse train switch

Units: [Dmnl]

RAAS pulse train duration= 5
Units: [Day [0,?]

RAAS pulse train end= 3000
Units: [Day] [0,?]

Optimal blood pressure= 120
Units: [mmhg]

RAAS pulse train switch= 0
Units: [Dmnl][0,1,1]

pulse blood loss= PULSE(blood loss start time , blood loss duration) * blood loss intensity * pulse blood loss switch
Units: [L]

RAAS ramp start= 0
Units: [Day] [0,?]

RAAS step= SMOOTH((STEP(RAAS percent increase step, RAAS step start) * RAAS step switch), RAAS pulse smooth time)
Units: [Dmnl]

RAAS step start= 30
Units: [Day]

EDV adjustment time= 1
Units: [Day]

RAAS step up down= SMOOTH(((STEP(RAAS percent increase, RAAS step up down end) -STEP(RAAS percent increase, RAAS step up down start))), RAAS pulse smooth time) * RAAS step up down switch
Units: [Dmnl]

blood loss duration= 0.05
Units: [Day]

blood loss start time= 1
Units: [Day]

RAAS hp 1 switch pulse= 0
Units: [Dmnl][0,1,1]

RAAS hp 1 switch ramp= 0
Units: [Dmnl][0,1,1]

RAAS hp 1 switch step= 0
Units: [Dmnl][0,1,1]

telmisartan treatment duration= 0.5
Units: [Day]

telmisartan treatment end time= 3000
Units: [Day]

telmisartan treatment repeat time= 1
Units: [Day]

telmisartan treatment start time= 900
Units: [Day] [300,1500,30]

RAAS pulse train repeat time= 60

Units: [Day] [0,?]

daily water removal adjustment time= 1

Units: [Day]

End diastolic volume= DELAY1(normal EDV * eff of blood volume on EDV, EDV adjustment time)

Units: [ml/beat]

implied water removal= DELAY1(Na removal, daily water removal adjustment time)/urine Na concentration

Units: [L/Day]

RAAS ramp finish= 300

Units: [Day] [0,?]

RAAS hp 3 switch step= 0

Units: [Dmnl][0,1,1]

na intake multiplication factor= 9

Units: [Dmnl

na load start time= 2

Units: [Day]

RAAS hp 4 switch pulse= 0

Units: [Dmnl][0,1,1]

chlorthalidone treatment duration= 0.5

Units: [Day]

chlorthalidone treatment end time= 3000
Units: [Day]

chlorthalidone treatment repeat time= 1
Units: [Day]

RAAS hp 4 switch step= 0
Units: [Dmnl][0,1,1]

telmisartan pulse= PULSE TRAIN(telmisartan treatment start time , telmisartan treatment duration , telmisartan treatment repeat time , telmisartan treatment end time)
Units: [Dmnl]

RAAS percent increase step= RAAS hp 1 percent step + RAAS hp 2 percent step + RAAS hp 3 percent step + RAAS hp 4 percent step
Units: [Dmnl]

RAAS percent increase= RAAS hp 1 percent + RAAS hp 2 percent + RAAS hp 3 percent + RAAS hp 4 percent
Units: [Dmnl]

RAAS step up down end= 20
Units: [Day]

RAAS step up down start= 35
Units: [Day]

RAAS step up down switch= 0
Units: [Dmnl][0,1,1]

na loading end time= 3

Units: [Day]

na loading step height= 1

Units: [Dmnl]

RAAS pulse train start= 1

Units: [Day] [0,?]

RAAS step switch= 0

Units: [Dmnl][0,1,1]

RAAS hp 4 switch ramp= 0

Units: [Dmnl][0,1,1]

SNS step up down switch= 0

Units: [Dmnl][0,1,1]

Upper normal blood pressure= 140

Units: [mmhg]

Hypertension grade 1= 150

Units: [mmhg]

Hypertension grade 2= 170

Units: [mmhg]

Hypertension grade 3= 180

Units: [mmhg]

SNS step up down end= 720

Units: [Day]

SNS step up down start= 1
Units: [Day]

SNS step up down= SMOOTH(((STEP(SNS percent increase, SNS step up down start) - STEP(SNS percent increase, SNS step up down end))), SNS pulse smooth time) * SNS step up down switch
Units: [Dmnl]

acute kidney damage= (STEP(time for damage to occur , kidney damage start time+ 1/time for damage to occur)-STEP(time for damage to occur, kidney damage start time))*kidney damage switch*percent of function loss
Units: [Dmnl/Day]

SNS hp 2 switch pulse= 0
Units: [Dmnl][0,1,1]

SNS hp 2 switch ramp= 0
Units: [Dmnl][0,1,1]

SNS hp 2 switch step= 0
Units: [Dmnl][0,1,1]

SNS hp 3 switch pulse= 0
Units: [Dmnl][0,1,1]

SNS hp 3 switch ramp= 0
Units: [Dmnl][0,1,1]

SNS hp 3 switch step= 1

Units: [Dmnl][0,1,1]

SNS hp 4 switch pulse= 0

Units: [Dmnl][0,1,1]

SNS hp 4 switch ramp= 0

Units: [Dmnl][0,1,1]

SNS hp 4 switch step= 0

Units: [Dmnl][0,1,1]

SNS percent increase= SNS hp 1 percent+SNS hp 2 percent+SNS hp 3 percent+SNS hp 4 percent

Units: [Dmnl]

SNS percent increase step= SNS hp 1 percent step + SNS hp 2 percent step + SNS hp 3 percent step + SNS hp 4 percent step

Units: [Dmnl]

SNS pulse= SMOOTH (PULSE(SNS pulse start , SNS pulse duration)*SNS percent increase , SNS pulse smooth time) * SNS pulse switch

Units: [Dmnl]

SNS pulse duration= 1

Units: [Day] [0,?]

SNS pulse smooth time= 7

Units: [Day]

SNS pulse start= 0

Units: [Day] [0,30]

SNS pulse switch= 0
Units: [Dmnl][0,1,1]

SNS pulse train= SMOOTH(PULSE TRAIN(SNS pulse train start , SNS pulse train duration , SNS pulse train repeat time , SNS pulse train end) , SNS pulse smooth time)*SNS percent increase*SNS pulse train switch
Units: [Dmnl]

SNS pulse train duration= 1
Units: [Day] [0,?]

SNS pulse train end= 1500
Units: [Day] [0,?]

SNS pulse train repeat time= 30
Units: [Day] [0,?]

SNS pulse train start= 1
Units: [Day] [0,?]

SNS pulse train switch= 0
Units: [Dmnl][0,1,1]

blood loss intensity= 10
Units: [L]

Blood volume= DELAY1(normal blood volume*eff of ECF volume on blood volume,blood volume adjustment time)-pulse blood loss
Units: [L]

SNS step start= 30

Units: [Day]

SNS step switch= 0
Units: [Dmnl][0,1,1]

ramp start= 0
Units: [Day] [0,?]

pulse water= pulse water intensity * PULSE(pulse water start time , pulse water duration) * pulse water switch
Units: [L/Day]

pulse water duration= 1
Units: [Day]

pulse water intensity= 20
Units: [L/Day]

pulse water start time= 2
Units: [Day]

SNS hp 1 switch step= 0
Units: [Dmnl][0,1,1]

percent of function loss= 0.7
Units: [Dmnl]

SNS hp 1 switch pulse= 0
Units: [Dmnl][0,1,1]

SNS hp 1 switch ramp= 0

Units: [Dmnl][0,1,1]

SNS ramp finish= 360
Units: [Day [0,?]

time for damage to occur= 3
Units: [1/Day]

kidney damage start time= 1
Units: [Day]

SNS step= SMOOTH((STEP(SNS percent increase step, SNS step start) * SNS step switch), SNS pulse smooth time)
Units: [Dmnl]

kidney function loss= (normal daily kidney function loss*eff of SBP on kidney damage)-acute kidney damage
Units: [Dmnl/Day]

kidney damage switch= 0
Units: [Dmnl][0,1,1]

na loading switch= 0
Units: [Dmnl][0,1,1]

days per year= 365
Units: [Day/year]

DBP80= 80
Units: [mmhg]

blood volume adjustment time= 3

Units: [Day]

average daily Na intake= 180+na loading

Units: [mEq/Day]

average daily water intake= (normal daily water intake + pulse water) * eff of osmolality on water intake

Units: [L/Day]

chlorthalidone weekly average dose= SMOOTH3 (Average free chlorthalidone in plasma , time to take weekly avg dose)

Units: [ng/ml]

pulse blood loss switch= 0

Units: [Dmnl][0,1,1]

pulse water switch= 0

Units: [Dmnl][0,1]

normal daily kidney function loss= yearly kidney function loss/days per year

Units: [Dmnl/Day]

amlodopine weekly average dose= SMOOTH3 (Average free amlodipine in plasma , time to take weekly avg dose)

Units: [ng/ml]

normal daily water intake= 2

Units: [L/Day]

normal vascular deterioration per day= yearly vascular deterioration/days per year

Units: [Dmnl/Day]

time to take weekly avg dose=7
Units: [Day]

eff of kidney function on GFR= WITH LOOKUP ((Kidney function), ([(0,0)-(1,1)], (0,0), (0.242363, 0.297203), (0.360489, 0.472028), (0.452138, 0.597902), (0.511202, 0.688811), (0.589409, 0.800699), (0.642159,0.856643), (0.690428,0.912587), (0.737271,0.944056), (0.792261,0.979021), (0.851324,0.99), (1,1)))
Units: [Dmnl]

Glomerular filtration rate= (normal GFR per min * eff of MAP on GFR * eff of kidney function on GFR)
Units: [ml/min]

daily average MAP= SMOOTH(Mean Arterial Pressure , time to average MAP)
Units: [mmhg]

SBP120= 120
Units: [mmhg]

Na intake= MAX(desired Na+average daily Na intake,0)
Units: [mEq/Day]

time to average SBP= 1
Units: [Day]

MAP93= 93.3
Units: [mmhg]

daily average DBP= SMOOTH(Diastolic BP , time to average DBP)

Units: [mmhg]

time to average MAP=7

Units: [Day]

daily average SBP= DELAY1 (Systolic BP , time to average SBP)

Units: [mmhg]

time to average DBP= 1

Units: [Day]

telmisertan weekly average dose= SMOOTH3(Average free telmisartan in plasma , time to take weekly avg dose)

Units: [ng/ml]

urine Na concentration= urine normal concentration * eff of ADH on urine Na concentration * eff of GFR on Na concentration

Units: [mEq/L]

urine normal concentration= 90

Units: [mEq/L]

telmisartan switch= 0

Units: [Dmnl][0,1,1]

initial operating point= Mean Arterial Pressure

Units: [mmhg]

initial RSNS operating point= Mean Arterial Pressure

Units: [mmhg]

implied SNS activity= (normal SNS activity+overactive SNS)*eff of baroreceptor on SNS
Units: [Dmnl]

amlodipine switch= 0
Units: [Dmnl][0,1]

chlorthalidone switch= 0
Units: [Dmnl][0,1,1]

yearly kidney function loss= 0.008
Units: [Dmnl/year]

implied normal tone= reference tone*eff of function on tone
Units: [Dmnl]

desired water= ((normal TBW-Total body water)/water adj time)
Units: [L/Day]

implied ADH= normal ADH*eff of AT2 on ADH*eff of osmolality on ADH
Units: [pg/ml]

eff of osmolality on water intake= WITH LOOKUP (Na concentration/normal Na concentration, ([(0,0) (2,5)], (0.00407332, 0.489511), (0.403259, 0.510489), (0.619145, 0.559441), (0.810591, 0.706294), (0.93279, 0.867133), (1,1), (1.08758, 1.18881), (1.2057, 1.78322), (1.29939, 2.67483), (1.40937, 3.74126), (1.47862, 4.24825), (1.58859, 4.63287), (1.71079, 4.79021), (1.78819, 4.86014), (1.89002, 4.91259), (1.98778, 4.91259)))
Units: [Dmnl]

eff of osmolality on ADH= WITH LOOKUP (Na concentration/normal Na

concentration, ([(0,0)-(2,2)], (0,0.503497), (0.358452, 0.503497), (0.578411, 0.566434), (1,1), (1.14053, 1.2028), (1.27495, 1.43357), (1.50713, 1.77622), (1.59267, 1.88811), (1.71894, 1.95804), (1.99593, 1.98601)))
Units: [Dmnl]

arterial tone change= (implied normal tone-Normal arterial tone)/tone adj time
Units: [1/Day]

Diastolic BP= Cardiac output * resistance at diastole
Units: [mmhg]

resistance at diastole= normal diastole resistance * eff of arterial tone on resistance * compliance
Units: [mmhg*min/ml]

eff of GFR on Na removal= Daily GFR/normal daily GFR
Units: [Dmnl]

eff of concentration on removal= Na concentration/normal Na concentration
Units: [Dmnl]

normal daily GFR= 180
Units: [L/Day]

normal Na concentration= 2160/14
Units: [mEq/L]

change in RSNS operating point= (Mean Arterial Pressure-RSNS operating point)/RSNS operating point adj time
Units: [mmhg/Day]

normal Na ratio= 0.007
Units: [Dmnl]

Na concentration= Total body salt/Extracellular fluid volume
Units: [mEq/L]

eff of MAP on GFR= WITH LOOKUP (Mean Arterial Pressure/reference MAP, ([(0.1, 0)-(2, 2)], (0.114053, 0.00947869), (0.219959, 0.356643), (0.270265, 0.496503), (0.339919, 0.643357), (0.409572, 0.762238), (0.479226, 0.839161), (0.575967, 0.909091), (0.688187, 0.951049), (0.784929, 0.972028), (0.916497, 1), (1, 1), (1.07515, 1), (1.14094, 1.00699), (1.20672, 1.02098), (1.26477, 1.03497), (1.38086, 1.06993), (1.50468, 1.11888), (1.6169, 1.17483), (1.71752, 1.25175), (1.79104, 1.37762), (1.86456, 1.52448), (1.99613, 1.97203)))
Units: [Dmnl]

reference MAP= 93.3
Units: [mmhg]

Na removal= implied Na removal
Units: [mEq/Day]

normal RSNS activity= 1
Units: [Dmnl]

cholorthalidone removal= Chlorthalidone concentration in plasma/chlorthalidone removal rate
Units: [(ng/ml)/Day]

eff of chlorthalidone dose on Na removal= WITH LOOKUP (chlorthalidone weekly average dose/average free chlorthalidone at standard dose, ([(0,0)-(2,2)], (0,0), (0.130346, 0.027972), (0.260692, 0.0839161), (0.342159, 0.146853), (0.427699,

0.244755), (1,1), (1.14053, 1.13986), (1.27088, 1.25874), (1.38493, 1.31469), (1.47862, 1.34965), (1.67821, 1.36364), (1.99185, 1.38462)))
Units: [Dmnl]

chlorthalidone removal rate= 10
Units: [Day]

change in average chlorthalidone= (Chlorthalidone concentration in plasma-Average free chlorthalidone in plasma)/average chlorthalidone adj time
Units: [(ng/ml)/Day]

average free chlorthalidone at standard dose= 3.57
Units: [ng/ml]

Average free chlorthalidone in plasma= INTEG (change in average chlorthalidone, 0)
Units: [ng/ml]

average free telmisartan at standard dose= 800
Units: [ng/ml]

Average free telmisartan in plasma= INTEG (change in average telmisartan, 0)
Units: [ng/ml]

average telmisartan adj time= 3
Units: [Day]

eff of amlodipine dose on HR= WITH LOOKUP (amlodopine weekly average dose/average free amlodipine at standard dose, ([(0,0)-(2,2)],(0,0),(0.130346,0.027972),(0.260692,0.0839161),(0.342159,0.146853),(0.427699,0.244755),(1,1
))
Units: [Dmnl]

average chlorthalidone adj time= 7
Units: [Day]

amlodipine dosing= implied amlodipine concentration/amlodipine adj time
Units: [(ng/ml)/Day]

chlorthalidone dosing= implied chlorthalidone conccentration/chlorthalidone adj time
Units: [(ng/ml)/Day]

telmisartan dosing=nimplied telmisartan concentration/telmisartan adj time
Units: [(ng/ml)/Day]

telmisartan removal= Telmisartan concentration in plasma/telmisartan removal rate
Units: [(ng/ml)/Day]

Chlorthalidone concentration in plasma= INTEG (chlorthalidone dosing-cholorthalidone removal,0)
Units: [ng/ml]

Telmisartan concentration in plasma= INTEG (telmisartan dosing-telmisartan removal, 0)
Units: [ng/ml]

eff of amlodipine dose on arterial tone= WITH LOOKUP (amlodopine weekly average dose/average free amlodipine at standard dose, ([(0,0)-(2, 2)], (0, 0), (0.130346, 0.027972), (0.260692, 0.0839161), (0.342159, 0.146853), (0.427699, 0.244755), (1, 1), (1.14053, 1.13986), (1.27088, 1.25874), (1.38493, 1.31469), (1.47862, 1.34965), (1.67821, 1.36364), (1.99185, 1.38462)))
Units: [Dmnl]

eff of amlodipine on dose on contractility= WITH LOOKUP (amlodopine weekly

average dose/average free amlodipine at standard dose, ([(0, 0)(2, 2)], (0, 0), (0.130346, 0.027972), (0.260692, 0.0839161), (0.342159, 0.146853), (0.427699, 0.244755), (1, 1), (1.14053, 1.13986), (1.27088, 1.25874), (1.38493, 1.31469), (1.47862, 1.34965), (1.67821, 1.36364), (1.99185, 1.38462)))
Units: [Dmnl]

change in average telmisartan= (Telmisartan concentration in plasma - Average free telmisartan in plasma)/average telmisartan adj time
Units: [(ng/ml)/Day]

telmisartan removal rate= 1.2
Units: [Day]

eff of telmisartan dose on AT2= WITH LOOKUP (telmisertan weekly average dose/average free telmisartan at standard dose, ([(0, 0)-(2, 2)],(0, 0),(0.130346, 0.027972), (0.260692, 0.0839161), (0.342159, 0.146853), (0.427699, 0.244755), (1, 1), (1.14053, 1.13986),(1.27088, 1.25874), (1.38493,1.31469), (1.47862, 1.34965), (1.67821, 1.36364), (1.99185, 1.38462)))
Units: [Dmnl]

amlodipine removal rate=2
Units: [Day]

amlodipine removal= Amlodipine concentration in plasma/amlodipine removal rate
Units: [(ng/ml)/Day]

average amlodipine adj time= 7
Units: [Day]

Amlodipine concentration in plasma= INTEG (amlodipine dosing-amlodipine removal, 0)

Units: [ng/ml]

change in average amlodipine= (Amlodipine concentration in plasma - Average free amlodipine in plasma)/average amlodipine adj time
Units: [(ng/ml)/Day]

eff of amlodipine dose on concentration= WITH LOOKUP (amlodipine daily dose/standard amlodipine dosing, ([(0,0)-(2, 1.51)], (0,0), (0.183299, 0.0791959), (0.362525, 0.248147), (0.615071, 0.517413), (0.847251, 0.818182), (1, 1), (1.15275, 1.19322), (1.22607, 1.28825), (1.30754, 1.37801), (1.4053, 1.45455), (1.50305, 1.47832), (1.77597, 1.4965), (1.98778, 1.5035)))
Units: [Dmnl]

Average free amlodipine in plasma= INTEG (change in average amlodipine, 0)
Units: [ng/ml]

average free amlodipine at standard dose= 15
Units: [ng/ml]

eff of MAP on baroreceptor= WITH LOOKUP (Mean Arterial Pressure/Baroreceptor operating point, ([(0.9, 0)-(1.1, 2)],(0.510183, 0.00699306),(0.672098, 0.020979), (0.812627, 0.027972), (0.889002, 0.0699301), (0.925662, 0.167832), (0.950102, 0.342657), (0.974542, 0.657343), (0.986762, 0.846154), (0.993686, 0.944056), (1, 1), (1.0224, 1.06294), (1.0387, 1.11888), (1.08147, 1.25874), (1.13238, 1.39161), (1.18228, 1.52448), (1.2169, 1.62238), (1.26986, 1.72727), (1.3167, 1.8042), (1.34929, 1.86713), (1.389, 1.90909), (1.42464, 1.94406), (1.46334, 1.97902), (1.49796, 1.97203)))
Units: [Dmnl]

implied baroreceptor activity= normal baroreceptor activity * eff of MAP on baroreceptor
Units: [burst/ms]

change in operating point= (Mean Arterial Pressure - Baroreceptor operating point) / operating point adj time
Units: [mmhg/Day]

eff of baroreceptor on PNS= WITH LOOKUP (Baroreceptor activity/normal baroreceptor activity, ([(0, 0)-(2, 2)], (0, 0.5), (0.0692464, 0.5), (0.175153, 0.503497), (0.378819, 0.552448), (0.582485, 0.65035), (0.745418, 0.734266), (0.892057, 0.853147), (1, 1), (1.1446, 1.23776), (1.222,1.40559), (1.30346, 1.53846), (1.39308, 1.66434), (1.52342, 1.79021), (1.66599, 1.91469), (1.76375, 1.96503), (1.89409, 1.9965), (1.96945, 2), (1.99796, 2)))
Units: [Dmnl]

baroreceptor activity change= (implied baroreceptor activity - Baroreceptor activity)/ baroreceptor activity adj time
Units: [burst/ms/Day]

eff of baroreceptor on SNS= WITH LOOKUP (Baroreceptor activity/normal baroreceptor activity, ([(0, 0.89)-(2, 2)], (0, 2), (0.0285132, 1.9965), (0.130346, 1.98059), (0.268839, 1.93706), (0.378819, 1.86713), (0.492872, 1.71329), (0.639511, 1.45455), (0.737271,1.24476),(0.786151,1.15392), (0.863544, 1.06294), (1, 1), (1.05295, 0.988112), (1.15071, 0.967133), (1.2668, 0.948951), (1.41752,0.932867), (1.56823,0.921678), (1.74745, 0.909091), (2, 0.9)))
Units: [Dmnl]

normal baroreceptor activity= 1000
Units: [burst/ms]

RSNS operating point= INTEG (change in RSNS operating point, initial RSNS operating point)
Units: [mmhg]

implied PNS activity= eff of baroreceptor on PNS*normal PNS activity
Units: [Dmnl]

RSNS operating point adj time= 3
Units: [Day]

eff of arterial tone on resistance= 1/(implied radiusˆ4)
Units: [Dmnl]

resistance at systole= eff of arterial tone on resistance*normal systole resistance
Units: [mmhg*min/ml]

Daily GFR= Glomerular filtration rate/daily filtration conversion
Units: [L/Day]

yearly vascular deterioration= 0.0035
Units: [Dmnl/year]

amlodipine adj time= 2
Units: [Day]

amlodipine concentration at standard dose= 30
Units: [ng/ml]

eff of telmisartan dose on concentration= WITH LOOKUP (telmisartan daily dose/standard telmisartan dosing, ([(0,0)-(2, 1.51)], (0, 0), (0.187373, 0.0580769), (0.309572, 0.131993), (0.411405, 0.237587), (0.627291, 0.506853), (0.847251, 0.818182), (1, 1), (1.15275, 1.19322), (1.22607, 1.28825), (1.30754, 1.37801), (1.4053, 1.45455), (1.50305, 1.47832), (1.77597, 1.4965), (1.98778, 1.5035)))
Units: [Dmnl]

telmisartan adj time= 1.1
Units: [Day]

telmisartan concentration at standard dose=1465
Units: [ng/ml]

implied chlorthalidone concentration= chlorthalidone concentration at standard dose * eff of chlorthalidone dose on concentration
Units: [ng/ml]

chlorthalidone concentration at standard dose=5
Units: [ng/ml]

chlorthalidone adj time=7
Units: [Day]

implied amlodipine concentration= amlodipine concentration at standard dose * eff of amlodipine dose on concentration
Units: [ng/ml]

standard amlodipine dosing= 5
Units: [mg]

implied telmisartan concentration= telmisartan concentration at standard dose * eff of telmisartan dose on concentration
Units: [ng/ml]

standard telmisartan dosing= 40
Units: [mg]

standard chlorthalidone dosing= 7

Units: [mg]

eff of chlorthalidone dose on concentration= WITH LOOKUP (chlorthalidone daily dose/ standard chlorthalidone dosing, ([(0, 0)-(2, 1.51)], (0, 0), (0.191446, 0.036958), (0.309572, 0.0686363), (0.354379, 0.095035), (0.391039, 0.131993), (0.480652, 0.227028), (0.643585, 0.480454), (0.879837, 0.807797), (1, 1), (1.15275, 1.19322), (1.31976, 1.36217), (1.42159, 1.42024), (1.52342, 1.4572), (1.63747, 1.4836), (1.77597, 1.4965), (1.98778, 1.5035)))
Units: [Dmnl]

Normal arterial tone= INTEG (arterial tone change, initial normal tone)
Units: [Dmnl]

normal SBP= 120
Units: [mmhg]

normal diastole resistance= 0.013333
Units: [mmhg*min/ml]

normal systole resistance= 0.02
Units: [mmhg*min/ml]

compliance= normal compliance * eff of function on compliance
Units: [Dmnl]

Mean Arterial Pressure= (Systolic BP+2*Diastolic BP)/3
Units: [mmhg]

eff of SBP on kidney damage= WITH LOOKUP (Systolic BP/normal SBP, ([(1, 1)-(2, 5)], (0, 1), (1, 1), (1.05703, 1.06993), (1.12424, 1.20979), (1.17312, 1.39161), (1.22811, 1.68531), (1.30143, 2.07692), (1.36456, 2.52448), (1.41752, 2.95804),

(1.48676, 3.61538), (1.54175, 4.14685), (1.57637, 4.48252), (1.63544, 4.72028), (1.72505, 4.91259), (1.88798, 4.98252), (2.00204, 4.98252)))
Units: [Dmnl]

normal compliance= 1
Units: [Dmnl]

tone adj time= 60
Units: [Day]

Systolic BP= Cardiac output * resistance at systole
Units: [mmhg]

eff of SBP on dysfunction= WITH LOOKUP (Systolic BP/normal SBP, ([(1, 1)-(2, 4)], (0, 1), (1, 1), (1.02648, 1.00699), (1.05255, 1.03147), (1.07515, 1.05245), (1.09593,1.12587), (1.11853, 1.20979), (1.13503, 1.28322), (1.15397, 1.40909), (1.17536, 1.55594), (1.25458, 2.45804), (1.31976, 3.17133), (1.37271, 3.59091), (1.39715, 3.72727), (1.43585, 3.8426), (1.47251, 3.91608), (1.5112, 3.93706), (1.56212, 3.95804), (1.65988, 3.95804), (1.75153, 3.96853)))
Units: [Dmnl]

Baroreceptor operating point= INTEG (change in operating point, initial operating point)
Units: [mmhg]

change in ADH= (implied ADH-Anti Diuretic Hormon)/ADH adj time
Units: [pg/ml/Day]

change in aldosterone= (implied aldosterone-Aldosterone)/ aldosterone adj time
Units: [ng/ml/Day]

initial AT2= 250
Units: [pg/ml]

aldosterone adj time= 3
Units: [Day]

initial aldosterone= 250
Units: [ng/ml]

initial ADH= 5
Units: [pg/ml]

ADH adj time= 3
Units: [Day]

Aldosterone= INTEG (change in aldosterone, initial aldosterone)
Units: [ng/ml]

Angiotensin 2 concentration= INTEG (change in AT2, initial AT2)
Units: [pg/ml]

Anti Diuretic Hormon= INTEG (change in ADH, initial ADH)
Units: [pg/ml]

AT2 adj time= 3
Units: [Day]

change in AT2= (implied AT2-Angiotensin 2 concentration)/AT2 adj time
Units: [pg/(ml*Day)]

initial renin activity= 5.5

Units: [pg/ml/hr]

eff of ADH on arterial tone= WITH LOOKUP (Anti Diuretic Hormon/normal ADH, ([(1, 0.8)-(2, 1)], (0, 1), (1, 1), (1.09369, 0.995105), (1.14664, 0.99021), (1.23014, 0.973427), (1.3279, 0.945455), (1.39919, 0.920979), (1.47454, 0.893007), (1.56415, 0.864336), (1.63136, 0.841958), (1.73523, 0.818182), (1.84114, 0.805594), (1.9389, 0.8), (1.99185, 0.8)))
Units: [Dmnl]

eff of ADH on urine Na concentration= WITH LOOKUP (Anti Diuretic Hormon/ normal ADH, ([(0, 0)-(2, 2.4)], (0.00407332, 0.146853), (0.10998, 0.146853), (0.289206, 0.174825), (0.439919, 0.230769), (0.659878, 0.394406), (0.855397, 0.688112), (1, 1), (1.13238, 1.46853), (1.23422, 1.9049), (1.31161, 2.11469), (1.41344, 2.24895), (1.51935, 2.32448), (1.62525, 2.34965),(2, 2.36643)))
Units: [Dmnl]

eff of aldosterone on Na removal= WITH LOOKUP (Aldosterone/ normal aldosterone, ([(0, 0)-(2, 2)], (0.00814664, 1.48951), (0.228106, 1.47552), (0.472505, 1.41958), (0.602851, 1.32168), (0.725051, 1.23776), (1, 1), (1.09572, 0.909091), (1.20978, 0.832168), (1.36049, 0.734266), (1.60081, 0.608392), (1.82892, 0.503497), (1.99185, 0.510489)))
Units: [Dmnl]

eff of AT2 on ADH= WITH LOOKUP (Angiotensin 2 concentration / normal AT2, ([(0, 0.5)-(2, 2)], (0.00407332, 0.510489), (0.313646, 0.524476), (0.615071, 0.573427), (0.761711, 0.646853), (0.87169, 0.734266), (1, 1), (1.13646, 1.29371), (1.34012, 1.74825), (1.44196, 1.93007), (1.49084, 1.96329), (1.56008, 2), (1.66191, 2), (1.98778, 2)))
Units: [Dmnl]

eff of AT2 on aldosterone= WITH LOOKUP (Angiotensin 2 concentration/ normal

AT2, ([(0, 0.78)-(2, 1.52)], (0.00814664, 0.783217), (0.1222, 0.783217), (0.305499, 0.805874), (0.501018, 0.846154), (0.782077, 0.916084), (1, 1), (1.07943, 1.04196), (1.29532, 1.17483), (1.43381, 1.29371), (1.49491, 1.35664), (1.62933, 1.45273), (1.66599, 1.4786), (1.75967, 1.4993), (1.89002, 1.51049), (2, 1.51049)))
Units: [Dmnl]

eff of AT2 on arterial tone= WITH LOOKUP (Angiotensin 2 concentration/normal AT2, ([(0, 0)-(2, 2)], (0.00814664, 1.23077), (0.505092, 1.23077), (0.708758, 1.2028), (0.806517, 1.16783), (0.904277, 1.1049), (0.953157, 1.05594), (1, 1), (1.05906, 0.902098), (1.15682, 0.79021), (1.28717, 0.713287), (1.41344, 0.678322), (1.54786, 0.657343), (1.98778, 0.643357)))
Units: [Dmnl]

implied aldosterone= normal aldosterone * eff of AT2 on aldosterone
Units: [ng/ml]

normal renin activity= 5.5
Units: [pg/ml/hr]

renin change= (implied renin activity-Renin activity)/renin adj time
Units: [pg/ml/hr/Day]

normal aldosterone= 250
Units: [ng/ml]

eff of renin on AT2= WITH LOOKUP (Renin activity/normal renin activity, ([(0,0.48)-(2, 2)], (0, 0.482517), (0.350305, 0.489511), (0.521385, 0.538462), (0.647658, 0.608392), (0.761711, 0.685315), (0.855397, 0.755245), (0.94501, 0.888112), (1, 1), (1.1446, 1.26573), (1.29939, 1.64336), (1.42974, 1.88811), (1.51528, 1.93622), (1.64969, 1.97203), (1.8167, 1.99301), (1.98778, 1.99301)))
Units: [Dmnl]

normal ADH= 5
Units: [pg/ml]

Renin activity= INTEG (renin change, initial renin activity)
Units: [pg/ml/hr]

normal AT2= 250
Units: [pg/ml]

renin adj time= 3
Units: [Day]

eff of function on tone= WITH LOOKUP (Vascular function/normal vascular function, ([(0.5, 0.9)-(1, 1)], (0.5, 0.9), (0.543788, 0.901049), (0.57943, 0.903497), (0.598778, 0.905594), (0.61609, 0.908741), (0.63442, 0.911888), (0.742362, 0.934266), (0.822811, 0.956993), (0.858452, 0.967133), (0.887984, 0.975874), (0.912424, 0.983566), (0.933809, 0.99021), (0.950102, 0.994755), (0.973523, 0.998252), (1, 1), (2, 1), (2.5, 1), (3, 1)))
Units: [Dmnl]

eff of function on compliance= WITH LOOKUP (Vascular function/normal vascular function, ([(0.6,0.4)-(1, 1)], (0.602444, 0.548951), (0.679837, 0.561538), (0.719756, 0.578322), (0.74582, 0.601399), (0.763747, 0.630769), (0.784114, 0.664336), (0.801222, 0.725175), (0.81833, 0.794406), (0.834623, 0.863636), (0.850917, 0.941259), (0.863951, 0.976923), (0.880244, 0.987413), (0.90224, 0.995804), (1, 1), (2, 1)))
Units: [Dmnl]

normal vascular function= 1
Units: [Dmnl]

water intake= MAX ((desired water + average daily water intake), 0)

Units: [L/Day]

desired Na= (normal Na-Total body salt)/Na adj time
Units: [mEq/Day]

vascular function loss= deterioration rate
Units: [1/Day]

water adj time= 3
Units: [Day]

normal TBW= 42
Units: [L]

Na adj time= 3
Units: [Day]

initial Na= 2160
Units: [mEq]

normal Na= 2160
Units: [mEq]

Total body salt= INTEG (Na intake-Na removal, initial Na)
Units: [mEq]

normal daily fitration= 180
Units: [L/Day]

normal GFR per min= 125
Units: [ml/min]

water removal= implied water removal

Units: [L/Day]

normal blood volume= 5

Units: [L]

normal contractility= 1

Units: [Dmnl]

eff of SNS on contractility= WITH LOOKUP (implied SNS activity/normal SNS activity, ([(1, 1)-(2, 4)], (0, 1), (1, 1), (1.06721, 1.05245), (1.1222, 1.25175), (1.16701, 1.52448), (1.23014, 1.91259), (1.28921, 2.25874), (1.32587, 2.47902), (1.37882, 2.77273), (1.44807, 3.10839), (1.52749, 3.42308), (1.58248, 3.62238), (1.69246, 3.8007), (1.82077, 3.92657), (1.93483, 3.96853), (2, 3.96853)))

Units: [Dmnl]

initial TBW= 42

Units: [L]

normal ESV= 40

Units: [ml/beat]

daily filtration conversion= 1000/1440

Units: [(ml*Day)/(min*L)]

End sytolic volume= (1/contractility) * normal ESV

Units: [ml/beat]

initial kidney function= 1

Units: [Dmnl][0,1]

Kidney function= INTEG (-kidney function loss, initial kidney function)
Units: [Dmnl]

normal water removal= 2.5
Units: [L/Day]

eff of blood volume on EDV= WITH LOOKUP (Blood volume/normal blood volume, ([(0, 0)-(2, 2)], (0, 0),(0.1, 0),(0. 248473, 0.0223777), (0.395112, 0.0788811), (0.501018, 0.149511), (0.615071, 0.276643),(0.794297,0.559161), (0.912424, 0.834615), (1, 1), (1.09572, 1.18776),(1.18534, 1.35021), (1.24236, 1.43497), (1.30346, 1.48441), (1.36456, 1.54091), (1.4501, 1.56916), (1.60081, 1.58329), (1.98371, 1.58329)))
Units: [Dmnl]

Stroke volume= End diastolic volume - End sytolic volume
Units: [ml/beat]

eff of ECF volume on blood volume= WITH LOOKUP (Extracellular fluid volume/normal ECF volume, ([(0.66,0.5)-(1.67, 1.5)], (0.66, 0.5), (1, 1), (1.28122, 1.39161), (1.3279, 1.44755), (1.35527, 1.47203), (1.389, 1.48252), (1.49084, 1.4965), (1.66705, 1.4965)))
Units: [Dmnl]

Extracellular fluid volume= Total body water * ECF volume ratio
Units: [L]

normal ECF volume= 14
Units: [L]

ECF volume ratio= 1/3
Units: [Dmnl]

Total body water= INTEG (water intake-water removal, initial TBW)
Units: [L]

deterioration rate= normal vascular deterioration per day * eff of SBP on dysfunction
Units: [1/Day]

Vascular function= INTEG (-vascular function loss, initial vascular function)
Units: [Dmnl]

initial vascular function= 1
Units: [Dmnl]

eff of SNS on arterial tone= WITH LOOKUP (implied SNS activity/normal SNS activity, ([(0.7, 0.25)-(1.4, 1.1)], (0.704481, 1.08846), (0.863544, 1.07692), (0.924033,1.06154), (0.962118, 1.03846), (0.984521, 1.01923), (1,1), (1.01141, 0.973077), (1.03493,0.926923),
(1.06293,0.846154),(1.0887,0.75),(1.11782,0.615385),(1.13238,0.526923), (1.16711, 0.361538), (1.18167, 0.311538), (1.20611, 0.276748), (1.22607, 0.26486), (1.24552, 0.257692), (1.39715, 0.258916)))
Units: [Dmnl]

normal PNS activity= 1
Units: [Dmnl]

eff of PNS on HR= WITH LOOKUP (implied PNS activity/normal PNS activity, ([(1,0.8)-(2, 1)], (0, 1), (1, 1), (1.01629, 0.972028), (1.03259, 0.948951), (1.06517, 0.923776), (1.11405, 0.901399), (1.21792, 0.874126), (1.29939, 0.856643), (1.39308, 0.841958), (1.50917, 0.828671), (1.62118, 0.818881), (1.70468, 0.81049), (1.75967, 0.806993), (1.82688, 0.802797), (1.90224, 0.800699), (2, 0.8)))
Units: [Dmnl]

normal SNS activity= 1
Units: [Dmnl]

normal EDV= 120
Units: [ml/beat]

operating point adj time= 3
Units: [Day] [0,?]

Hearth Rate= INTEG (HR change, initial HR)
Units: [beat/min]

initial normal tone= 1
Units: [Dmnl]

initial baroreceptor activity= 1000
Units: [burst/ms]

Baroreceptor activity= INTEG (baroreceptor activity change, initial baroreceptor activity)
Units: [burst/ms]

baroreceptor activity adj time= 3
Units: [Day] [0,?]

Cardiac output= Hearth Rate * Stroke volume
Units: [ml/min]

HR adj time= 3
Units: [Day]

HR change= (implied heart rate-Hearth Rate)/HR adj time

Units: [beat/min/Day]

initial HR= 75

Units: [beat/min]

reference tone= 1

Units: [Dmnl]

normal HR= 75

Units: [beat/min]

FINAL TIME = 3000

Units: [Day] The final time for the simulation.

INITIAL TIME = 0

Units: [Day] The initial time for the simulation.

SAVEPER = TIME STEP

Units: [Day] [0,?]

TIME STEP = 0.0625

Units: [Day] [0,?]

APPENDIX B: MODEL VIEW

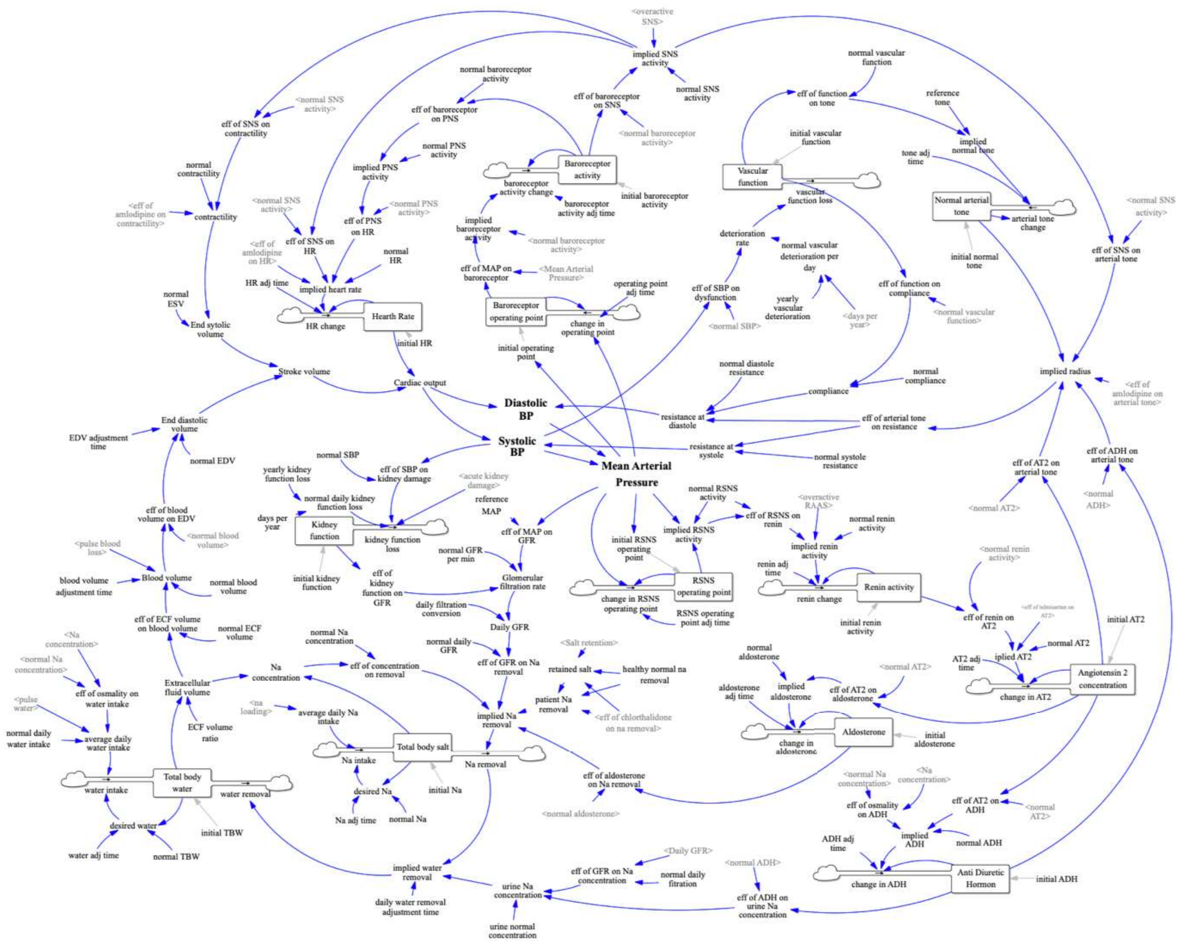

Figure B.1. Main structure.

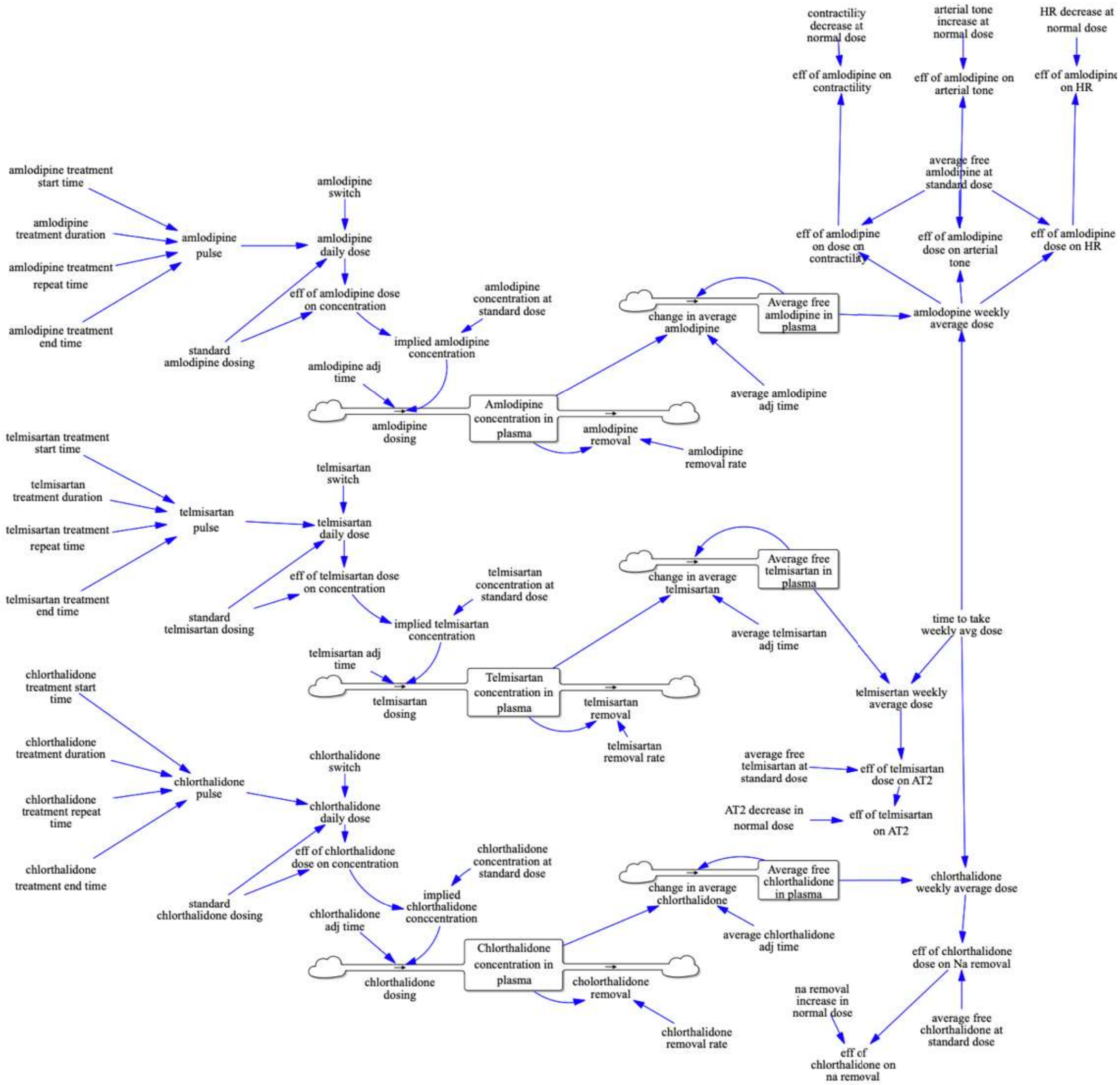

Figure B.2. Treatment view.

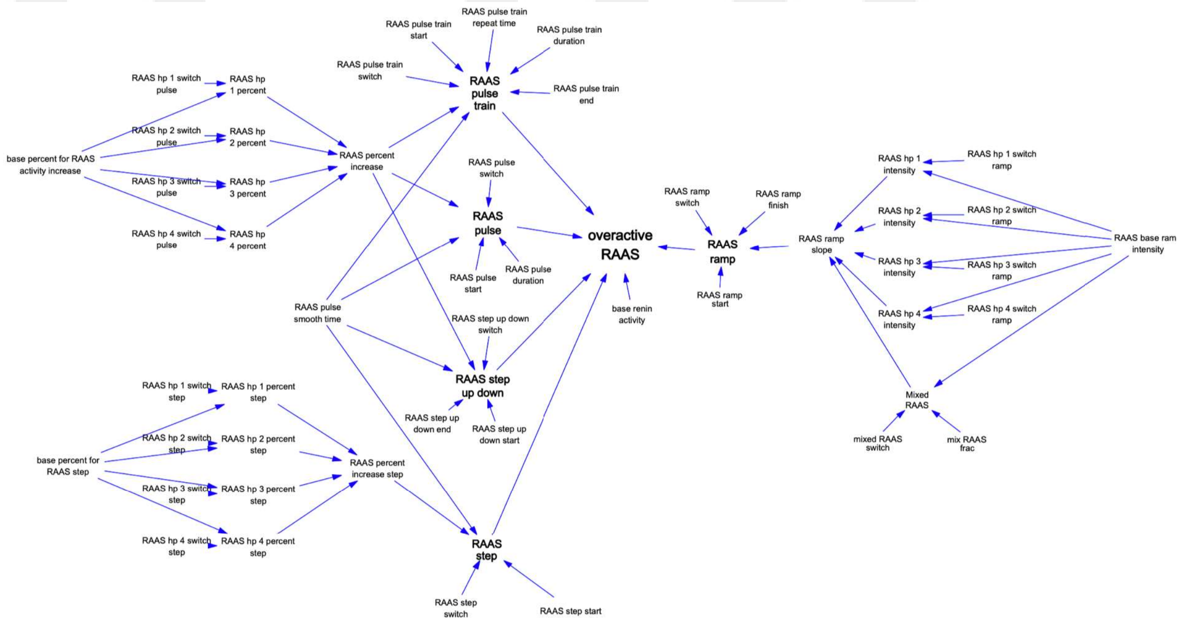

Figure B.3. Scenario view.